# UNIVERSITY OF ZAGREB

## FACULTY OF MECHANICAL ENGINEERING AND NAVAL ARCHITECTURE

International Master of Science Programme: Sustainable Energy Engineering

# Autonomous solar-hydrogen power system

## Master thesis

## Motalleb Miri

Zagreb - 2012

# UNIVERSITY OF ZAGREB

## FACULTY OF MECHANICAL ENGINEERING AND NAVAL ARCHITECTURE

International Master of Science Programme: Sustainable Energy Engineering

# Autonomous solar-hydrogen power system

## Master thesis

Supervisor:
Associate prof. dr. sc. Mihajlo Firak

Candidate:
Motalleb Miri  BSc.

Zagreb - 2012

## DATA FOR BIBLIOGRAPHICAL CARD:

UDK: 620.92

Key words: SOLAR ENERGY, PASIVE HOUSE, PHOTOVOLTAIC SYSTEM, HYDROGEN, FUEL CELL, ELECTROLYSER, COMPUTER SIMULATION

Scientific scope: TECHNICAL SCIENCES

Scientific field: SUSTAINABLE ENERGY ENGINEERING

Institution at which work has been made: UNIVERSITY OF ZAGREB, FMENA

Advisor: Associate prof. dr. sc. MIHAJLO FIRAK

Number of pages: 110

Number of figures: 83

Number of tables: 20

Number of titles listed in References: 23

Date of presentation: 2012


Committee:    Associate prof. dr. sc MIHAJLO FIRAK

Prof. dr. sc. FRANO BARBIR

Associate prof. dr.sc. DRAŽEN LONČAR


Institution at which work is filled: UNIVERSITY OF ZAGREB, FACULTY OF MECHANICAL ENGINEERING AND NAVAL ARCHITECTURE (FMENA)

Zagreb, 09-12-2006.

# Master Thesis Proposal

Candidate: **Miri Motalleb, B.Sc.**

Title: **Autonomous solar-hydrogen power system**

Thesis Contents:

The problems of providing energy on a local and a global level have grown in importance in recent years. The aim of the thesis is to analyse the present situation in detail and to estimate further development. Assuming that the solar energy use takes an increased share in the total energy consumption and taking into consideration the development of the technology of production and use of hydrogen, it is necessary to conceive a solar-hydrogen autonomous system for supplying an isolated household with heat and power energy and the energy for personal transport (autonomous solar-hydrogen system plus transport - ASVS+T).

The annual cycle of heat, electrical, and transportation load of a particular type of household has to be defined, i.e. the temporal arrangement and intensity of using energy during a year has to be specified.
It is also necessary to choose a location in the Republic of Croatia where this type of a supposed household would be situated, to define the geometry and orientation of the building and to assume that it is built according to the standard of a passive house.
Furthermore, the available solar energy across the superficial area (all the outer surfaces) of the supposed building should be defined on a yearly basis and with the maximum resolution considering the accessible meteorological data.
After defining the ASVS+T concept, as well as the incoming and needed energy, it is necessary to choose required components and then to approximately size them. The chosen components should be analyzed on the level of the system and of the process; their dynamical and mathematical model should be defined and then verified by computer simulation using the collected technical data.
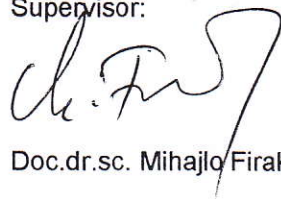The mathematical model of single components and of the whole system should be transferred to simulation models using Matlab and Simulink. Finally, it is necessary to simulate the ASVS+T model using Simulink for the supposed scenario (annual cycle) and also for the critical weekly and daily periods (exceptionally rich and exceptionally poor with incoming solar energy).
To summarize, based on simulation results, it is necessary to determine the required changes of the starting assumptions concerning the presumed superficial area of the building, and concerning the chosen technical ASVS+T concept.
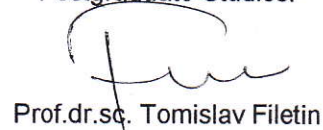
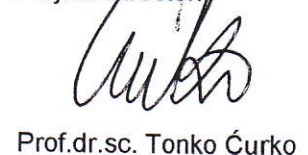Thesis proposed: 23. 01. 2007,

Thesis submitted:

Supervisor:

Doc.dr.sc. Mihajlo Firak

Chairman of Committee for
Postgraduate Studies:

Prof.dr.sc. Tomislav Filetin

Project Director:

Prof.dr.sc. Tonko Ćurko

Zagreb, 09.12.2006.

# Zadatak za magistarski rad

| | |
|---|---|
| Kandidat: | **Miri Motalleb, dipl.ing.** |
| Naslov: | **Autonomni solarno-vodikov energetski sustav** |

Sadržaj zadatka:

Zadnjih godina problem opskrbe energijom na lokalnoj i globalnoj razini dobiva na važnosti. U radu je potrebno provesti argumentiranu diskusiju trenutne situacije i dati procjenu razvoja budućih zbivanja.

Pod pretpostavkom povećanog udjela korištenja solarne energije u ukupnoj potrošnji energije i sazrijevanja tehnologija proizvodnje i korištenja vodika, potrebno je koncipirati solarno-vodikov autonomni energetski sutav za snabdjevanje toplinskom i električnom energijom kućanstva uključivo i energiju za osobni transport (ASVS+T).

Potrebno je definirati godišnji ciklus toplinskog, električnog i transportnog opterećenja pretpostavljenog kućanstva, tj. odrediti vremenski raspored i intenzitet korištenja energije tokom jedne godine.

Također je potrebno odabrati lokaciju na području RH gdje bi takvo kućanstvo bilo smješteno, pretpostaviti geometriju i orjentaciju zgrade te da je zgrada građena prema standardu pasivne gradnje. Zatim treba odrediti raspoloživu sunčevu energiju po oplošju pretpostavljene zgrade tokom jedne godine s najvećom mogućom rezolucijom s obzirom na dostupne meteorološke podatke.

Nakon definiranja koncepta ASVS+T, kao i dozračene i potrebne energije, treba odabrati potrebne komponente i okvirno ih dimenzionirati.

Odabrane komponente treba analizirati na razini sustava i procesa i zatim postaviti njihove dinamičke matematičke modele te izvršiti njihovu verifikaciju simulacijom na računalu korištenjem prikupljenih tehničkih podataka.
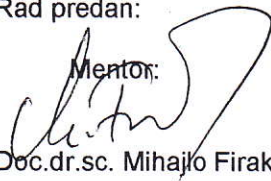
Matematički model pojedinih komponenti i cijelog sustava treba prevesti u simulacijski model korištenjem Matlab-a i Simulink-a.
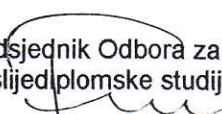
Na kraju je potrebno provesti simulaciju ASVS+T modela u Simulinku za pretpostavljeni scenarij (godišnji ciklus) kao i za kritične tjedne i dnevne periode (izrazito bogate i izrazito siromašne dozračenom sunčevom energijom).

Zaključno, treba provesti diskusiju dobivenih rezultata i utvrditi eventualno potrebne promjene polaznih pretpostavki u smislu pretpostavljene površine za prikupljanje sunčeve energije i u smislu odabrane tehničke koncepcije ASVS+T.

Zadatak zadan: 23. 01. 2007.

Rad predan:

| Mentor: | Predsjednik Odbora za poslijediplomske studije: | Voditelj projekta: |
|---|---|---|
| Doc.dr.sc. Mihajlo Firak | Prof.dr.sc. Tomislav Filetin | Prof.dr.sc. Tonko Ćurko |

Zagreb, 09-12-2006.

# Master Thesis Proposal

Candidate: **Miri Motalleb, B.Sc.**

Title: **Autonomous solar-hydrogen power system**

Thesis Contents:

The problems of providing energy on a local and a global level have grown in importance in recent years. The aim of the thesis is to analyse the present situation in detail and to estimate further development. Assuming that the solar energy use takes an increased share in the total energy consumption and taking into consideration the development of the technology of production and use of hydrogen, it is necessary to conceive a solar-hydrogen autonomous system for supplying an isolated household with heat and power energy and the energy for personal transport (autonomous solar-hydrogen system plus transport - ASVS+T).

The annual cycle of heat, electrical, and transportation load of a particular type of household has to be defined, i.e. the temporal arrangement and intensity of using energy during a year has to be specified.

It is also necessary to choose a location in the Republic of Croatia where this type of a supposed household would be situated, to define the geometry and orientation of the building and to assume that it is built according to the standard of a passive house.

Furthermore, the available solar energy across the superficial area (all the outer surfaces) of the supposed building should be defined on a yearly basis and with the maximum resolution considering the accessible meteorological data.

After defining the ASVS+T concept, as well as the incoming and needed energy, it is necessary to choose required components and then to approximately size them. The chosen components should be analyzed on the level of the system and of the process; their dynamical and mathematical model should be defined and then verified by computer simulation using the collected technical data.
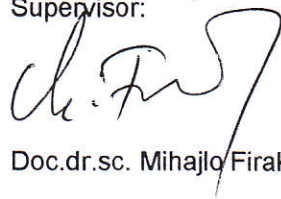
The mathematical model of single components and of the whole system should be transferred to simulation models using Matlab and Simulink. Finally, it is necessary to simulate the ASVS+T model using Simulink for the supposed scenario (annual cycle) and also for the critical weekly and daily periods (exceptionally rich and exceptionally poor with incoming solar energy).

To summarize, based on simulation results, it is necessary to determine the required changes of the starting assumptions concerning the presumed superficial area of the building, and concerning the chosen technical ASVS+T concept.
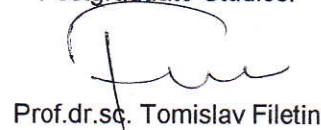
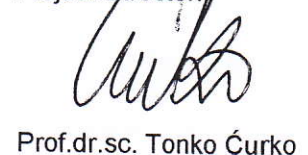Thesis proposed: 23. 01. 2007,

Thesis submitted:

Supervisor:

Doc.dr.sc. Mihajlo Firak

Chairman of Committee for Postgraduate Studies:

Prof.dr.sc. Tomislav Filetin

Project Director:

Prof.dr.sc. Tonko Ćurko

S v e u č i l i š t e   u   Z a g r e b u
**Fakultet strojarstva i brodogradnje**
International Master of Science Programme: Sustainable Energy
Engineering

Zagreb, 09.12.2006.

# Zadatak za magistarski rad

Kandidat:     **Miri Motalleb, dipl.ing.**

Naslov:       **Autonomni solarno-vodikov energetski sustav**

Sadržaj zadatka:

Zadnjih godina problem opskrbe energijom na lokalnoj i globalnoj razini dobiva na važnosti. U radu je potrebno provesti argumentiranu diskusiju trenutne situacije i dati procjenu razvoja budućih zbivanja.

Pod pretpostavkom povećanog udjela korištenja solarne energije u ukupnoj potrošnji energije i sazrijevanja tehnologija proizvodnje i korištenja vodika, potrebno je koncipirati solarno-vodikov autonomni energetski sutav za snabdjevanje toplinskom i električnom energijom kućanstva uključivo i energiju za osobni transport (ASVS+T).

Potrebno je definirati godišnji ciklus toplinskog, električnog i transportnog opterećenja pretpostavljenog kućanstva, tj. odrediti vremenski raspored i intenzitet korištenja energije tokom jedne godine.

Također je potrebno odabrati lokaciju na području RH gdje bi takvo kućanstvo bilo smješteno, pretpostaviti geometriju i orjentaciju zgrade te da je zgrada građena prema standardu pasivne gradnje. Zatim treba odrediti raspoloživu sunčevu energiju po oplošju pretpostavljene zgrade tokom jedne godine s najvećom mogućom rezolucijom s obzirom na dostupne meteorološke podatke.

Nakon definiranja koncepta ASVS+T, kao i dozračene i potrebne energije, treba odabrati potrebne komponente i okvirno ih dimenzionirati.

Odabrane komponente treba analizirati na razini sustava i procesa i zatim postaviti njihove dinamičke matematičke modele te izvršiti njihovu verifikaciju simulacijom na računalu korištenjem prikupljenih tehničkih podataka.
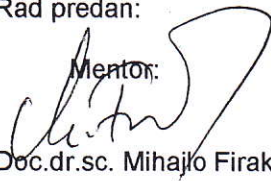
Matematički model pojedinih komponenti i cijelog sustava treba prevesti u simulacijski model korištenjem Matlab-a i Simulink-a.
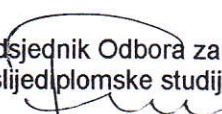
Na kraju je potrebno provesti simulaciju ASVS+T modela u Simulinku za pretpostavljeni scenarij (godišnji ciklus) kao i za kritične tjedne i dnevne periode (izrazito bogate i izrazito siromašne dozračenom sunčevom energijom).

Zaključno, treba provesti diskusiju dobivenih rezultata i utvrditi eventualno potrebne promjene polaznih pretpostavki u smislu pretpostavljene površine za prikupljanje sunčeve energije i u smislu odabrane tehničke koncepcije ASVS+T.

Zadatak zadan:  23. 01. 2007.

Rad predan:

Mentor:

Doc.dr.sc. Mihajlo Firak

Predsjednik Odbora za
poslijediplomske studije:

Prof.dr.sc. Tomislav Filetin

Voditelj projekta:

Prof.dr.sc. Tonko Ćurko

# ACKNOWLEDGEMENTS

**TABLE OF CONTENTS:**

**LIST OF TABLES:**

**LIST OF FIGURES:**

## NOMENCLATURE

### List of symbols

| | |
|---|---|
| $A$ | area, $m^2$ |
| $A_{el}$ | area of electrode, $m^2$ |
| $A_{FC}$ | the active area of the fuel cell electrode, $cm^2$ |
| $Ag$ | glass area, $m^2$ |
| $As$ | surface area, $m^2$ |
| $a$ | ohmic resistance of electrolyte, $\Omega m^2$ |
| $b, c$ | coefficients for overvoltage on electrodes |
| C | battery capacity, As |
| $C_p$ | specific heat of air , kJ/(kg ºC), ($C_p$ = 1.0 ) |
| dt | infinitesimal part of time, s |
| $E_{cell}$ | fuel cell working voltage, V |
| $E_{Nerst}$ | Nernst voltage, V |
| $F$ | Faraday's constant, C/mol, (F=96500) |
| $F_s$ | special allowance factor for Fluorescent lamp,  (Fs = 2.19) |
| $F_u$ | use factor |
| $G_{f,liq}$ | Gibbs free energy of hydrogen in liquid state, J/mol,($G_{f,liq}$= 228170) |
| $h_{amb}$ | enthalpy of ambient air, kJ/kg |
| $h_{supply}$ | enthalpy of supply air, kJ/kg |
| $I$ | current through cell, A |
| i | current density, $A/cm^2$ |
| $i_o$ | exchange current density, $A/cm^2$ |
| $Im$ | output current of module, A |
| $I_{ac}$ | AC current, A |
| $I_B$ | battery current, A |
| $I_E$ | electrolyser current, A |
| $i_L$ | limiting current density, $A/cm^2$ |
| $I_{load}$ | momentarly current of the load, A |
| $I_{mp}$ | maximum power current, A |
| $I_{ph}$ | light generated current, A |
| $I_s$ | reverse saturation current, A |
| $I_{sc}$ | short circuit current, A |
| $k$ | Boltzmann constant, J/K, ( $k$ = 1.38 x $10^{-23}$) |
| $m_{supply}$ | mass air-flow, kg/s |
| $n$ | the quantity of released hydrogen, mol |
| $n_c$ | number of cells in stack |
| $n_d$ | diode ideality factor |

| $N$ | number of solar cell in series string |
|---|---|
| $N_p$ | number of PV modules in parallel |
| $N_s$ | number of PV modules in series |
| $n_{st}$ | quantity of hydrogen in storage tank, mol |
| $P_{solar}$ | heat flow through the window, kW |
| $P_{load}$ | electrical loads, W |
| $P_{PV}$ | power of photovoltaic array, W |
| $q$ | electric charge, C, ($q = 1.6 \times 10^{-19}$) |
| $Q_{reg}$ | external heat delivered to the regenerator, kW |
| $Q_v$ | solar radiation, Wh/m2 |
| $R_B$ | battery internal resistance, $\Omega$ |
| $R_h$ | resistance of heater, $\Omega$ |
| $R_i$ | total cell internal resistance, $\Omega$ cm$^{-2}$ |
| $R_{load}$ | ohmic resistance of electrical load, $\Omega$ |
| $R_s$ | series resistance, $\Omega$ |
| $R_{sh}$ | shunt resistance, $\Omega$ |
| $T$ | cell temperature, K |
| $T_i$ | indoor air temperature, ºC |
| $T_o$ | outdoor air temperature, ºC |
| $T_o$ | outdoor air temperature, ºC |
| $U_c$ | operation cell voltage, V |
| $U$ | overall heat transfer coefficient, W/(m$^2$ ºC) |
| $U$ | heat transfer coefficient, W/(m$^2$ ºC) |
| $U_B$ | battery voltage, V |
| $U_E$ | electrolyser voltage, V |
| $U_{load}$ | momentary voltage of the load, V |
| $U_{oc}$ | battery clamps voltage, V |
| $U_{PV}$ | terminal voltage of module, V |
| $U_{rev}$ | reversible cell voltage, V |
| $V$ | volumetric flow of ventilation air, m$^3$/s |
| $V$ | volumetric flow of ventilation air, m$^3$/s |
| $V_{ac}$ | AC voltage, V |
| $V_{act}$ | activation loss, V |
| $V_{cell}$ | fuel cell voltage, V |
| $V_{conc.}$ | concentration loss, V |
| $V_{mp}$ | maximum power voltage, V |
| $V_{oc}$ | open circuit voltage, V |
| $V_{ohmic}$ | ohmic loss, V |
| $V_{st}$ | hydrogen storage tank volume, m$^3$ |

| $W_{cell}$ | Power output of a fuel cell, W |
|---|---|
| $W_{comp}$ | total compressor work, W |
| $W_L$ | total installed wattage, W |
| $Z$ | compressibility factor |

**Greek letter**

| $\alpha$ | transfer coefficient,($\alpha$=1) |
|---|---|
| $\rho$ | density of air at temperature Ti, kg/m$^3$, ($\rho$ =1.2) |
| $\Delta t$ | time step, h |
| $\eta_{DCDCB}$ | DC/DC battery converter efficiency |
| $\eta_{DCDCE}$ | DC/DC electrolyser converter efficiency |
| $\eta_{MPP}$ | MPP tracker efficiency |

**Acronyms**

| FC | Fuel cell |
|---|---|
| FF | fill factor |
| MPPT | maximum power point tracker |
| PV | photovoltaic |
| SOC | battery state of charge |

**ABSTRACT**

Solar-hydrogen autonomous system for supplying isolated real passive house in real climate with power energy, energy for personal transport and heating/cooling system have been established and discussed.

Simulation and analysis of a model of an autonomous power system based only on a renewable source (solar irradiance) integrated with a hydrogen system for energy backup has been performed. Commercially available passive house in island of Hvar in Croatia, and real commercial components (photovoltaic module, fuel cell stack and electrolyser) were acquired.

In order to minimize the level of modeling and simulation complexity, just electric - hydrogen system have been modeled and result of dynamic simulation has been presented. For heating and cooling of the house only static simulation (calculation in Excel) has been performed instead of dynamic simulation.

The electric-hydrogen system is composed of a PV array integrated with an electrolyser, with a storage tank where the hydrogen is stored as compressed gas and with a PEM fuel cell stack. Such a system has no pollutant emissions and is environmentally friendly.

Matlab-Simulink software has been used to design the system and to analyze its functioning during one certain day of operation. The analysis has been affected by considering three scenarios in order to simulate different situations (with and without solar irradiance) with high energy demands by the user to prove the control system function during the system operation.

Simulations results show that concept, design, mathematical models and Simulink schemes work as it assumed. All of that can be used as valuable tool for passive house autonomous electric-hydrogen system design.

**Keywords:** solar energy, passive house, photovoltaic system, hydrogen, fuel cell, electrolyser, computer simulation

**SAŽETAK**

U radu je izveden i analiziran sunčevo-vodikov autonomni sustav za snabdijevanje električnom energijom izolirane realne pasivne kuće u realnim klimatskim uvjetima, energijom za osobni transport i sustavom za grijanje i hlađenje.

Napravljena je simulacija i analiza modela autonomnog sustava za proizvodnju električne energije zasnovanog samo na obnovljivom izvoru energije (sunčevom zračenju) koji uključuje i vodikov podsustav za pohranu energije. Pretpostavljene su komercijalno dobavljiva pasivna kuća smještena na otoku Hvaru u Hrvatskoj, i realne komercijalno dobavljive komponente (fotonaponski modul, svežanj gorivnih članaka i elektrolizator).

Da bi se smanjila kompleksnost modeliranja i simulacije, izvršeno je modeliranje, simulacija i dan prikaz rezultata samo za dinamiku električno - vodikovog sustava. Umjesto simulacije dinamike grijanja i hlađenja kuće izvršen je samo proračun stacionarnog stanja u Excelu.

Električko-vodikov sustav sastavljen je od PV polja koje je integrirano s elektrolizatorom, rezervoarom za pohranu u kojem se pohranjuje vodik u formi komprimiranog plina i svežnjem PEM gorivnih članaka. Takav sustav ne ispušta štetne tvari i prihvatljiv je za okolinu.

Matlab-Simulink računalni program korišten je u projektiranju sustava i analizu funkcioniranja električko-vodikovog sustava tokom jednog određenog dana. Analiza je provedena na temelju tri pretpostavljena scenarija da bi se simulirale različite situacije (sa i bez sunčevog zračenja, uz visoke i niske potrebe korisnika za električnom energijom) i time provjerio regulacijski sustav.

Rezultati simulacije pokazuju da koncept, projekt, matematički modeli i Simulink sheme funkcioniraju kako je zamišljeno. Sve to može biti korišteno kao vrijedan alat kod projektiranja autonomnog električno-vodikovog sustava za pasivnu kuću.

**Ključne riječi**: sunčeva energija, pasivna kuća, fotonaponski sustav, vodik, gorivni članak, elektrolizator, računalna simulacija

# 1   Introduction

## 1.1   Global energy demand

Renewable energy sources (solar, wind, etc) are attracting more attention as alternative energy sources to conventional fossil fuel energy sources. This is not only due to the diminishing fuel sources, but also due to environmental pollution and global warming problems.

The potential of renewable energy sources is unequally higher. Especially through direct utilization of the sun's radiation energy the global demand could be met many times over.

In the long run, there will be no alternative to an optimized tapping of the potentials of renewable energy sources. Especially, the utilization of solar energy through solar cells and solar-thermal power plants will play a key role. Long-term scenarios forecast that by 2100, the utilization of solar energy will meet more than 50%of the global energy demand.(Fig.1)
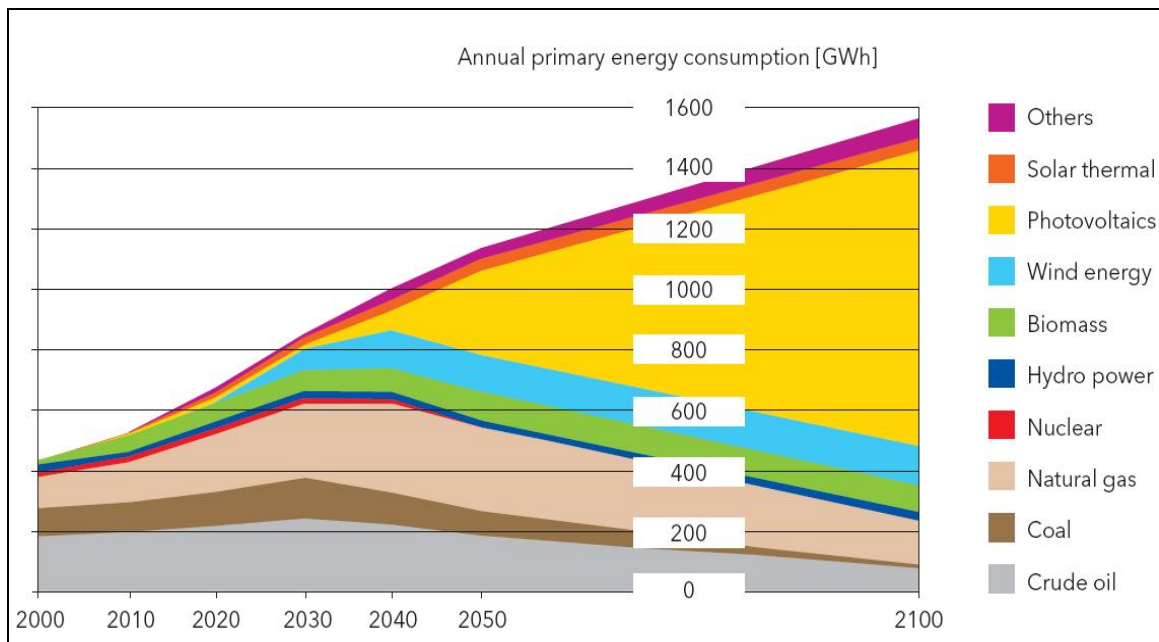


**Figure 1.  Scenario of the development of the global energy demand [1]**

Among these sources is the solar energy, which is the most promising, as the fabrication of less costly PV devices becomes a reality. Control problems arise due to large variances of PV output power under different insulation levels. To overcome this problem, PV power plants are integrated with other power sources or storage system such as hydrogen generator, storage and fuel cells.

One of the major challenges for PV systems remains matching their sun dependent power supply curve with that of the time dependent power demand of the residence. To solve this problem an energy storage device must be used in conjunction with the PV array. This device must store excess PV energy and subsequently deliver power at the desired time and rate. The energy storage device that is most commonly used with PV systems today is the battery but hydrogen based technology is under way.

Under assumption of increased part of using solar energy in entire energy consumption, and developing of technology of production and using hydrogen, it is necessary to conceive solar-hydrogen autonomous system for supplying isolated household with heat and power energy and energy for personal transport (ASVS+T).

## 1.2    Aim and scope of the work

The goal of this thesis work is to use solar energy in entire energy consumption, and to apply of technology of production and using hydrogen to operate solar-hydrogen autonomous system for supplying isolated passive house with heat and power energy and energy for personal transport. Chosen geographical location is the remote island of Hvar, Croatia.  What is going to be done in this project is to define the whole system for solar heating, solar cooling, solar power (electric) supply and ensure energy for local transport (pick up truck), Then find and test mathematical model of the power system (Fig.2).
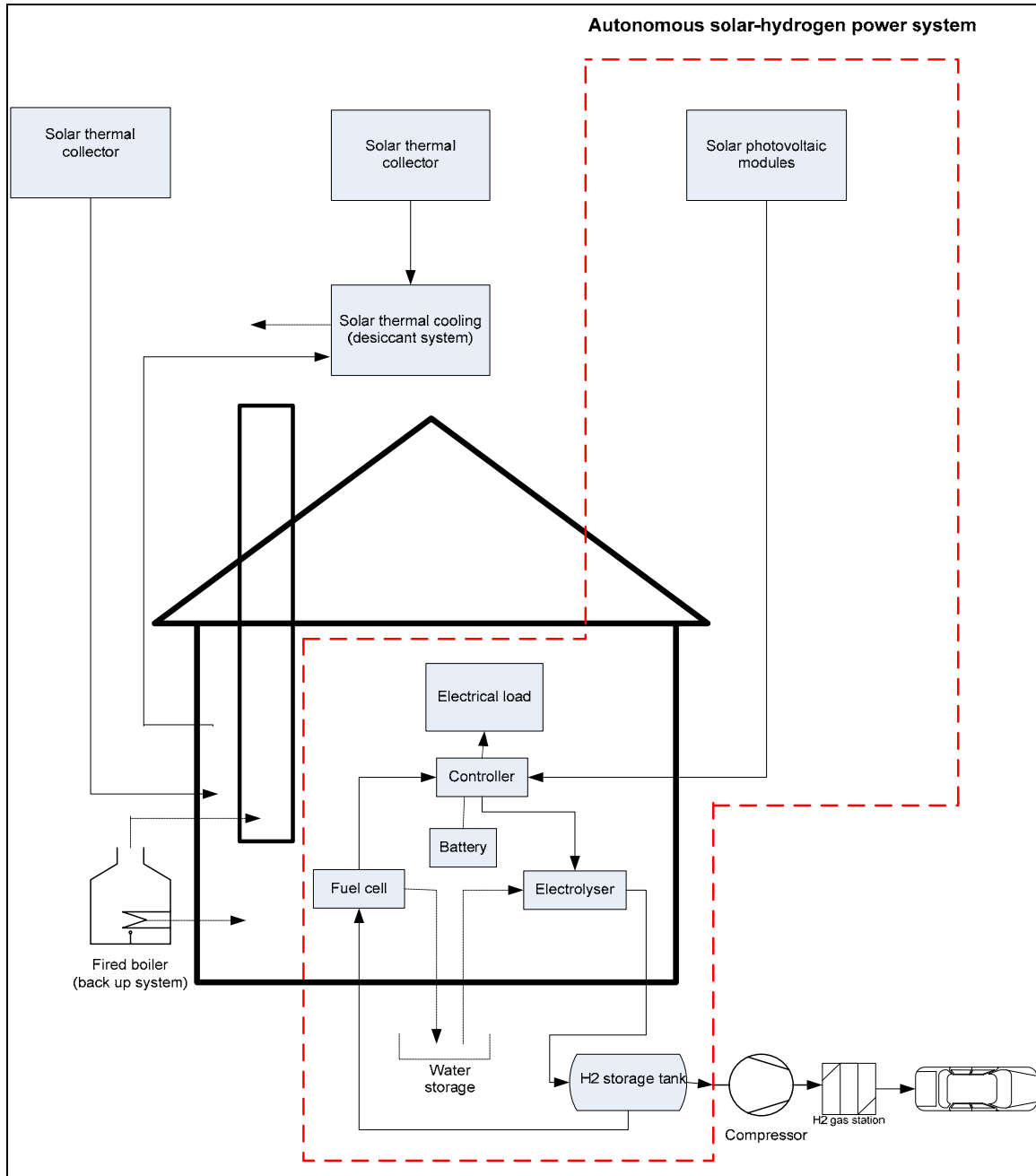
**Figure 2. Energy supply of isolated household assumed in this work**

After collecting technical data and in order to analyze the performance of the model, MATLAB/Simulink is used.

## 1.3    Purpose of the project

The purpose of this project is to define and simulate solar –hydrogen autonomous power system based on renewable energy sources which particularly in this project is solar energy. Therefore, it's necessary to conceive solar-hydrogen power system

specified for remote island. Especially recent developments in PEM fuel cells are beginning to make possible a promising alternative to batteries for storage of energy from solar electric power systems. With this in mind, we are going to design an energy production/storage system based on PV, battery and fuel cell concept. With such an integrated system, is expected to provide reliable, environmentally valuable power to remote installations. Optimization of this system would be possible by successive computer simulations under various scenarios.

## 1.4    Power system design

The proposed PV–Electrolyser–FC system is shown in Fig.3 The major components of the system are: a PV array, an Electrolyser, a hydrogen storage tank, proton exchange membrane (PEM) fuel cell stack, and the loads which are households and transport vehicles. A control system is employed to monitor the state of the system, and control power and hydrogen flows. The power generation system with a PV system has two application types: a local (isolated) type and an interconnected (grid connected) type. The isolated type system works independent of other power systems, where the load locally consumes the electric power from the PV system. The output power of the PV system, however, fluctuates depending on solar radiation and PV cell temperature. Then a storage system must be used to deliver the required power at lower radiation levels and during the night.

The electrolyser consists of a number of cells isolated from one another in separate cell compartments.

Proton Exchange Membrane (PEM) fuel cells stack is used. The PEM uses a polymer membrane as its electrolyte. With such solid polymer electrolyte, electrolyte loss is not an issue with regard to stack life. H2 produced by the electrolyser is consumed at the anode, yielding electrons at the anode and producing H2 ions, which enter the electrolyte. At the cathode, H2 combines with O2 ions to produce water, which is rejected from the back of the cathode into the oxidant gas stream as the PEM operates at 75°C; water produced is carried out of the FC by excess oxidant flow. [2]
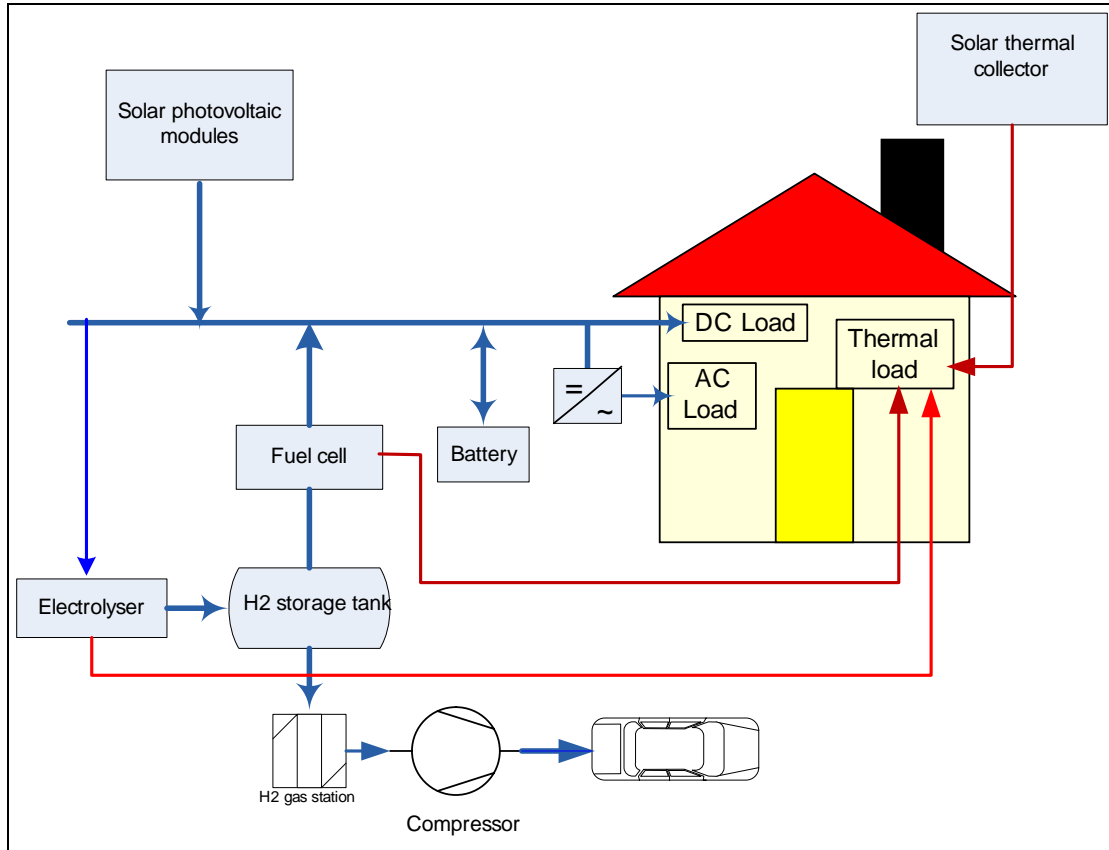
**Figure 3. Isolated hybrid PV-FC power system**

In this system, electricity generated in the photovoltaic array is sent to battery and excess electricity to the electrolyser to produce hydrogen which is stored for a period of time to be converted, when required, into electricity using the fuel cell. The fuel cell can be considered as a back up generator to meet the load requirement. The heat which is produced by fuel cell and electrolyser can be used appropriately in heat and mass flow management system of the household. This system was not considered here because it would add too much complexity in this work.

The system must have energy production and storage capabilities. It must also be designed to meet hourly, daily, weekly and seasonal variations in energy demand.

## 2   Household description

After defining the concept of the household energy system in the following, description of components are given

## 2.1 Passive house

A passive house is a building in which a comfortable interior climate can be maintained without active heating and cooling systems. [2]  The Passive House standard offers a cost-efficient way of minimizing the energy demand of new buildings in accordance with the global principle of sustainability, while at the same time improving the comfort experienced by building occupants.(Fig.4)

It thus creates the basis on which it is possible to meet the remaining energy demand of new buildings completely from renewable sources, while keeping within the bounds set by the limited availability of renewable and the affordability of extra costs.

 The Passive House philosophy builds upon two basic principles:

Principle1:
**Optimize what is essential anyway**
Principle2:
**Minimize losses before maximizing gains**

South-facing Passive Houses are also solar houses. Efficiency potentials having been exploited, the passive gain of incoming solar energy through glazing dimensioned to provide sufficient daylight covers about 40% of the minimized heat losses of the house. To achieve this, in the most cases newly developed, windows have low-emissivity triple glazing and super insulated frames. These let in more solar heat than they lose. The benefit is enhanced if the main glazing areas are oriented to the south and are not shaded
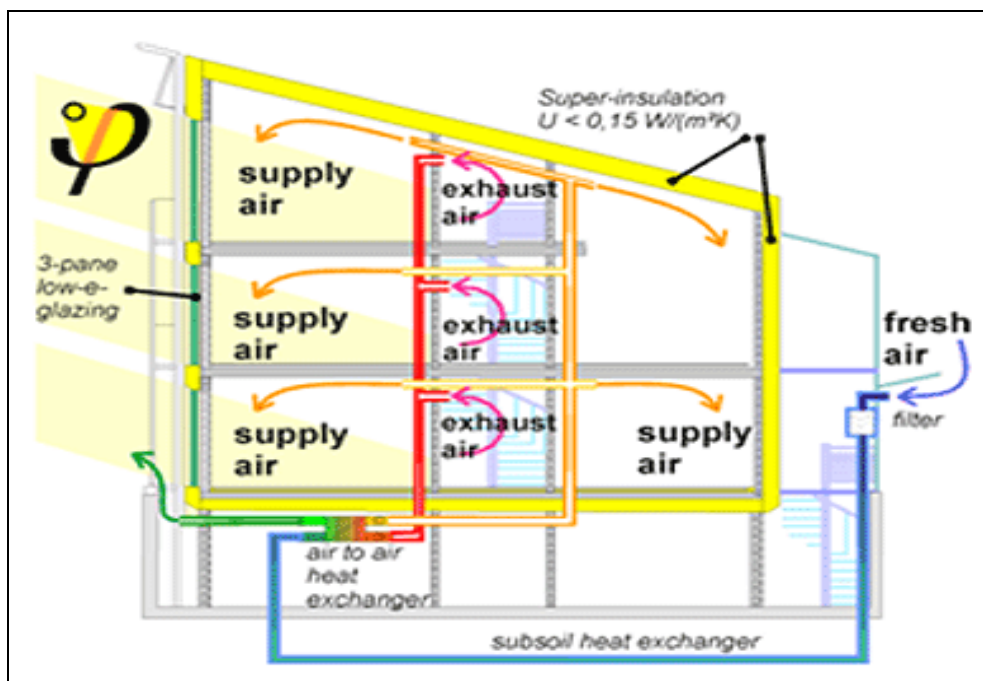


**Figure 4. Schematic of passive house[3]**

Fig.5 shows that the combined energy consumption of a passive house is less than the average new European home requires for household electricity and hot water alone.
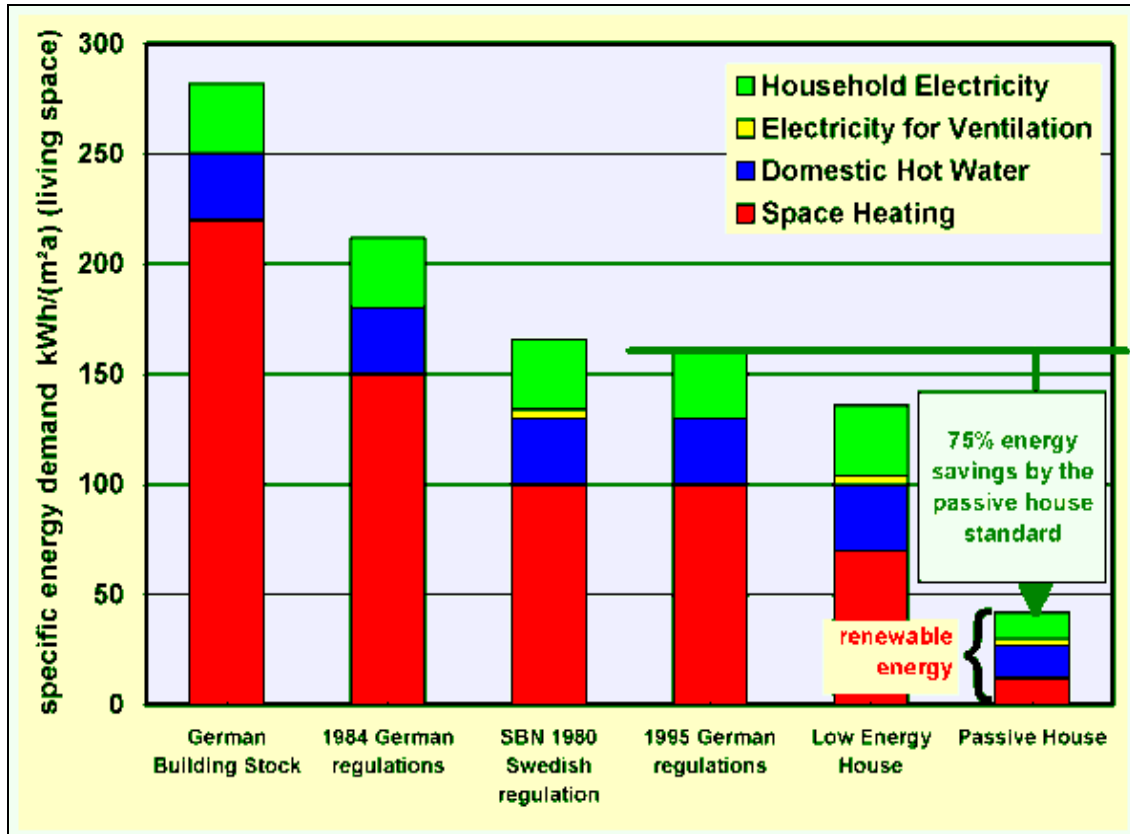
**Figure 5. Comparison of energy consumption in passive house with other building [4]**

The combined end energy consumed by a passive house is therefore less than a quarter of the energy consumed by the average new construction that complies with applicable national energy regulations.

A dwelling which achieves the Passive House standard typically includes:

- very good levels of insulation with minimal thermal bridges
- well thought out utilization of solar and internal gains
- excellent level of air tightness
- good indoor air quality, provided by a whole house mechanical ventilation system with highly efficient heat recovery

For Europe (40° - 60° Northern latitudes), a dwelling is deemed to satisfy the Passive House criteria if:

- the total energy demand for space heating is less than 15 kWh/m$^2$/yr treated floor area;
- the total primary energy use for all appliances, domestic hot water and space heating and cooling is less than 120 kWh/m$^2$/yr

The following listing explains the upgrade:

**Passive solar gain:** The passive gain of incoming solar heat through the windows will cover close to 40% of the heat losses if all guidelines are followed.

**Windows**: The standard triple glazing with one low emission shield and argon fill has a glazing U-value of 1.0 W/(m$^2$°C)

**External doors:** The standard door has a U-value of 1.0 W/(m$^2$°C)

**Wall:** The standard wall insulation consists of 145mm of semi rigid Rock wool insulation carefully fitted between 45x145mm studs spaced 600mm apart with minimized cold bridging. The U-value is 0.25 W/(m$^2$°C) using Swedish calculation methods.

Roof: Single storey houses. This is the ideal situation when building to fully passive specification. Simple and cheap Cellulose-fiber insulation is blown to a thickness of 500mm over the entire ceiling. U-value 0.066 W/(m$^2$°C)

**Floor:** The standard base unit provides good insulation of U-value 0.1 W/(m$^2$°C)

**Air tightness:** The entire building envelope must be totally airtight. The vapour barrier must be overlapping 500 mm and sealed everywhere. All windows and doors must meet the required air-leakage standards less than 0.6 air changes per hour

**Ventilation:** The ventilation heat-recovery system can be set to slightly lower speed for a passive house. The ventilation system for a standard passive house is designed for a 0.5 air-exchange per hour

**Tap water:** Around 60-70% of the hot water required for a house can be got from solar collectors on the roof. This is only possible when one half of the roof is oriented to south.

Theses are the criteria that must be considered when a passive house constructed.

The use of passive house heating and cooling requires an integrated approach to building design. it mainly consider proper location, design and construction materials choice. The initial feature of the passive system is, however, the minimization of all possible heat losses. Such state can be achieved by proper orientation of a building, appropriate surface to volume ratio and adequate insulation.

### 2.1.1　Floor plans, building section and views

For the purpose of this work passive house built by company Marles Ltd. [5].
The house is built using a mixed modular system: ceilings, partition walls between rooms, and prefabricated reinforced concrete slabs; the highly insulated facade and roof are lightweight prefabricated wood elements. In addition, triple-glazed windows with specially insulated window frames as well as a home ventilation system with a high efficiency heat exchanger were installed.

Fig.6 shows the south and north views of the houses with the large window Surfaces.


**Figure 6. North and South view of passive house chosen for this work [5]**

Fig.7 shows the floor plan of the house. One gains entry, into the ground floor through a door on the north side



10 m

Kitchen

Living room

7.7 m

Bathroom

Hallway

Bedroom

Store room

Staircase
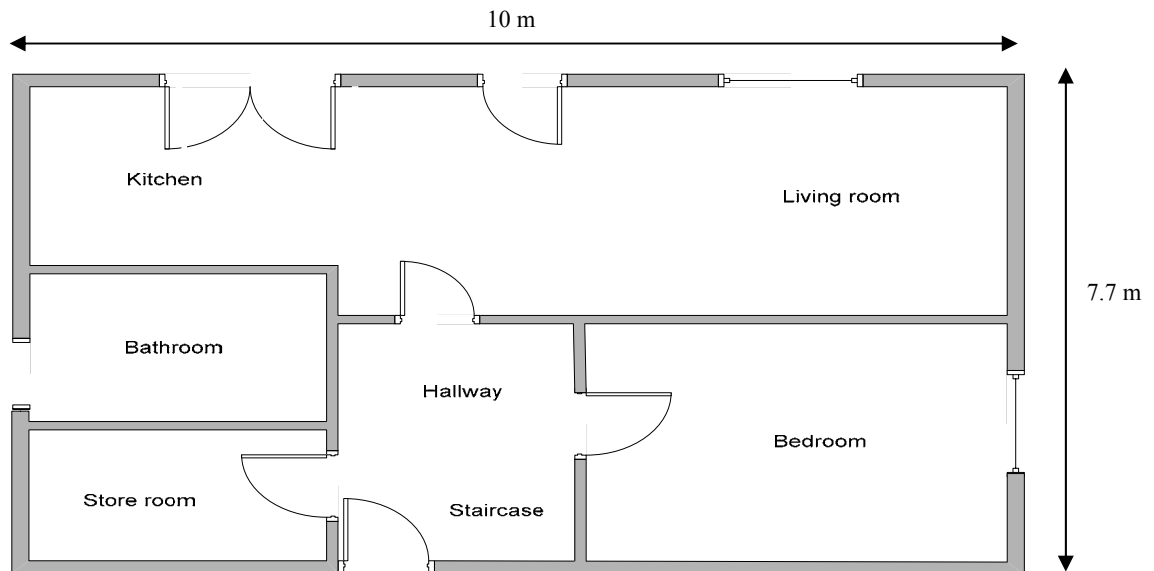
**Figure 7. Floor plan of the house [5]**

In the first floor, on the south there are bedrooms for parents, guestroom with a door to the patio and children's room.
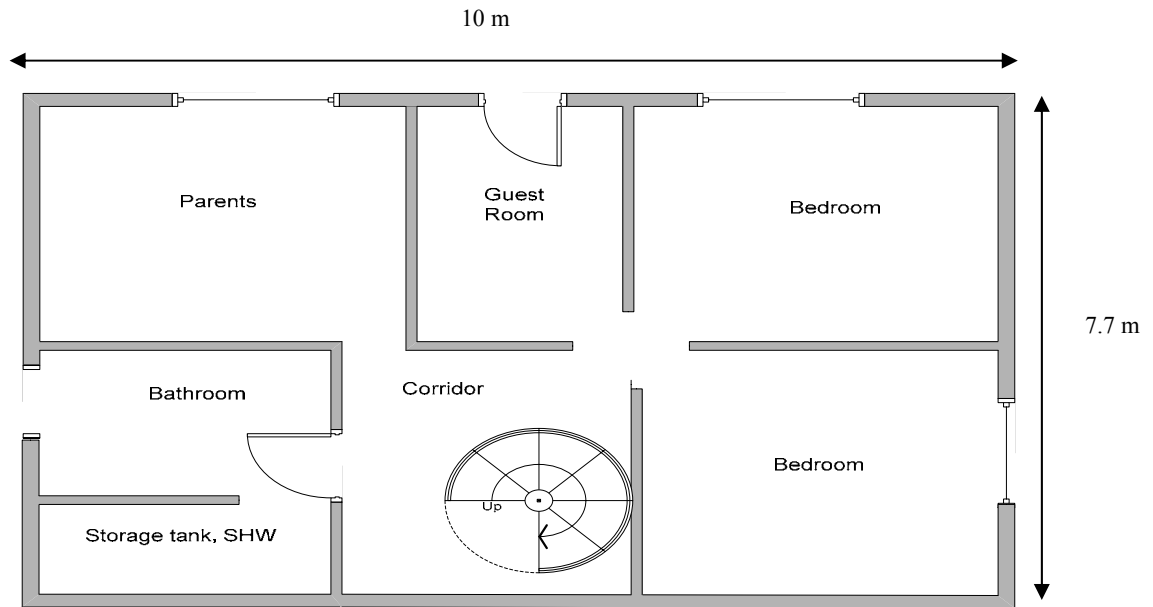
**Figure 8. First floor plan of the house [5]**

In the construction of Passive Houses a great deal of attention must be paid to air tightness of the building envelope, especially at connections between different elements, such as windows and doors.
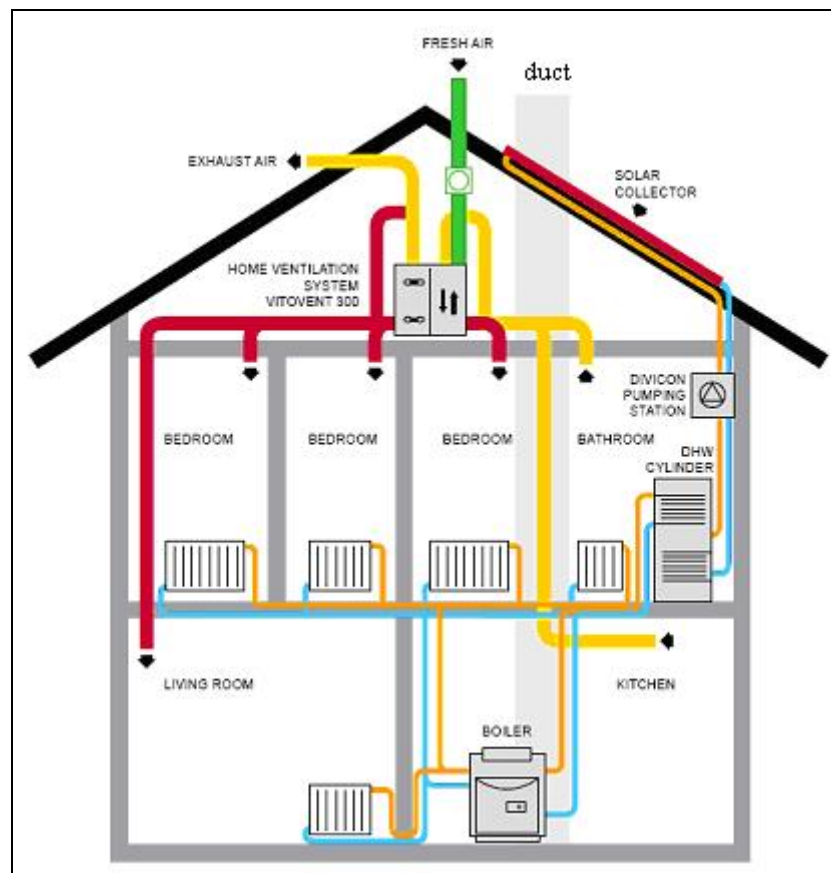


**Figure 9. Heat recovery system in passive house concept [6]**

Table 1 shows the standard details of the highly insulated building envelope.

**Table 1. Specification of the walls and window [3]**

| | Material | U-Value | Thickness (total) |
|---|---|---|---|
| External wall | Prefabricated lightweight wood element Plaster board Particleboard Mineral wool insulation Particleboard ventilated board casing | 0.126 W/(m²°C) | 340 mm |
| External wall(gable side) | Prefabricated concrete element (165 mm) with thermal insulation compound system (400 mm) out of polystyrene hard foam EPS, plastered on the outside | 0.097 W/(m²°C) | 575 mm |
| Roof | Plaster board 12,5 mm Particle board 19 mm Mineral wool 400 mm/I truss Particle board 25 mm Roof sealing | 0.095 W/(m²°C) | 456 mm |
| Floor | Wood flooring Tread absorbing insulation (5 mm PE foam) Concrete slab (150 mm) Insulation (300 mm) | 0.125 W/(m²°C) | 475 mm |
| Window | triple-glazed low -emissive | 0.83 W/(m²°C) | (2 * 15 mm pane separation, argon gas filling) |

The roof is built from prefabricated lightweight wood elements with 400 mm thickness, which span from one partition wall to the next. An internal polyethylene foil forms the airtight layer.

The outer wall elements for the north and south facades are also built using prefabricated lightweight wood elements. An internal polyethylene foil forms the airtight layer.

The outer wall of the gable sides is, like the house partition walls, built from load carrying reinforced-concrete slabs. This is protected on the outside against heating losses by a 400 mm polystyrene external thermal insulation compound system. The concrete itself forms the airtight layer for the gable wall.

The floor slab consists of 240 mm prefabricated steel-reinforced slabs, which is insulated underneath by factory-made 300 mm polystyrene external thermal insulation

(420 mm for the end-of-terrace houses). The concrete floor itself also forms the airtight layer.

To achieve the Passive House standard it is not only necessary to have good standard insulation for the building envelope surfaces, but most importantly a thermal-bridge free and airtight connection between the building elements.

### 2.1.2 Dimensions of the house

Following tables presents characteristic of the house that is consist of two floors.

**Table 2.  Size of the house**

|  | North | South | East | West |
|---|---|---|---|---|
| L,W, (m); H=5,4 m | 7.7 | 10 | 7,7 | 10 |
| Total Area [m$^2$] | 61.6 | 61.6 | 39.2 | 39.2 |
| Doors [m$^2$] | 1.6 | 3.2 | *** | *** |
| Windows [m$^2$] | *** | 12 | 0.5 | 5.25 |
| Total Exterior Wall Area [m$^2$] | 60 | 46.4 | 38.7 | 33.95 |
| Total Roof Area [m$^2$] | 77 | | | |

| Gross floor area [m$^2$] | 144 | Ceiling Height [m] | 2.8 | Volume [m$^3$] | 431.2 |
|---|---|---|---|---|---|
| Total exterior glass area [m$^2$] | 20.95 | Triple  pane [m$^2$] | 20.95 | Total door area [m$^2$] | 1.6 |

It's necessary to mention that door in the ground floor is made by wood but in the first floor, it's made of glass. Since it's more look like a window in the calculation it's considered as a glass area.

### 2.1.3 Passive house energy flows

The house was considered from the island of Hvar, It's located on eastern shores of Adriatic Sea (43°30′N 16°26′E). Hvar has a Mediterranean climate: hot, dry summers (maximum air temperature in July reaches 36°C) and warm, wet winters. Hvar is one of the sunniest places in Croatia.
In order to find energy consumption demand, heat losses need to be calculated. The heating season period, last from October 15th until April 15th, while cooling season starts, first of June and finishes on September 15th.
Selecting the indoor temperature is very important from thermal comfort view points. Standard handbooks don't specify specific design temperature and humidity conditions for load calculation but a design temperature of 22°C is commonly used.

#### 2.1.3.1 House heat losses

Every difference in temperature between the inside and the outside of the structure results heat flow between outside and inside of the building. Three main type of heat losses exist.

- transmission losses through walls, roofs and windows

- ventilation losses, when the warm inside air is exchanged by fresh outside air
- Infiltration losses, leaking into the building through cracks and other openings which is taken into account zero in our case.

Heat load can be estimated at any given time by simply subtracting heat gains received by the structure interior from the heat losses experienced by the building.

Q heating = Q heat loss – Q heat gains =

$$= [(UA + \rho\, C_p\, V \text{ ventilation})(T_i - T_o) - (Q_{solar} + Q_{people} + P_{el.\ appliances})]\Delta t \qquad (2.1)$$

Where:

| | |
|---|---|
| $\Delta t$ | time step, h |
| U | overall heat transfer coefficient, $W/(m^2\,°C)$ |
| A | surface area, $m^2$ |
| $\rho$ | density of air at temperature Ti, $kg/m^3$, ($\rho = 1.2$) |
| $C_p$ | specific heat of air, $kJ/(kg\ °C)$, ($C_p = 1.0$) |
| V | volumetric flow of ventilation air, $m^3/s$ |
| Ti | indoor air temperature, $°C$ |
| To | outdoor air temperature, $°C$ |

In general the scale of the heat losses from a building depends on the outdoor air temperature, surface area and construction and insulation of walls, roof, floor, windows, and door along with ventilation flow rate. In table 3, calculation is given for one month just to estimate how much energy needs to be supplied.

**Table 3. Heat losses through the envelope of the house in a day of January**

| hours | Ti [°C] | Qloss-walls | Qloss-windows | Qloss-Roof | Qloss-Floor | Qloss[kWh]-Total |
|-------|---------|-------------|---------------|------------|-------------|------------------|
| 1 | 6,5 | 1,23 | 1,14 | 1,05 | 1,08 | 4,49 |
| 2 | 6,5 | 1,23 | 1,14 | 1,05 | 1,08 | 4,49 |
| 3 | 6,3 | 1,25 | 1,16 | 1,07 | 1,10 | 4,57 |
| 4 | 6,2 | 1,26 | 1,17 | 1,08 | 1,10 | 4,60 |
| 5 | 6,2 | 1,26 | 1,17 | 1,08 | 1,10 | 4,60 |
| 6 | 6,1 | 1,27 | 1,17 | 1,09 | 1,11 | 4,64 |
| 7 | 6 | 1,28 | 1,18 | 1,10 | 1,12 | 4,68 |
| 8 | 6,2 | 1,26 | 1,17 | 1,08 | 1,10 | 4,60 |
| 9 | 6,4 | 1,24 | 1,15 | 1,06 | 1,09 | 4,53 |
| 10 | 7 | 1,17 | 1,09 | 1,00 | 1,03 | 4,29 |
| 11 | 7,6 | 1,11 | 1,03 | 0,95 | 0,97 | 4,06 |
| 12 | 8,2 | 1,04 | 0,97 | 0,89 | 0,92 | 3,82 |
| 13 | 8,9 | 0,97 | 0,90 | 0,83 | 0,85 | 3,55 |
| 14 | 9,2 | 0,94 | 0,87 | 0,80 | 0,82 | 3,43 |
| 15 | 9,4 | 0,92 | 0,85 | 0,79 | 0,81 | 3,36 |
| 16 | 9,1 | 0,95 | 0,88 | 0,81 | 0,83 | 3,47 |
| 17 | 8,8 | 0,98 | 0,91 | 0,84 | 0,86 | 3,59 |
| 18 | 8,4 | 1,02 | 0,95 | 0,88 | 0,90 | 3,75 |
| 19 | 8 | 1,07 | 0,99 | 0,91 | 0,94 | 3,90 |
| 20 | 7,5 | 1,12 | 1,04 | 0,96 | 0,98 | 4,10 |
| 21 | 7,2 | 1,15 | 1,07 | 0,99 | 1,01 | 4,21 |
| 22 | 7 | 1,17 | 1,09 | 1,00 | 1,03 | 4,29 |
| 23 | 6,8 | 1,19 | 1,11 | 1,02 | 1,05 | 4,37 |
| 24 | 6,6 | 1,21 | 1,13 | 1,04 | 1,07 | 4,45 |
| Ave. | | 27,27 | 25,27 | 23,37 | 23,96 | 99,86 |
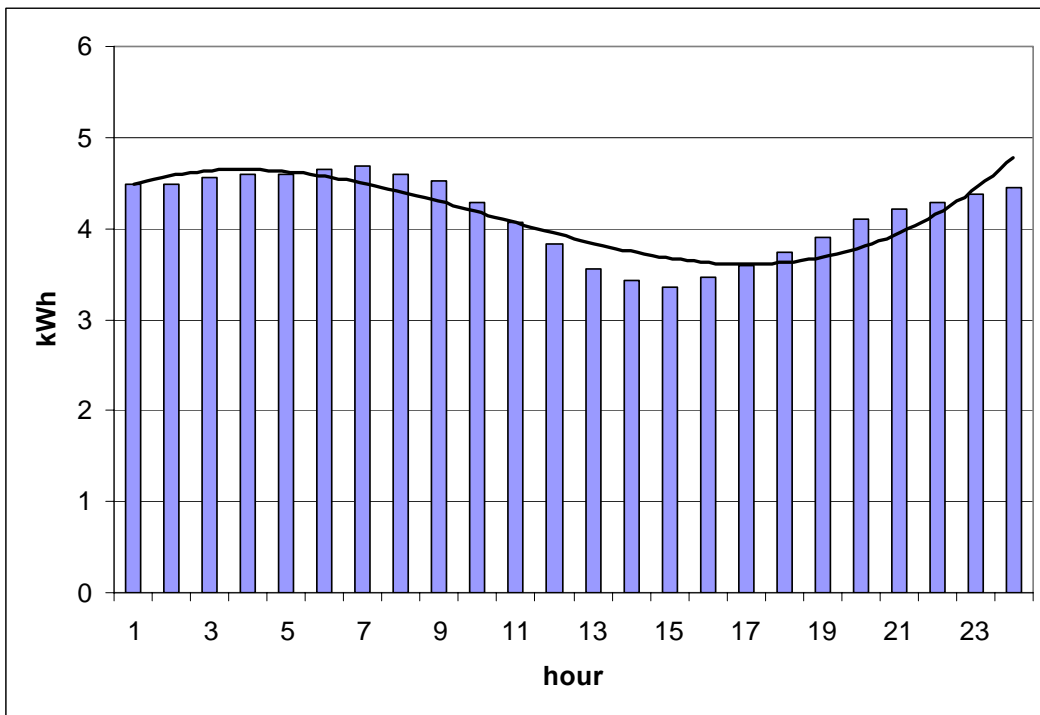


**Figure 10. Total heat losses of the house through envelope**

This figure shows trend of energy loss during the days in January.

### 2.1.3.2 Heat gains generated within the house

Heat gain is the rate at which energy is generated within the building. Heat gain usually occurs in the following forms:

- Solar irradiation
- Latent and sensible heat generated by occupants within the house
- Heat generated by electrical appliances and other equipments

The heat supplied by people, lights, motors and machinery may be estimated, but any allowance for these heat sources requires careful consideration.

### 2.1.3.3 Solar irradiation through the windows

Solar irradiation received by the house depends on the orientation of the house and windows, as well as the surface area and optical properties of the glazing. It also varies with the time of a day and year, and orientation of the window. Since it affects on heating or cooling load demand, therefore it's very important to have measured data for deferent orientation. Monthly average daily values of radiation are available. Basic equation for the solar energy which is absorbed through the windows is given below:

$$Q_{solar} = 0.9 \, Q_v \, A_{window} \qquad\qquad (2.2)$$

Where:

| | |
|---|---|
| $Q_{solar}$ | heat flow through the window, kW |
| 0.9 | transmission coefficient for double-glazed windows |
| $Q_v$ | solar radiation, $Wh/m^2$ |
| $A_{window}$ | area of window in given direction, $m^2$ |

Table 4. Solar irradiation during a day in January

| hour | $Q_v [Wh/m^2]$ | $P_{solar} [kWh]$ |
|---|---|---|
| 1 | 0.0 | 0 |
| 2 | 0.0 | 0 |
| 3 | 0.0 | 0 |
| 4 | 0.0 | 0 |
| 5 | 0.0 | 0 |
| 6 | 0.0 | 0 |
| 7 | 0.0 | 0 |
| 8 | 6.9 | 0.11 |
| 9 | 74.0 | 1.18 |
| 10 | 145.1 | 2.32 |
| 11 | 204.3 | 3.26 |
| 12 | 237.8 | 3.80 |
| 13 | 237.8 | 3.80 |
| 14 | 204.3 | 3.26 |
| 15 | 145.1 | 2.32 |
| 16 | 74.0 | 1.18 |
| 17 | 6.9 | 0.11 |
| 18 | 0.0 | 0 |
| 19 | 0.0 | 0 |
| 20 | 0.0 | 0 |
| 21 | 0.0 | 0 |
| 22 | 0.0 | 0 |
| 23 | 0.0 | 0 |
| 24 | 0.0 | 0 |
| Total | 1336.3 | 21.35 |

### 2.1.3.4 Occupants heat gain

The heat gain from human beings has two components, sensible and latent. The total and relative amounts of sensible and latent hear vary depending on the level of activity. The data on heat gain from occupants that can be used for calculation is given in table 5.

**Table 5. Heat gain from occupants**

| One man | 140 | W/person |
|---|---|---|
| One women | 130 | W/person |
| Three children | 105 | W/person |
| Total | 585 | W/person |

In the following table hourly heat gain in the same month is shown.

**Table 6. Heat gain from occupants of the house**

| hour | Occupancy factor | $P_{gain}$[kWh] |
|---|---|---|
| 1 | 0.8 | 0.44 |
| 2 | 0.8 | 0.44 |
| 3 | 0.8 | 0.44 |
| 4 | 0.8 | 0.44 |
| 5 | 0.8 | 0.44 |
| 6 | 0.8 | 0.44 |
| 7 | 0.8 | 0.44 |
| 8 | 0.6 | 0.35 |
| 9 | 0.6 | 0.35 |
| 10 | 0.6 | 0.35 |
| 11 | 0.6 | 0.35 |
| 12 | 0.6 | 0.35 |
| 13 | 0.6 | 0.35 |
| 14 | 0.7 | 0.41 |
| 15 | 0.7 | 0.41 |
| 16 | 0.7 | 0.41 |
| 17 | 0.7 | 0.41 |
| 18 | 0.8 | 0.47 |
| 19 | 0.8 | 0.47 |
| 20 | 0.8 | 0.47 |
| 21 | 0.8 | 0.47 |
| 22 | 0.8 | 0.47 |
| 23 | 0.8 | 0.47 |
| 24 | 0.8 | 0.47 |
| **Total** | **0.7** | **10.09** |

The main source of errors in the computation of heat gain arises from poor estimation of occupancy factor. Great care should be taken to be realistic about the allowance for the number of people and period of occupancy in the house.

### 2.1.3.5 The heat gain from electric lighting

Lighting is one of the major internal load components; an accurate estimate of the space heat is needed. Accurate calculation is somewhat difficult since the rate of heat gain at any given moment can be quite different. Generally the rate of heat gain from electric lighting may be calculated by the following formula:

$$Q_{light} = 3.14 \, W_L \, F_u \, F_s \qquad (2.3)$$

$W_L$              total installed wattage
$F_u$              use factor
$F_s = 2.19$       special allowance factor for Fluorescent lamp

**Table 7. Heat gain through lighting system**

| hour | Use factor | Q light [kWh] |
|------|------------|---------------|
| 1 | 0.0 | 0.00 |
| 2 | 0.0 | 0.00 |
| 3 | 0.0 | 0.00 |
| 4 | 0.0 | 0.00 |
| 5 | 0.0 | 0.00 |
| 6 | 0.2 | 1.16 |
| 7 | 0.2 | 1.16 |
| 8 | 0.0 | 0.00 |
| 9 | 0.0 | 0.00 |
| 10 | 0.0 | 0.00 |
| 11 | 0.0 | 0.00 |
| 12 | 0.0 | 0.00 |
| 13 | 0.0 | 0.00 |
| 14 | 0.0 | 0.00 |
| 15 | 0.0 | 0.00 |
| 16 | 0.0 | 0.00 |
| 17 | 0.0 | 0.00 |
| 18 | 0.0 | 0.00 |
| 19 | 0.5 | 2.89 |
| 20 | 0.7 | 4.04 |
| 21 | 0.7 | 4.04 |
| 22 | 0.6 | 3.47 |
| 23 | 0.6 | 3.47 |
| 24 | 0.6 | 3.47 |
| **Total** | **0.2** | **23.68** |

The primary source of heat from lighting comes from the light- emitting elements or lamps.

Compact fluorescent lamps (CLF) are considered in this house. Modern CFLs typically have a life time of between 6,000 and 15,000 hours, whereas incandescent lamps are usually manufactured to have a life time of 750 hours or 1000 hours.

In order to compare the actual energy efficiency of CFLs with various other lamp technologies such as incandescent, LED and halogen, it is necessary to consider their luminous efficacy; including the subjective usefulness of different frequencies of light.

Whilst CFLs are an important development in energy conservation for most lighting, LED lighting may have the potential to compete with CFLs in the near future. LED lamps have current efficiencies of 30% with higher levels attainable, and a lifetime of around 50,000 hours, but currently are struggling to deliver the required domestic light output while maintaining a reasonable working lifespan. Comparisons of cost and energy consumption of LED with the other lamps are shown in the table 8.

**Table 8. Comparison of Cost and energy for LED lamp with others**

|  | Incandescent | CFL | LED |
|---|---|---|---|
| Wattage [W] | 30-50 | 10 - 16 | 1 - 3 |
| Fixture cost | $20 - $100 | $125 - $200 | $30 - $250 |
| lamp life [h] | 3000 - 19000 | 13000 | 10yrs |
| Annual energy use [kWh] | 263 - 438 | 88 - 140 | 26-Sep |
| Annual energy cost | $21 - $35 | $7 - $11 | $0.7 - $2 |
| 10-Year Energy cost | $210 - $350 | $70 - $112 | $7 - $21 |

The above table compares life-cycle costs of the three lamp types, assuming that electricity costs $.08 per kWh, that the cost of purchasing and changing a lamp is $10, and that there are no other maintenance requirements for any of the exit sign types.

### 2.1.3.6    Appliances heat gain

Estimation of heat gain in this category tends to be more subjective than for people and lights. However, considerable data are available in the table 9.

**Table 9. Appliances energy consumption**

| Refrigerator | 0.28 | kWh/day |
|---|---|---|
| Freezer | 0.5 | kWh/day |
| Dishwasher | 1.2 | kWh/application |
| Washing machine | 0.95 | kWh/application |
| Dryer | 0.4 | kWh/application |
| Computer | 1 | kWh/day |
| TV | 0.5 | kWh/day |
| Electric stove | 2 | kWh/day |
| Miscellaneous | 0.5 | kWh/day |
| Total | 6.99 | kWh/day |

As a special feature, the passive house described here was equipped by the appliances with optimized energy consumption which have the best grade of energy certificate.

**Figure 11. Energy labeling for appliances, a) Refrigerator b) Washing machine**
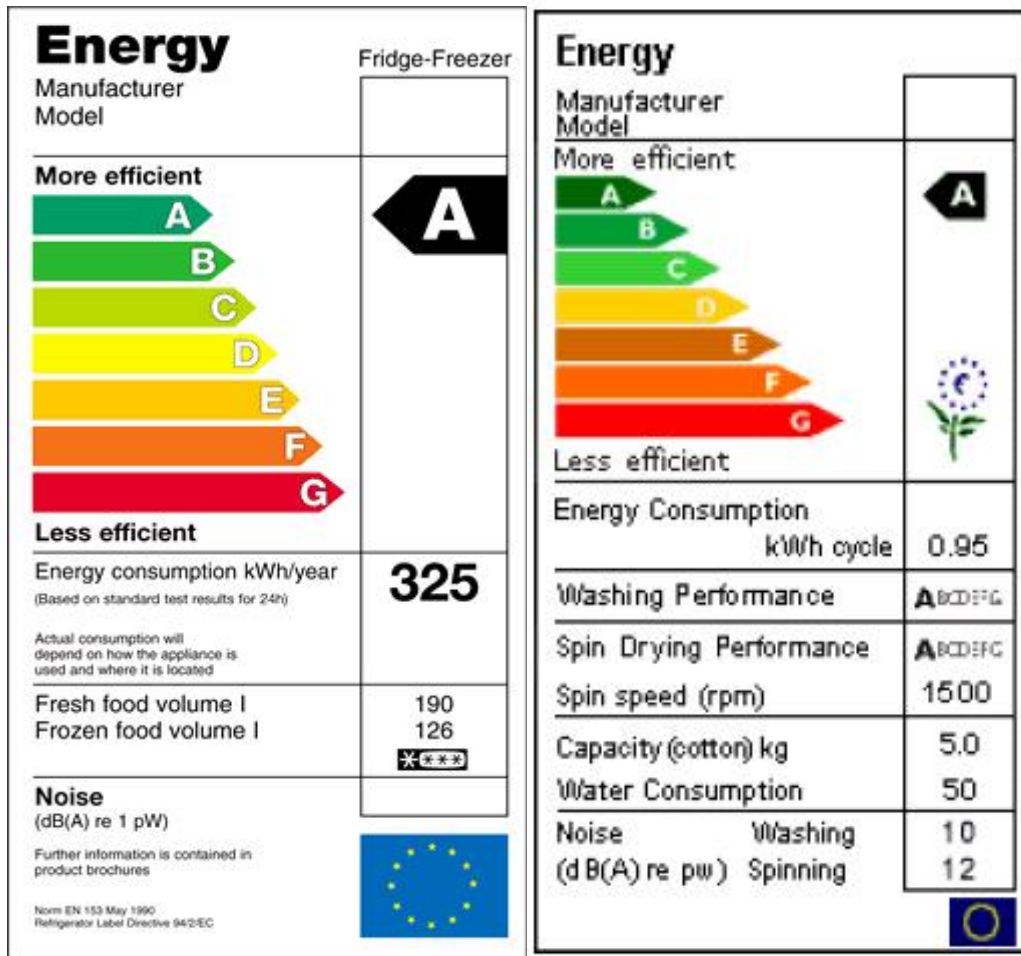
European Union has approved energy labeling in order to improve energy efficiency of appliances. New regulation for energy efficiency is applied for refrigerator, freezer, Dishwasher, clothe washer, dryer and lamps so far. [7]

### 2.1.3.7 Heating energy demand

After calculation of all heat loss and internal heat gain, monthly or annual energy demand can be estimated by subtracting heat gains received by the structure interior from the heat losses experienced by the building.net energy demand is calculated by following equation:

$$Q_{heating} = Q_{heat\ loss} - Q_{solar} - Q_{poeple} - P_{el.appliances} \qquad (2.4)$$

**Table 10. Total heating load demand**

| hour | Q heat loss[kWh] | Q heat gain[kWh] | Q supply[kWh] |
|---|---|---|---|
| 1 | 4,49 | 0,44 | 4,05 |
| 2 | 4,49 | 0,44 | 4,05 |
| 3 | 4,57 | 0,44 | 4,13 |
| 4 | 4,60 | 0,44 | 4,17 |
| 5 | 4,60 | 0,44 | 4,17 |
| 6 | 4,64 | 1,59 | 3,05 |
| 7 | 4,68 | 1,59 | 3,09 |
| 8 | 4,60 | 0,46 | 4,14 |
| 9 | 4,53 | 1,53 | 2,99 |
| 10 | 4,29 | 2,67 | 1,62 |
| 11 | 4,06 | 3,61 | 0,44 |
| 12 | 3,82 | 4,15 | -0,33 |
| 13 | 3,55 | 4,15 | -0,60 |
| 14 | 3,43 | 3,67 | -0,24 |
| 15 | 3,36 | 2,73 | 0,63 |
| 16 | 3,47 | 1,59 | 1,88 |
| 17 | 3,59 | 0,52 | 3,07 |
| 18 | 3,75 | 0,47 | 3,28 |
| 19 | 3,90 | 3,36 | 0,55 |
| 20 | 4,10 | 4,51 | -0,41 |
| 21 | 4,21 | 4,51 | -0,30 |
| 22 | 4,29 | 3,93 | 0,36 |
| 23 | 4,37 | 3,93 | 0,44 |
| 24 | 4,45 | 3,93 | 0,51 |
| Total | 99,86 | 55,12 | 44,74 |

In the next figure the net energy supply is presented. As it can be seen due to internal heat gain in sometimes even don't need to feed energy to the passive house.
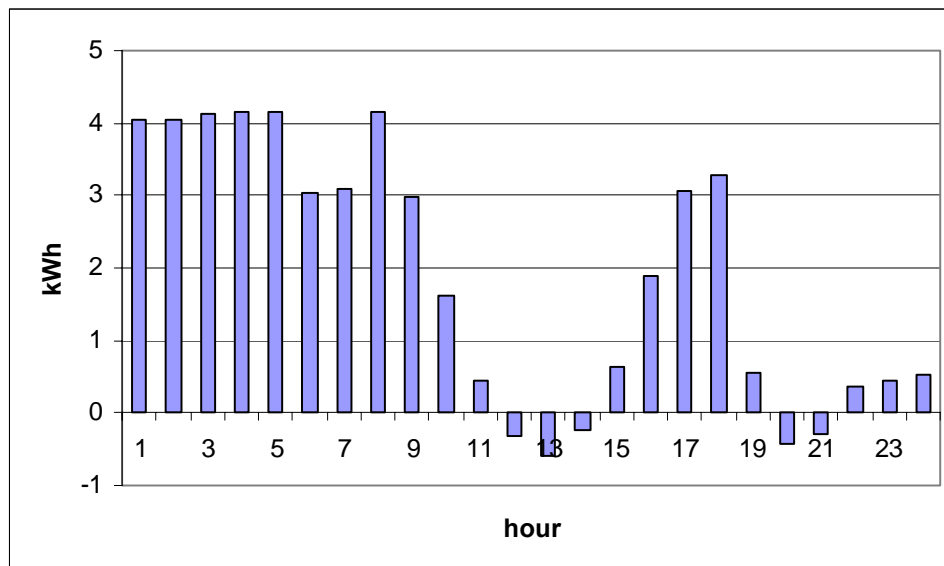


**Figure 12. Required Energy supply in the passive house in a day**

High-efficiency technology has proven itself in this case to be a decisive prerequisite and opportunity for a long-term sustainable energy supply.

**According to the calculation maximum heating peak load will be 5.5 kW and total thermal energy requirement for heating will be 4395.7 kWh per year.**

## 2.2 Solar hot water system

Solar hot water heating for domestic use is one of the most popular and economically feasible applications of solar energy.

Generally, domestic solar water system is installed to meet 100% demand during the year of the required energy.

Solar systems, like any other system, need to be operated with the maximum possible performance. This can be achieved by proper design, construction, installation, and orientation. The orientation of the collector is described by its azimuth and tilt angles. Generally, systems installed in the northern hemisphere are oriented due south and tilted at a certain angle.

The common approach used in excel program to calculate the tilt angle which maximizes the amount of solar radiation received by the collector.

Calculations are carried out in excel file which is given in the following. The system is assumed to operate with a daily hot water load of 50 Lit/person day at 45°C flowing during the day.

**2.2.1    Description of system**

The schematic diagram of the system studied in the present work is shown in Fig.18. It consists of a flat-plate collector, connected to a vertical storage tank. A check valve is added to the pipes connecting the collector and the storage tank to prevent reverse circulation at times of low or no solar radiation. An auxiliary heater and a thermostat are placed in the storage tank, to meet the required load energy when the useful energy gained by the collector is going to be sufficient to meet the load. A daily load of 50 L/person day at a temperature of 45°C was delivered to the user and distributed over a 24-hour period.
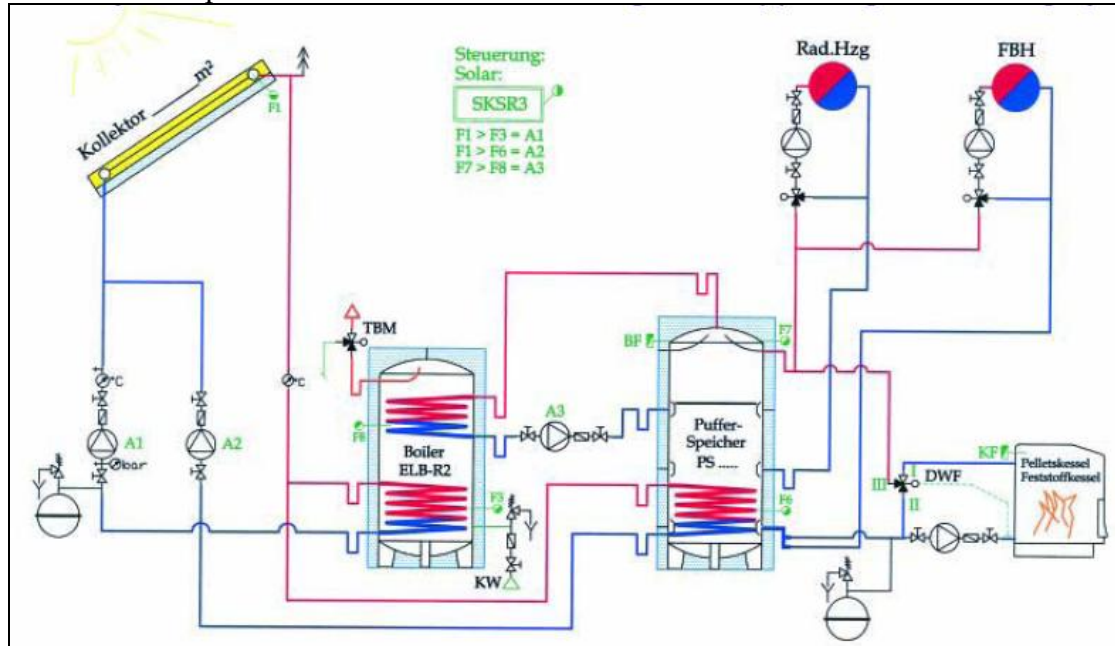


**Figure 13.  Schematic of diagram of considered system [8]**

**2.2.2 Effect of collector area on solar gain**

The case study is sized for meeting the water heating demand for the house, subjected to the climate of the Hvar Island

Parameters, considered in this work as follow:

- The house consist of 4 persons
- Consumption of water is 50 L/person day
- Temperature of fresh water is 15 °C
- Volume of storage tank is 300 kg
- Area of collector is 5 -35 m$^2$
- Required energy is  5.7 kWh/day

Calculation in excel sheet shows the area of collectors extremely depends on solar radiation during a year. Since we are going to fulfill all hot water demand by collectors it needs to be installed in a big area. Figure 17 represent solar gain during a year when the collector area is 35m$^2$.
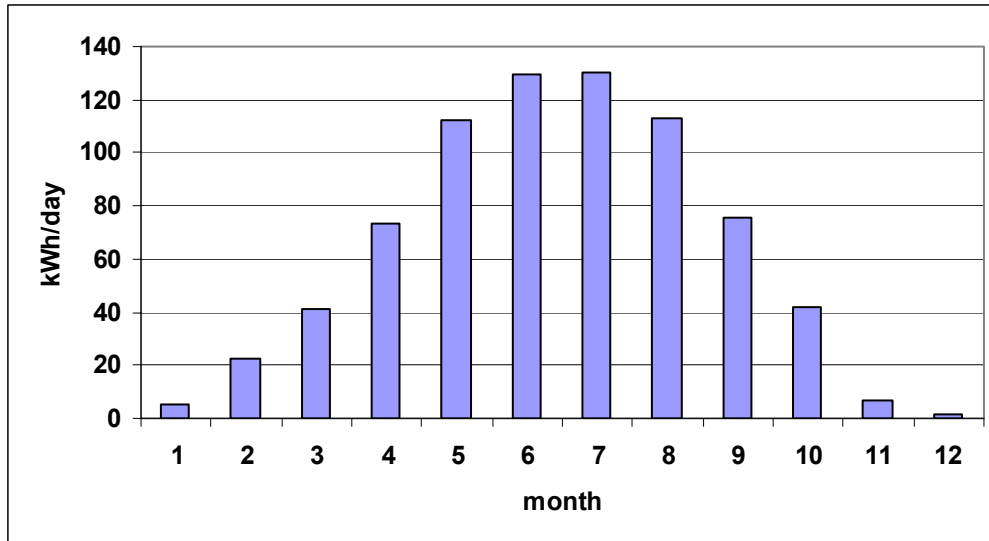
**Figure 14. Solar gain during a year in Hvar Island [20]**

Following table illustrates how much percentage can be covered if we select area of the collector less than 35 m$^2$.

**Table 11. Effect of collector size on solar gain**

| Area [m$^2$] | Percentage |
|---|---|
| 35 | 92 |
| 30 | 84 |
| 25 | 75 |
| 20 | 75 |
| 15 | 75 |
| 10 | 75 |
| 5 | 67 |

This table shows with selecting collector area 10m$^2$, it can be covered more than 75% of total hot water demand. Because of technical problem and economical point of view it is not possible to cover 100% of hot water needed.

## 2.3 Solar cooling system

### 2.3.1 Cooling load calculation

The cooling capacity is calculated based on building location and orientation, building materials, insulation; glazing characteristics, outside temperature, solar radiation through windows and walls, heat accumulation in the walls, internal gains. The cooling load is calculated as a sum of the external cooling load and the internal cooling load same as the way which is done for heating load. But in this situation outside temperature is bigger that inside temperature. Therefore heat transfer direction is from outside to the inside of the house.

### 2.3.1.1  External cooling load

External cooling load is calculated as sum of cooling load through external walls and roofs, cooling load due to transmission through windows, cooling load due to radiation through windows.

Cooling load can be estimated by the following formula:

Q cooling = Q transmission loss + Q heat gains =

$$= [(UA + \rho \, C_p \, V \text{ ventilation}) (T_o - T_i) + (Q_{solar} + Q_{people} + Q_{el. \, appliances})] \, \Delta t \qquad (2.5)$$

Where:

| | |
|---|---|
| $\Delta t$ | time step, hour |
| U | overall heat transfer coefficient, W/(m²°C) |
| A | surface area, m² |
| $\rho$ | density of air at temperature Ti, kg/m³, ($\rho$ =1.2) |
| $C_p$ | specific heat of air , kJ/(kg ºC), ($C_p$ = 1.0 ) |
| V | volumetric flow of ventilation air, m³/s |
| Ti | indoor air temperature, ºC |
| To | outdoor air temperature, ºC |

The result of calculation for month of July is given in the table 12 which shows the transmission loss through the envelope.

**Table 12.  Transmission losses through the envelope of the house in July**

| hours | Ti (°C) | Qloss-walls | Qloss-windows | Qloss-Roof | Qloss-Floor | Qloss[kWh]-Total |
|---|---|---|---|---|---|---|
| 1 | 22,5 | 0,37 | 0,35 | 0,32 | 0,33 | 1,37 |
| 2 | 22 | 0,32 | 0,30 | 0,27 | 0,28 | 1,17 |
| 3 | 21,6 | 0,28 | 0,26 | 0,24 | 0,24 | 1,01 |
| 4 | 22,2 | 0,34 | 0,32 | 0,29 | 0,30 | 1,25 |
| 5 | 21 | 0,21 | 0,20 | 0,18 | 0,19 | 0,78 |
| 6 | 21,5 | 0,27 | 0,25 | 0,23 | 0,23 | 0,98 |
| 7 | 22,1 | 0,33 | 0,31 | 0,28 | 0,29 | 1,21 |
| 8 | 23 | 0,43 | 0,39 | 0,37 | 0,37 | 1,56 |
| 9 | 24,2 | 0,55 | 0,51 | 0,47 | 0,49 | 2,03 |
| 10 | 25,6 | 0,70 | 0,65 | 0,60 | 0,62 | 2,58 |
| 11 | 26,8 | 0,83 | 0,77 | 0,71 | 0,73 | 3,04 |
| 12 | 28,1 | 0,97 | 0,90 | 0,83 | 0,85 | 3,55 |
| 13 | 29,4 | 1,11 | 1,03 | 0,95 | 0,97 | 4,06 |
| 14 | 30,3 | 1,20 | 1,12 | 1,03 | 1,06 | 4,41 |
| 15 | 30,6 | 1,24 | 1,15 | 1,06 | 1,09 | 4,53 |
| 16 | 30,6 | 1,24 | 1,15 | 1,06 | 1,09 | 4,53 |
| 17 | 30,1 | 1,18 | 1,10 | 1,01 | 1,04 | 4,33 |
| 18 | 29,3 | 1,10 | 1,02 | 0,94 | 0,96 | 4,02 |
| 19 | 28 | 0,96 | 0,89 | 0,82 | 0,84 | 3,51 |
| 20 | 26,7 | 0,82 | 0,76 | 0,70 | 0,72 | 3,00 |
| 21 | 25,8 | 0,72 | 0,67 | 0,62 | 0,64 | 2,65 |
| 22 | 24,5 | 0,59 | 0,54 | 0,50 | 0,51 | 2,15 |
| 23 | 23,6 | 0,49 | 0,45 | 0,42 | 0,43 | 1,80 |
| 24 | 23 | 0,43 | 0,39 | 0,37 | 0,37 | 1,56 |
| | | **16,68** | **15,45** | **14,29** | **14,65** | **61,07** |

### 2.3.1.2 Internal cooling load

The internal cooling load of a room is made up of the partial cooling loads due to heat emission from persons, heat emission from equipment, lighting and solar radiation. Since the formula is illustrated in heating load section (2.1.3.1), here just the result of calculation is presented.

In the following table share of each part in cooling load is given.

Table 13. Total cooling load for a day in July

| hour | Solar radiation [kWh/m²] | $Q_{solar}$ [kWh] | $Q_{people}$ [kWh] | $Q_{light}$ [kWh] | $Q_{convection}$ loss [kWh] | Total [kWh] |
|---|---|---|---|---|---|---|
| 1 | 0.0 | 0 | 0.44 | 0 | 1.37 | 1.80 |
| 2 | 0.0 | 0 | 0.44 | 0 | 1.17 | 1.61 |
| 3 | 0.0 | 0 | 0.44 | 0 | 1.01 | 1.45 |
| 4 | 0.0 | 0 | 0.44 | 0 | 1.25 | 1.69 |
| 5 | 0.0 | 0 | 0.44 | 0 | 0.78 | 1.22 |
| 6 | 0.0 | 0 | 0.44 | 1.16 | 0.98 | 2.57 |
| 7 | 0.088 | 1.42 | 0.44 | 1.16 | 1.21 | 4.22 |
| 8 | 0.243 | 3.88 | 0.35 | 0 | 1.56 | 5.79 |
| 9 | 0.422 | 6.74 | 0.35 | 0 | 2.03 | 9.13 |
| 10 | 0.595 | 9.52 | 0.35 | 0 | 2.58 | 12.45 |
| 11 | 0.733 | 11.72 | 0.35 | 0 | 3.04 | 15.11 |
| 12 | 0.809 | 12.93 | 0.35 | 0 | 3.55 | 16.83 |
| 13 | 0.809 | 12.93 | 0.35 | 0 | 4.06 | 17.34 |
| 14 | 0.733 | 11.72 | 0.41 | 0 | 4.41 | 16.54 |
| 15 | 0.595 | 9.52 | 0.41 | 0 | 4.53 | 14.46 |
| 16 | 0.422 | 6.74 | 0.41 | 0 | 4.53 | 11.68 |
| 17 | 0.243 | 3.88 | 0.41 | 0 | 4.33 | 8.62 |
| 18 | 0.088 | 1.42 | 0.47 | 0 | 4.02 | 5.90 |
| 19 | 0.0 | 0 | 0.47 | 2.89 | 3.51 | 6.87 |
| 20 | 0.0 | 0 | 0.47 | 4.04 | 3.00 | 7.52 |
| 21 | 0.0 | 0 | 0.47 | 4.04 | 2.65 | 7.17 |
| 22 | 0.0 | 0 | 0.47 | 3.47 | 2.15 | 6.08 |
| 23 | 0.0 | 0 | 0.47 | 3.47 | 1.80 | 5.73 |
| 24 | 0.0 | 0 | 0.47 | 3.47 | 1.56 | 5.49 |
| Total | 5.785 | 92.42 | 10.09 | 23.68 | 61.07 | 187.26 |

### 2.3.1.3 Cooling load demand

After calculation of all losses and internal heat gain (apply the same terminology), monthly or annual cooling demand can be estimated by including heat gains received by the structure of the building.net energy demand is calculated by following equation:

$$Q_{cooling} = Q_{transmission} + Q_{solar} + Q_{poeple} + Q_{el.appliances} \qquad (2.6)$$

In the Fig.15 profile of total cooling demand during the days in July is presented.
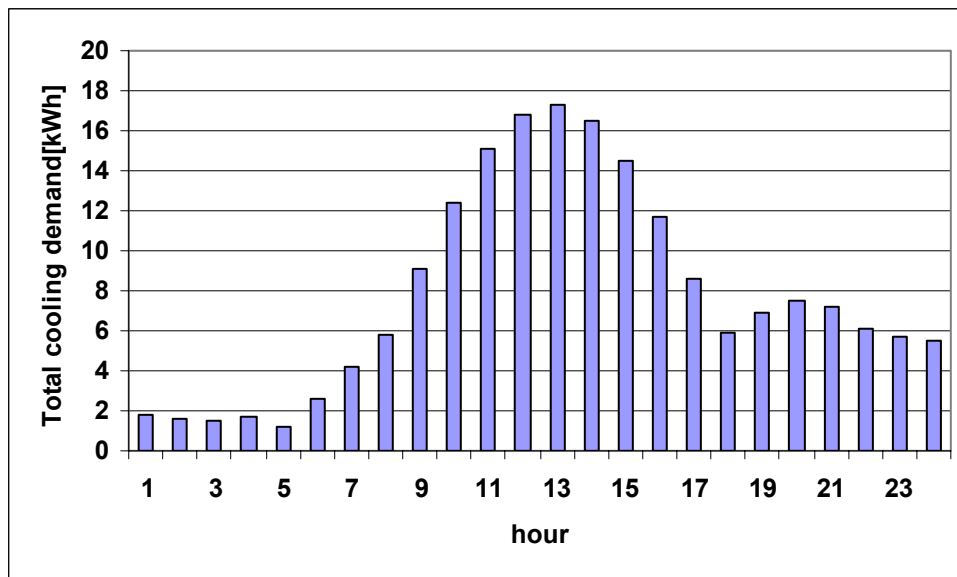
**Figure 15. Total daily cooling load during a month in July**

**Based on calculation of cooling load, maximum peak is 17.3 kW and total cooling load is 5204.07 kWh per year.**

### 2.3.2 Choosing the cooling system for passive house

Main goal of passive cooling system is to create thermal comfort during summer, when over heating may occur. Cooling the building and increasing the comfort zone range is done with as much as possible utilization of natural forces, energies and heat sinks. There are a number of possible solutions available such as:
- Cooling with ventilation
- Evaporative cooling
- Heat pump system
- Dehumidification with a desiccant

According to metrological data, since Hvar has relatively high humidity, cooling with ventilation and evaporative cooling don't work properly and efficiently.
Following figure shows relative humidity during a year in Hvar.
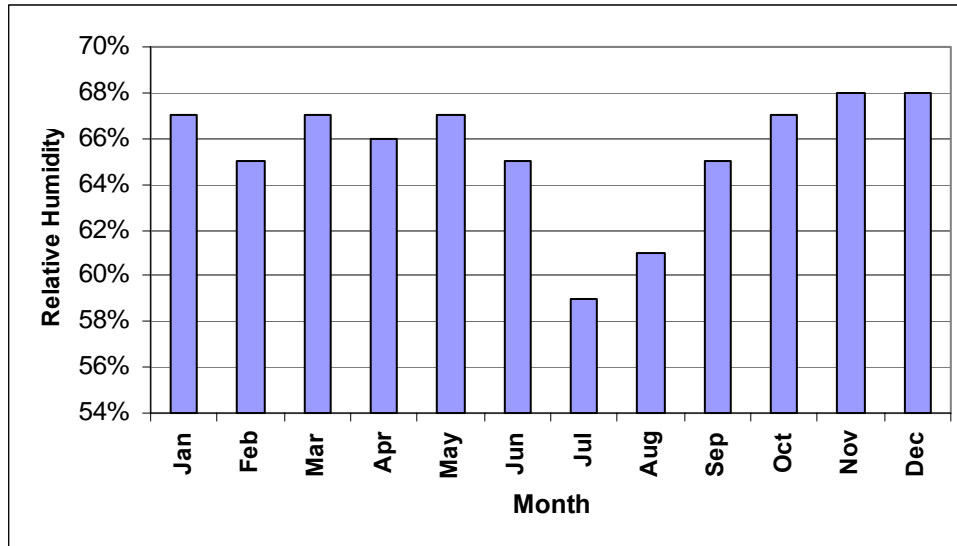
**Figure 16. Relative humidity in Hvar**

The main goal of our system is to meet the cooling loads and reduce the conventional energy consumption by introducing solar heat as the major driving energy source for the system.

A fundamental decision, which is independent of the air- conditioning technology selection, concerns the fraction of solar energy use relative to the entire plant energy needs. The possible options are a solar-driven system with no other heat source and no other cold production devices. Solar energy can be converted directly into electricity using photovoltaic panels, to drive a vapour compression chiller with an electric motor or to install solar thermally driven air conditioning system.
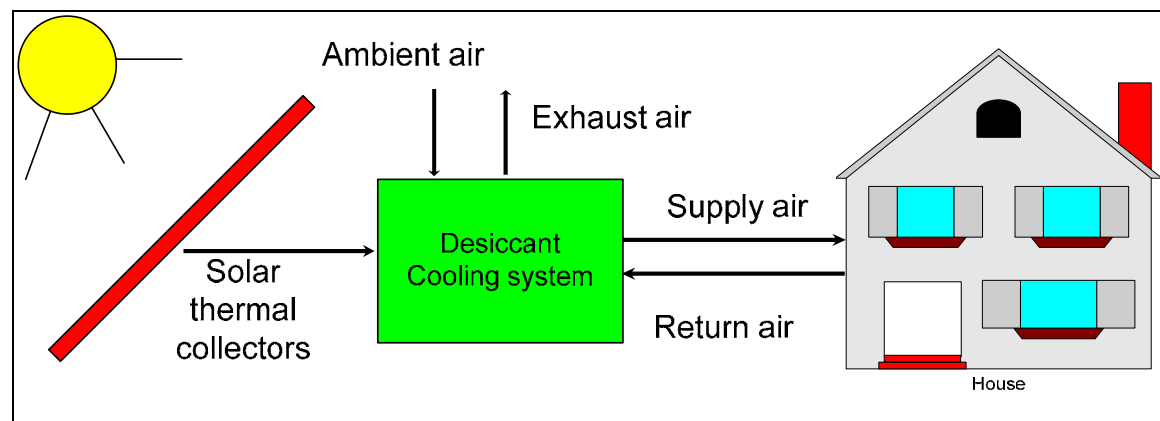


**Figure 17. Basic system scheme**

Thermally driven chiller-based and desiccant systems are key solutions for solar-assisted air conditioning systems. Since among these technology desiccant cooling system is better option for low demand (single family), we are dealing with this system in this section.

Desiccant systems are used to produce conditioned fresh air directly. They are not intended to be used as systems where a cold liquid medium such as chilled water is used for heat removal, e.g., as for thermally driven chiller based systems. Therefore,

they can be used only if the air conditioning systems include some equipment to remove the surplus internal loads by supplying conditioned ventilation air to the building. This air flow consists of ambient air, which needs to be cooled and dehumidified in order to meet the required supply air conditions. Desiccant cooling machines are designed to carry out these tasks. [9]

The most commonly used desiccant cooling process, which is based on the use of desiccant wheels, works as follows (see figure18)

The ambient air (1) is dehumidified in a desiccant wheel, causing the air temperature to increase; the process is nearly adiabatic (2). The regenerator heat recovery leads to cooling of the air inlet to the humidifier, by means of indirect evaporative cooling (3). Depending on the air inlet temperature and humidity supplied, the temperature is reduced by direct evaporative cooling in the humidifier, with a simultaneous increase in humidity up to condition (4). The coil on the supply stream is in operation only for heating condition. The fan releases heat, leading to an increase in the temperature of the supply air, which brings about the supply air condition (5). An increase in temperature of up to 1 °C is usually expected. A proper design of the fan is recommended so as to minimize the heat added to the supply air.

The return air from the room is in state (6). The air is then humidified as close as possible to saturation (7).



**Figure 18. Schematic drawing of a desiccant cooling air handling**

This state is the one which guarantees the maximum potential for indirect cooling of the supply air stream through the heat exchanger for hear recovery. The heat recovery from (7) to (8) leads to an increase in the temperature of the air, which is then used as regeneration air. The air is subsequently reheated in the coil until it reaches state (9). The temperature of the latter is adjusted such as to guarantee the regeneration of the sorption wheel (9to10).

It's important to mention that in many desiccant systems a bypass is installed which allows that some of the air coming from the heat recovery unit bypasses the regeneration air heater and the desiccant wheel. Depending on the actual condition up

to more than 20% of the air can go through the bypass thus saving regeneration heat and also electricity because of the reduced pressure drop along the desiccant wheel.

The COP $_{thermal}$ of a desiccant cooling system is defined as the ratio between the enthalpy change from ambient air to supply air, multiplied by the mass air-flow, and the external heat delivered to the regeneration heater, Q $_{reg}$:

$$COP_{thermal} = m_{supply} (h_{amb} - h_{supply})/Q_{reg} \qquad (2.7)$$

Where:
$m_{supply}$     mass air-flow, kg/s
$h_{amb}$     enthalpy of ambient air, kJ/kg
$h_{supply}$     enthalpy of supply air, kJ/kg
$Q_{reg}$     external heat delivered to the regenerator, kW

The value of COP of a desiccant cooling system depends strongly on the conditions of ambient air, supply air and return air. Under normal design conditions, a COP of about 0.7 is achieved and the cooling power lies in the range of about 5-6 kW per 500 m$^3$/h of supply air.
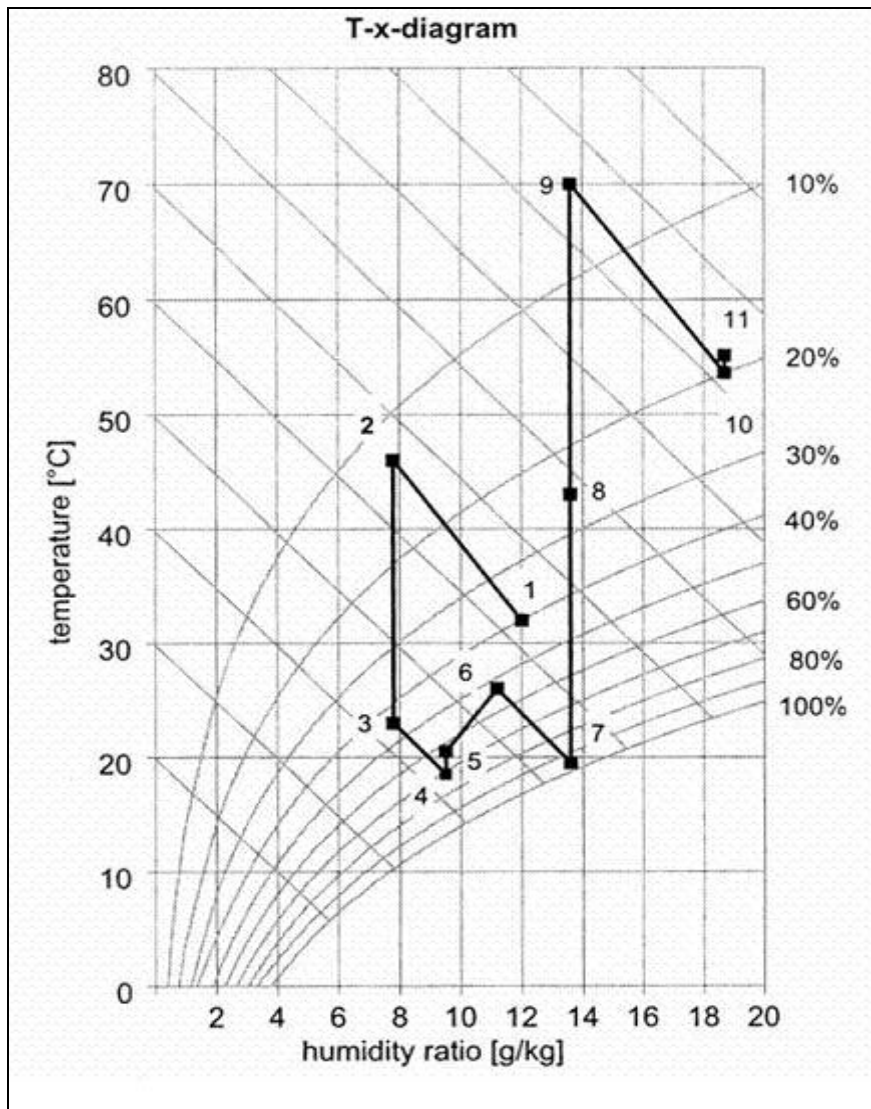
**Figure 19. Typical desiccant cooling process in the T - x diagram (refer to Fig. 18) [9]**

Fresh air conditions have a considerable effect on the amount of cooling that can be achieved. If the outdoor air is properly pretreated, the ventilation air can be cooled to lower temperatures via subsequent indirect and direct evaporative cooling.

### 2.3.3 Specification of selected desiccant system

A desiccant-based air conditioning system is a hybrid system of desiccant dehumidification, evaporative cooling, refrigeration, and regeneration systems to cool and dehumidify the space air and maintain it at a required temperature and relative humidity with adequate outdoor ventilation air, at the same time improving the efficiency of energy use.

According to total demand calculation the maximum cooling load is 7.8 kW. So the following system could be suitable for our model.
The conditioned space occupies an area of about 144 m$^2$. The system was selected according to the calculated cooling and heating loads of the conditioned space.
Main operating parameters:

Area of collector: 35m$^2$
Cooling capacity: 10 kW
Desiccant: composite silica-gel
Power of motor for desiccant wheel: 120 W
Power of cooling power pump: 300 W
Ventilation rate of conditioned space: 500 m$^3$/h

## 2.4 Transport system

For transport system a pickup truck was considered to serve the family. (Fig. 20)



**Figure 20. Hydrogen engine pickup truck [10]**

The advantages of fuel cell car are:
- Professional engine calibration
- Pure hydrogen fuel resulting in zero hydrocarbon emissions
- Burns clean Hydrogen today!

Specification of this car is given in table 14.

**Table 14. Specification of fuel cell car**

| Type of the car | | Pick up Truck |
|---|---|---|
| Motor | Max output | 146 kW |
| | Type | AC synchronous motor |
| Fuel cell stack | Type | PEFC(Proton exchange membrane) |
| | Output | 150 kW |
| Fuel | Type | Compressed hydrogen |
| | Storage: | High pressure hydrogen tank (350bar) |
| | Tank capacity | 150 L |
| Max. speed | | 160 km/h |
| Energy storage | | Lithium ion battery |
| Fuel Economy | | 22.5 km/kg City/ 32.3kg Highway |
| Vehicle range | | 237-339 km |

Based on consumption of the car and our assumption for driving which is 45 km per day, total demand for hydrogen is 2 kg/day.

## 2.5    Power system

In order to determine energy consumption of the building, it needs to analyze heating, cooling and electrical energy demand and consumption.

Cooling load is met by desiccant cooling system. Heating load is fulfilled by solar hot water system. Also heat generated during fuel cell and electrolyser operation can be used as heating source. But it is not considered in this work because of increasing complexity caused by different temperature levels of these various heat sources. The special consideration in this direction should be done in further development of this project. In fact, for heating and cooling static simulation (calculation) has been performed instead of dynamic simulation. In part 2.1.3 has been calculated and presented in excel table for heating demand (static simulation). In part 2.3.1 cooling load has been calculated.

In this study in order to minimize the level of modeling and simulation complexity, just electrical part has been modeled and result of dynamic simulation has been presented (Fig. 21).
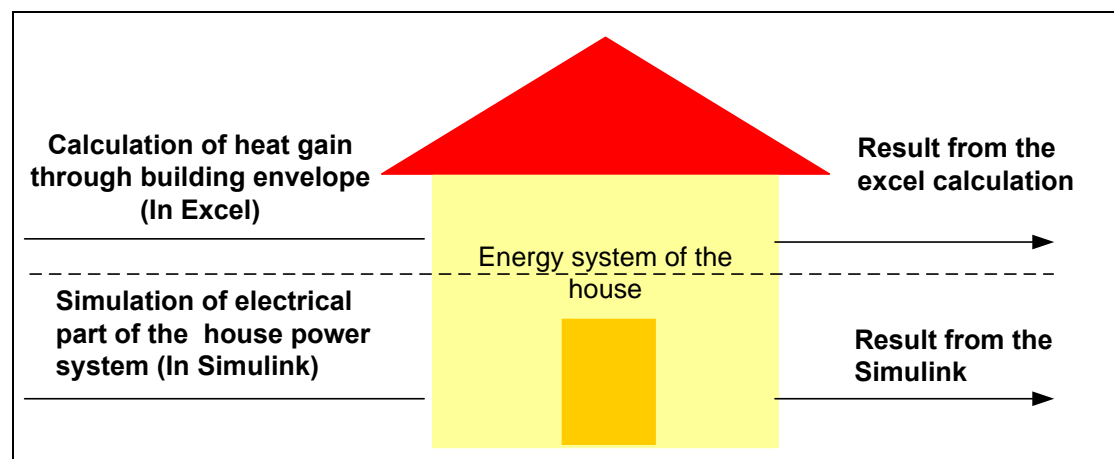


**Figure 21.  Schematic of calculation of the whole energy system of the house**

Also, even though transport necessities have been discussed in parts 2.4, 3.2.4, amount of hydrogen needed for transport purpose and appropriate PV modules area have not been specially considered during simulations because a) transport vehicle is filled with hydrogen manually and b) because overall optimization of the PV field area and hydrogen tank volume was not performed.  Further work should be done concerning this problem.

In the next chapter only mathematical models and dynamical simulation of electrical part of the house energy system (Fig. 2) is presented.

# 3 Synthesis and analysis of the power system

## 3.1 Power system components overview

### 3.1.1 Photovoltaic cell, module, array

A typical silicon PV cell is composed of a thin wafer consisting of an ultra-thin layer of phosphorus-doped (N-type) silicon on top of a thicker layer of boron-doped (P-type) silicon. An electrical field is created in the cell where these two materials are in contact, called the P-N junction. When sunlight strikes the surface of a PV cell, this electrical field provides momentum and direction to light-stimulated electrons, resulting in a flow of current when the solar cell is connected to an electrical load.
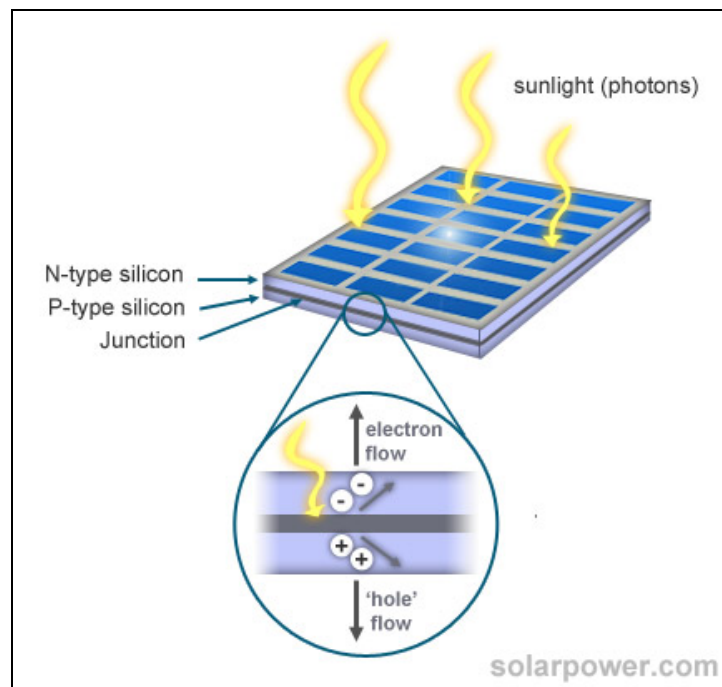


**Figure 22. principle of photovoltaic system**

Regardless of size, a typical silicon PV cell produces about 0.5 – 0.6 volt DC under open-circuit, no-load conditions.

**Figure 23. Solar cell, module, panel, array**

The current (and power) output of a PV cell depends on its efficiency and size (surface area), and is proportional the intensity of sunlight striking the surface of the cell. For example, under peak sunlight conditions a typical commercial PV cell with a surface area of 160 cm$^2$ will produce about 2 watts peak power. If the sunlight intensity were 40 percent of peak, this cell would produce about 0.8 watts. Photovoltaic modules can be placed on 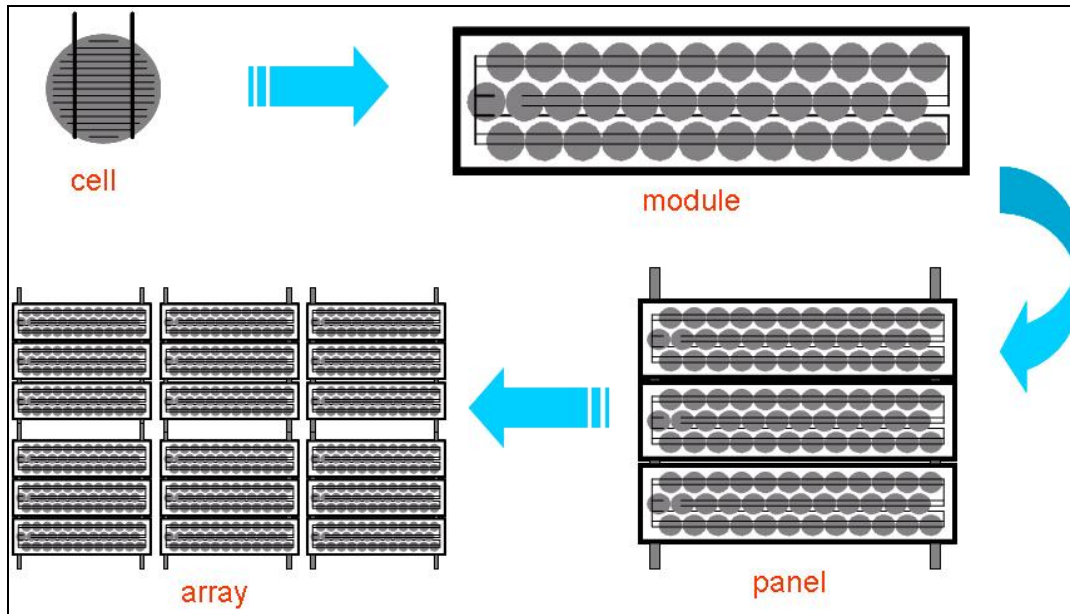almost any building surface which receives sunshine for most of the day. Roofs are the usual location for PV systems on houses.

A PV generator can contain several arrays. Each array is composed of several solar cells.

The area required for mounting a PV array depends on the output power desired and the type of module used. An area of around 8 m$^2$ will be required to mount an array with a rated power output of 1kW, if mono-crystalline modules are used (the most efficient modules type). If multi-crystalline modules are used an area of around 10 m$^2$ will be required for a 1kWp system. These areas can be scaled up or down depending on the output power desired. 1- 3 kWp is a typical power output for a domestic system, although smaller or larger systems can be installed.
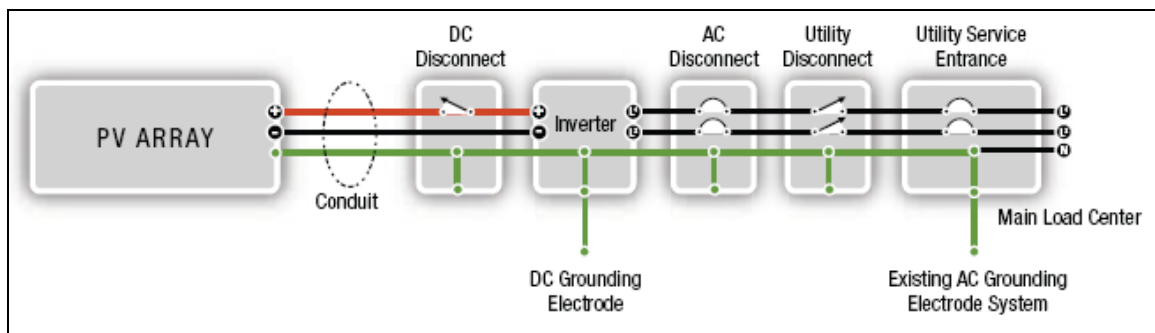


**Figure 24.  Schematic diagram of a typical residential PV system**

The operation of a PV-cell also depends on the circuit in which it is connected. When the resistance of the circuit, connected between the terminals of the cell, is zero (R =

0), the voltage difference is small. In this case, the current flowing in the circuit is known as the short-circuit current (Isc). When the resistance of the circuit is very large (R = ∞), the current is small and the voltage between the cell's terminals is known as the open-circuit voltage (Voc). The short-circuit current (Isc) and the open-circuit voltage (Voc) are both shown in Fig.26. The current in an ideal PV-cell is equal to the short-circuit current (I = Isc) and as the voltage approaches the open-circuit voltage (Voc), it decreases rapidly.



**Figure 25.  Photovoltaic Panels**

The power produced by a PV-cell (P = IV) is greatest at the point (Imp, Vmp) where mp is maximum power.

This is the point on the IV-curve where the area of a rectangle drawn beneath the curve, i.e.: IV is the greatest. From below figure, it can be seen that this point is on the "knee" of the IV-curve. The quality of a cell's semiconductor junction can be described by the fill factor (FF), which is the ratio of the cell's maximum power to the product of the short circuit current and open-current voltage.

The fill factor is defined as    $FF = I_{mp} \, V_{mp} / I_{sc} \, V_{oc}$

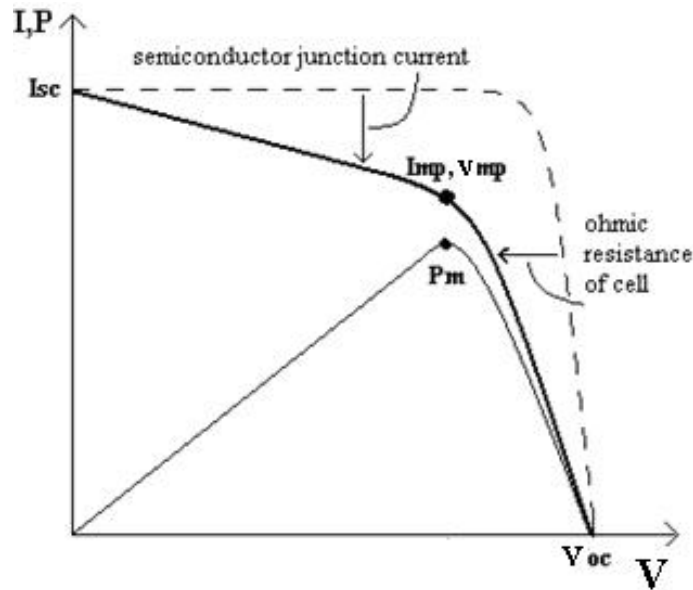**Figure 26. The produced current (thick line) and power (narrow line) in a PV-cell as a function of voltage. The ideal IV-curve is represented as the dash-line.**

The closer the value of the fill factor is to unity, the better the operation of the PV-cell. The fill factor is lowered by the ohmic resistance of the cell. When the temperature of a cell increases, both the short-circuit voltage and fill factor decrease.

The efficiency ($\eta$) of a PV-cell is defined as    $\eta = P_m / GA$

Where A is the active surface area of the cell and $P_m$ is the maximum power. The efficiency varies from 5 to 18%, depending on the construction and materials used in the cell.

As for every technology there is always a balancing set of characters for the positive and negative side of PV Modules. For any application we must weigh between them to check their suitability for the specific reasons there are to be utilized. In general their advantages and disadvantages are respectively:

**Advantages:**

− Production of high quality electrical power (better than utility power in most cases),

− On-site green power production – absolutely no emissions,

− Longevity, 20-30 year lifetime for most components, some will last longer,

− Reliability, long periods between regular maintenance, 6-12 months,

− Provision of an uninterrupted power supply

− Silent & low maintenance, replaces noisy & unreliable generators,

− Solid State, no moving parts, nothing to break,

− Available anywhere in the world where there is light, (even if no direct sun!)

− Transportable, lightweight, good for mobile applications,

− Modular-expandable & easily up-gradable.

**Disadvantages:**

− High initial cost

− Higher overall cost depending on situation

### 3.1.2    Electrolyser and electrolysis

Water Electrolysis is a very simple process that takes water and passes a supply of electricity through it using immersed electrodes to split into positive hydrogen (H+) and negative oxygen (O-) ions. These hydrogen and oxygen ions migrate through the water towards the cathode and anodes respectively, where electron transfers allow for the diatomic $H_2$ and $O_2$ molecules to form at high purity.
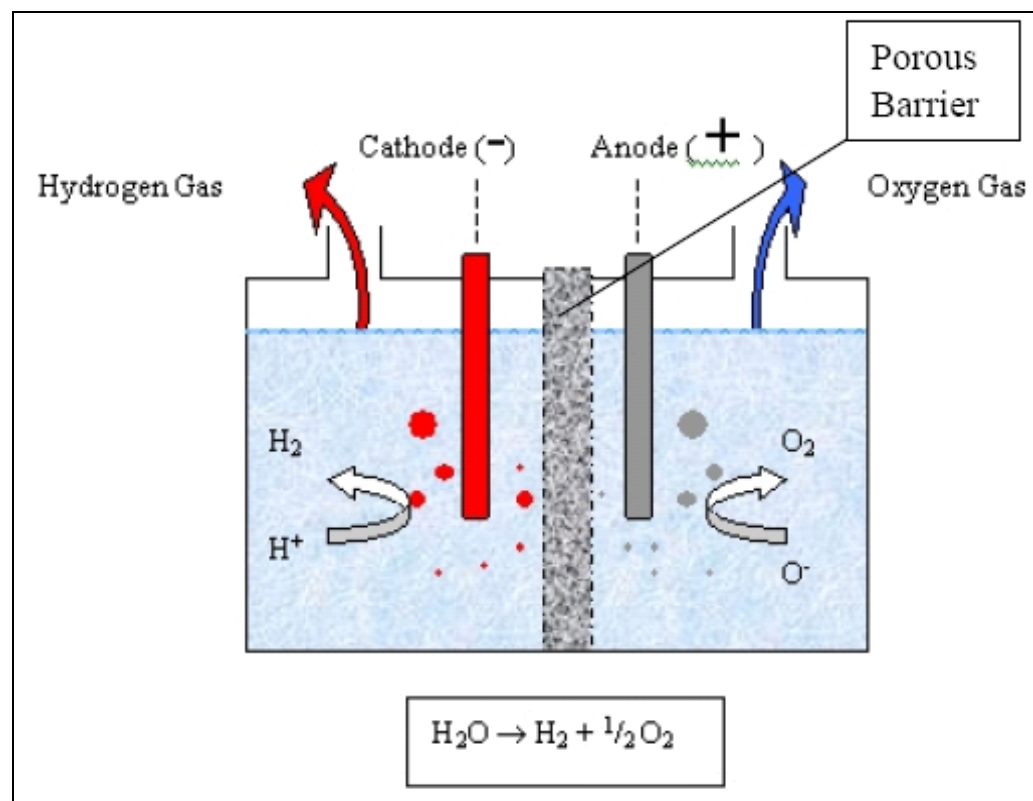


**Figure 27.  Water electrolyser**

A porous barrier or salt bridge is placed in the tank where the electrolysis process takes place. It must be added to the system in order to allow the current flow.
Both the porous barrier and the salt bridge contain an ionic substance in solution. It is used to prevent the quick mixing of various solutions, while permitting the exchange of ions.

Electrolysis of hydrogen is currently around 75% energy efficient and could be theoretically increased to more than 90 % in the future [11]. Therefore this process appears to be an efficient method of producing high purity hydrogen in large

quantities with little or no environmental impact. However the electrical energy required in running such a process would have to come from renewable power sources such as wind, photovoltaic, hydroelectric or geothermal generators for it to be truly environmentally friendly and sustainable in the future as it comes from photovoltaic system in our study.

Considering a most effective strategy regarding the supply of hydrogen to the consumer, water electrolysis from non fossil fuel power generation is appointed as the preferred method of hydrogen production.

The electrolysers that are based on Polymer – Electrolyte Membrane (PEM) separators and alkaline (referring to the nature of its liquid electrolyte), can be used for this study, because they can achieve high efficiencies.
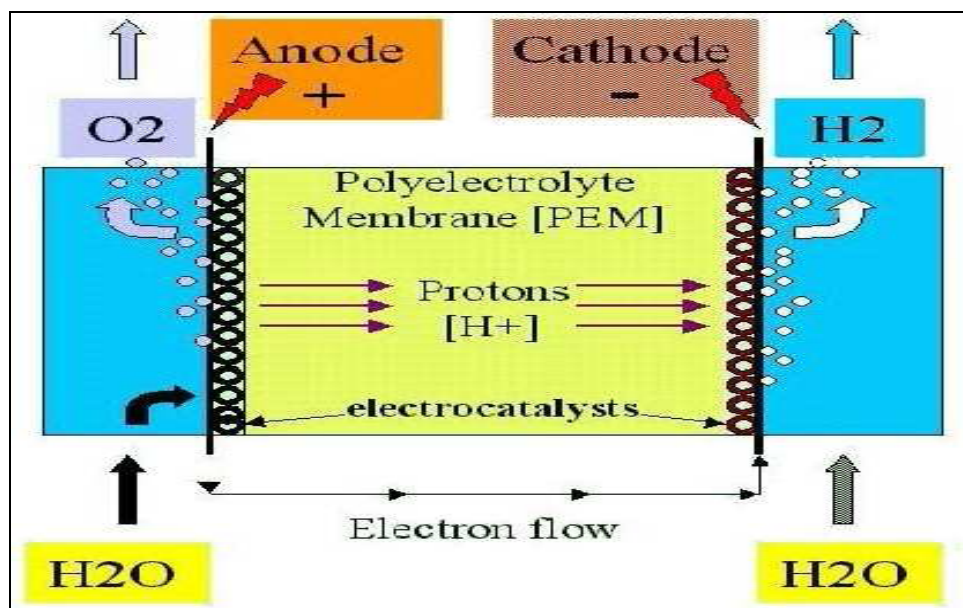


**Figure 28. Schematic Diagram of a Proton Exchange Membrane Electrolyser**

Water electrolysis [11] takes place in the electrolyser (Fig. 28), whereby electrical energy drives the electrolysis of a water molecule to its elementary components, oxygen and hydrogen:

$$2H_2O \rightarrow 2H_2 + O_2 \qquad (3.1)$$
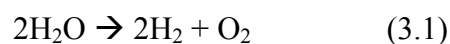
The quantity of released hydrogen on the electrolyser cathode is, according to the Faraday 1st law, dependent on the amount of charge flowing through the electrolyser, $I$, during time $t$:

$$I\,t = z\,F\,n \qquad (3.2)$$

Where:

$z = 2$        - number of released electrons per $H_2O$ molecule
$F = 96500$       - Faraday's constant, C/mol
$n$           - The quantity of released hydrogen, mol

The I –*V* characteristic of electrolyser as a function of current density is shown in the Fig.29.



**Figure 29. Typical I-V curve for an electrolyser at high and low temperature [12]**

Water electrolysis to produce gaseous hydrogen and oxygen is a long-established process. The water electrolyser essentially takes in pure water and dc electricity and outputs H2 and O2; it is the reverse of a hydrogen fuel cell.

There are three principal types of water electrolyser:- alkaline (referring to the nature of its liquid electrolyte), proton-exchange membrane (referring to its solid polymeric electrolyte), and solid-oxide (referring to its solid ceramic electrolyte).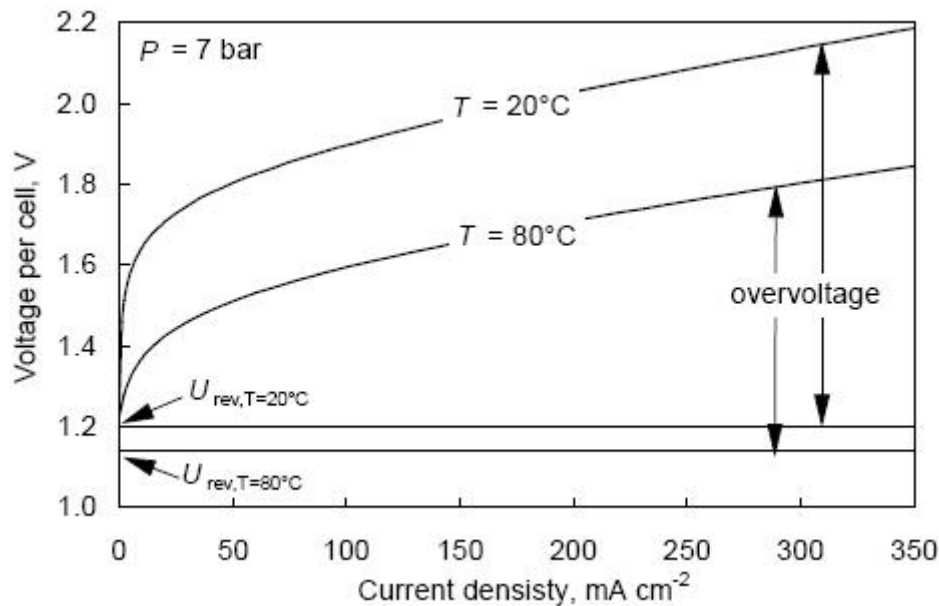 The alkaline and PEM electrolysers are well proven devices with thousands of units in operation, while the solid-oxide electrolyser is as yet unproven. The PEM electrolyser is particularly well suited to highly distributed applications. The alkaline electrolyser currently dominates global production of electrolytic hydrogen.

### 3.1.3 Hydrogen and hydrogen storage tank

Hydrogen is characterized by a very low boiling point (-253°C) and a low density at normal condition (0.08245 kg/m$^3$). Therefore, at ambient conditions hydrogen only exists as a gas.

Hydrogen has a very high energy content by weight (about three times more than gasoline), but it has a very low energy content by volume (liquid hydrogen is about four times less than gasoline). This makes hydrogen a challenge to store,
Developing safe, reliable, compact, and cost-effective hydrogen storage technologies is one of the most technically challenging barriers to the widespread use of hydrogen as an energy carrier.

Hydrogen can be stored mechanically and/or chemically. Apart from storage in chemical compounds, the four basic hydrogen storage concepts are [12]:

- Liquid hydrogen (LH$_2$) storage
- Adsorber storage (e.g., H$_2$ in superactivated carbon, H2 in carbon nanostructures)
- Metal hydride (MH) storage (H$_2$ in metal alloys)
- Pressurized hydrogen (PH2) gas storage

Metal hydrides are very attractive for hydrogen storage in consideration of their inherent safety and good performance characteristics.
This system is able to store hydrogen inside of the metallic structure of the hydride: it's a more compact and safe solution in comparison with the traditional high pressure bottles.

An alternative design is to store the hydrogen in a near-ambient temperature and atmospheric metal hydride (MH) storage. One advantage of the MH-storage is that requires less space than a 120 bar pressure vessel with the same capacity. However, the greatest advantage of the MH-storage is that it can be coupled directly to a low-pressure electrolyser, thus eliminating the need for a compressor [12].

### 3.1.4    High pressure compressor

A compressor is needed in the model to compress hydrogen from a short-term low-pressure H2-tank up to a long-term high pressure H2-storage in order to be used for hydrogen based car.
Compressed gaseous hydrogen can be stored either in aboveground portable or stationary tanks. Hydrogen, produced by electrolysis of water, is compressed to a high pressure to refill a car with a working pressure of 350 bar.

### 3.1.5    PEM Fuel Cell

Fuel cells are electrochemical devices that convert the chemical energy of a reaction directly into electrical energy. The basic physical structure or building block of a fuel cell consists of an electrolyte layer in contact with a porous anode and cathode on either side. A schematic representation of a fuel cell with the reactant/product gases and the ion conduction flow directions through the cell is shown in Fig. 30.
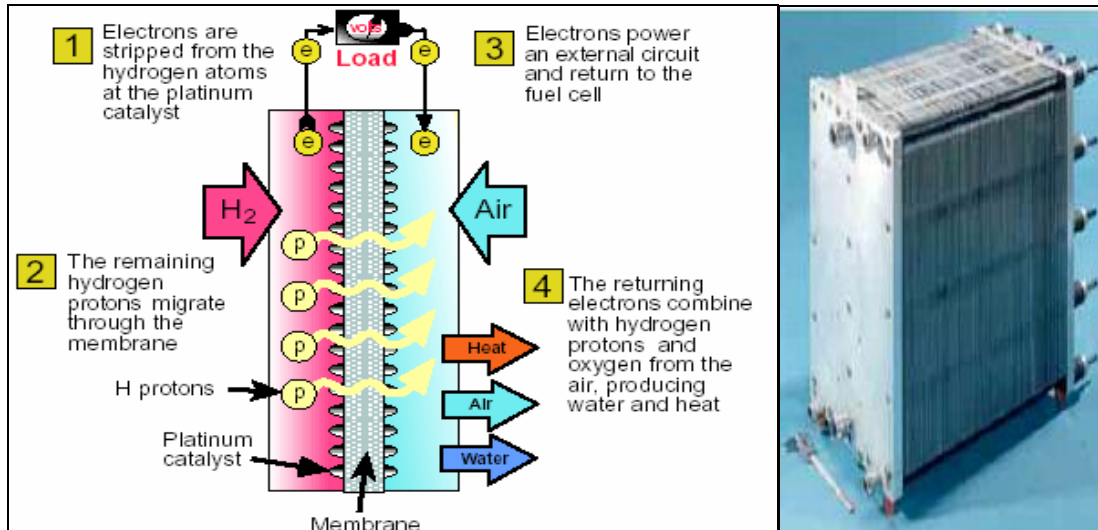
**Figure 30. Schematic of Fuel Cell [20]**

In a typical fuel cell, gaseous fuels are fed continuously to the anode (negative electrode) compartment and an oxidant (i.e., oxygen from air) is fed continuously to the cathode (positive electrode) compartment; the electrochemical reactions take place at the electrodes to produce an electric current.

The most common classification of fuel cells is by the type of electrolyte used in the cells and includes:

− Polymer Electrolyte Fuel Cell (PEFC) or Proton Exchange Membrane Fuel Cell (PEMFC)
− Alkaline Fuel Cell (AFC)
− Phosphoric Acid Fuel Cell (PAFC)
− Molten Carbonate Fuel Cell (MCFC)
− Intermediate Temperature Solid Oxide Fuel Cell (IT SOFC), and
− Tubular Solid Oxide Fuel Cell (T SOFC)

A variety of fuel cells are in different stages of development. They can be classified by use of diverse categories, depending on the combination of type of fuel and oxidant, whether the fuel is processed outside (external reforming) or inside (internal reforming) the fuel cell, the type of electrolyte, the temperature of operation, whether the reactants are fed to the cell by internal or external manifolds, etc.

These fuel cells are listed in the order of approximate operating temperature, ranging from ~80°C for PEMFC, ~100°C for AFC, ~200°C for PAFC, ~650°C for MCFC, ~800°C to 1000°C for SOFC. The operating temperature and useful life of a fuel cell dictate the physicochemical and thermo-mechanical properties of materials used in the cell components (i.e., electrodes, electrolyte, interconnect, current collector, etc.).

Following table shows major differences of the fuel cell types.

**Table 15.  Comparison of five fuel cell technologies [20]**

| Fuel Cell | Electrolyte | Operating Temperature (°C) | Electrochemical Reactions |
|---|---|---|---|
| Polymer Electrolyte/ Membrane (PEM) | Solid organic polymer poly-perfluorosulfonic acid | 60 - 100 | Anode: $H_2 \rightarrow 2H^+ + 2e^-$ <br> Cathode: $\frac{1}{2}O_2 + 2H^+ + 2e^- \rightarrow H_2O$ <br> Cell: $H_2 + \frac{1}{2}O_2 \rightarrow H_2O$ |
| Alkaline (AFC) | Aqueous solution of potassium hydroxide soaked in a matrix | 90 - 100 | Anode: $H_2 + 2(OH)^- \rightarrow 2H_2O + 2e^-$ <br> Cathode: $\frac{1}{2}O_2 + H_2O + 2e^- \rightarrow 2(OH)^-$ <br> Cell: $H_2 + \frac{1}{2}O_2 \rightarrow H_2O$ |
| Phosphoric Acid (PAFC) | Liquid phosphoric acid soaked in a matrix | 175 - 200 | Anode: $H_2 \rightarrow 2H^+ + 2e^-$ <br> Cathode: $\frac{1}{2}O_2 + 2H^+ + 2e^- \rightarrow H_2O$ <br> Cell: $H_2 + \frac{1}{2}O_2 \rightarrow H_2O$ |
| Molten Carbonate (MCFC) | Liquid solution of lithium, sodium and/ or potassium carbon-ates, soaked in a matrix | 600 - 1000 | Anode: $H_2 + CO_3^{2-} \rightarrow H_2O + CO_2 + 2e^-$ <br> Cathode: $\frac{1}{2}O_2 + CO_2 + 2e^- \rightarrow CO_3^{2-}$ <br> Cell: $H_2 + \frac{1}{2}O_2 + CO_2 \rightarrow H_2O + CO_2$ <br> (CO$_2$ is consumed at cathode and produced at anode) |
| Solid Oxide (SOFC) | Solid zirconium oxide to which a small amount of ytrria is added | 600 - 1000 | Anode: $H_2 + O^{2-} \rightarrow H_2O + 2e^-$ <br> Cathode: $\frac{1}{2}O_2 + 2e^- \rightarrow O^{2-}$ <br> Cell: $H_2 + \frac{1}{2}O_2 \rightarrow H_2O$ |

The type of fuel cell currently receiving the most attention is the PEM fuel cell; PEM stands variously for "proton exchange membrane" or "polymer electrolyte membrane".

The fuel cell types have significantly different operating regimes. As a result, their materials of construction, fabrication techniques, and system requirements differ. These distinctions result in individual advantages and disadvantages that govern the potential of the various cells to be used for different applications.
Fuel cells have many characteristics that make them favorable as energy conversion devices. The advantages that fuel cells and fuel cell plants offer are:

- Direct energy conversion (no combustion)
- No moving parts in the energy converter
- Quiet
- Demonstrated high availability of lower temperature units
- Sitting ability
- Fuel flexibility
- Demonstrated endurance/reliability of lower temperature units
- Good performance at off-design load operation
- Modular installations to match load and increase reliability
- Remote/unattended operation
- Size flexibility
- Rapid load following capability

General negative features of fuel cells include:

- Market entry cost high
- Unfamiliar technology to the power industry
- No infrastructure

The overall performance of the PEM fuel cell can be improved by increasing one (or all) of the following conditions (with typical values in parenthesis): (1) Temperature of the PEM (20–80°C), (2) Hydrogen and/or oxygen pressure (1–5 bar), (3) Flow rates of hydrogen and air (2–2.5 times stoichiometry), and (4) Oxygen concentration in oxygen-mixtures (80% in air)
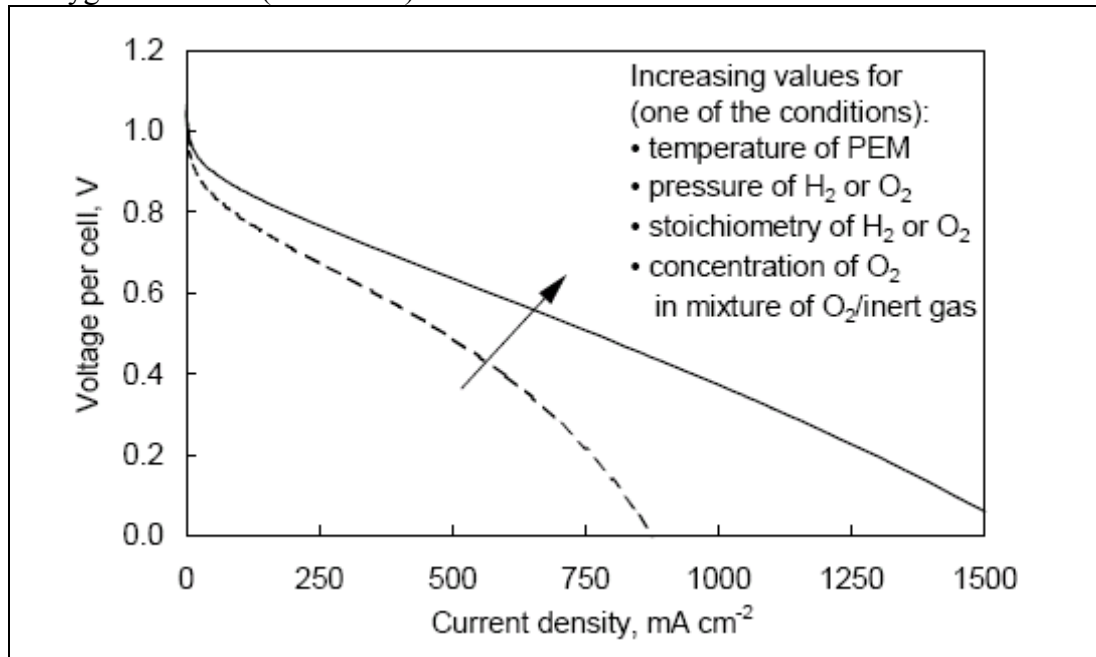


**Figure 31. The influence of increasing values for temperature, pressure, and reaction conditions (varied one at a time) on the *I–U* curve for a typical H2/O2 PEM fuel cell [12]**

### 3.1.6    Battery as electricity storage

The battery is typically used in photovoltaic-hydrogen system. In our system battery has priority because it has less inefficiency comparing to the fuel cell. Neither electrolyser nor fuel cell can start without electricity, therefore battery should be considered in the system. The key physical properties of the battery are its nominal voltage, capacity curve, lifetime curve, minimum state of charge. The capacity curve shows the discharge capacity of the battery in ampere-hours versus the discharge current in amperes. Manufacturers determine each point on this curve by measuring the ampere-hours that can be discharged at a constant current out of a fully charged battery.

The term state of charge SOC is used as an indication of the depth to switch the battery charge. The minimum state of charge is the state of charge below which the battery must not be discharged to avoid permanent damage.

 It is obvious that as long as the battery state of charge SOC is high the battery voltage is high. When the battery continually discharges, its voltage decreases gradually.

### 3.1.7    MPP tracker and DC/DC converters

If a DC/DC-converter is connected directly to a PV array with the purpose of finding the maximum operation power (for given solar irradiation intensity), it is called a maximum power point tracker (MPPT). In an actual system, the MPPT is an external device to the PV array. Numerically, the MPPT model always finds the maximum power point of the PV array *I–U* curve.
Output from MPP tracker is therefore momentary available power. When this power is transferred to the load, certain losses will occur, but generally efficiency of MPP tracker is about 0.95 (In this work MPP tracked efficiency is assumed to be one). In this work loads or electrical loads are supposed to be ohmic resistance type. Also under such assumption next equations are valid:

$$P_{pv} \text{ (at MPP)} = \eta_{MPP}.P_{load} \qquad\qquad (3..3)$$

$$P_{load} = R_{load}\, I_{load}{}^2 \qquad\qquad (3.4)$$

By known the load resistance ($R_{load}$) and PV power at MPP appropriate working voltage will be established.
Real electrical design of the MPP trackers which should ensure realisation of above equations are the question beyond of this work [21]. Here is supposed that certain electrical ohmic load use all available power with current and voltage in accordance with working characteristic of that load. There are supposed three main electrical loads: appliances, electrolyser and battery. In part 3.2.7 of this work, DC/DC converter will be further described.

### 3.1.8    Control system objective

The main objective of the control strategy is to utilize excess renewable energy (RE) in system to charge short- and/or long-term energy storage. And opposite, if there is deficit RE energy the system's control strategy decides whether to use long- or short term energy storage to supply the load. In order to fulfill these choices, the *state of system* must be known at all time. The control strategy of this study includes *hydrogen state of charge* (H2 soc), battery *state of charge* (SOC), in addition, weather/load prediction and actual power balance in system could be taken into account.

The electric power produced by the PV modules is managed by a control of electrical part of power system. It sends the power to the different elements of the system following a pre-defined priority order. The power request of the user has the first priority (batteries). The excesses of power are sent to the electrolyser to produce hydrogen (storage tank).

Actually all power system must include a control strategy that describes the interactions between its components.
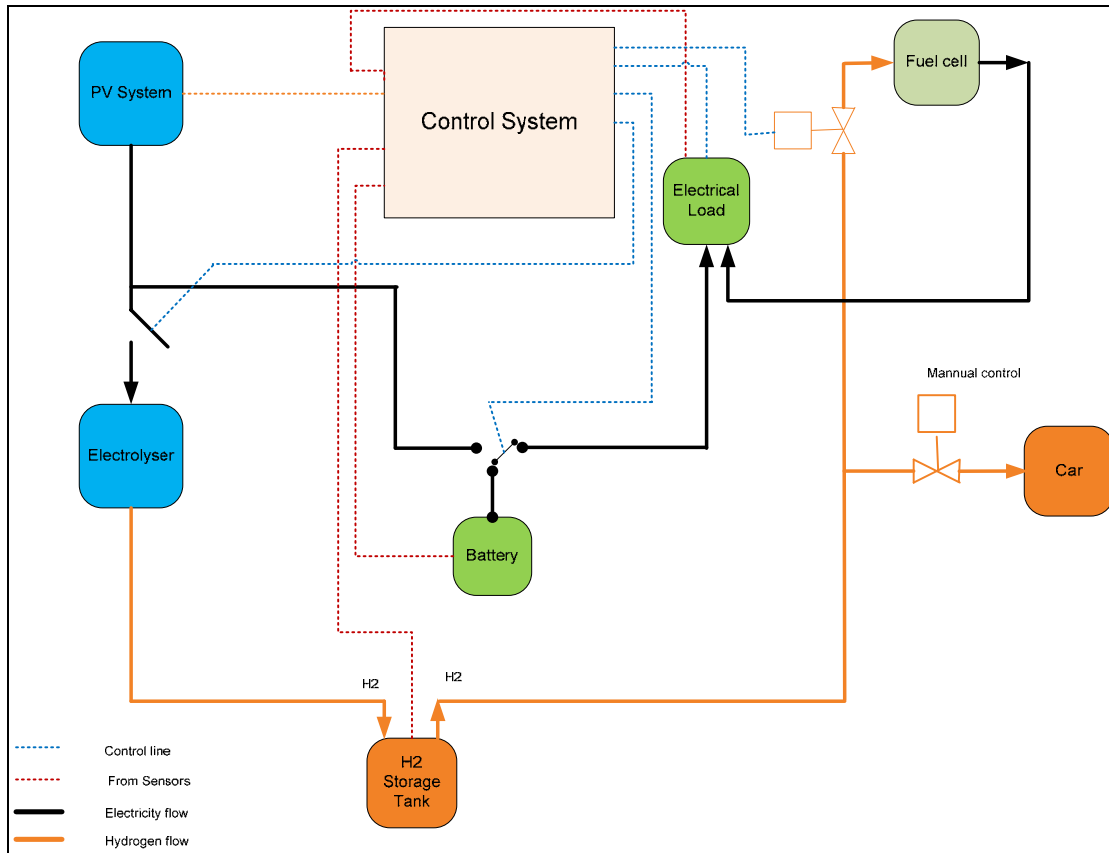


**Figure 32. Schematic of control system**

### 3.1.9    Electric loads

The profile of the request for electric and thermal power has been defined using statistical data for a passive house situated in the island of Hvar.

The electric energy demand has been evaluated along one complete year of operation. For each month, a reference day has been constructed, and in the reference day, the electric energy demand is given for every hour of operation.

The loads existing in the PV stand-alone system are both DC (television, lighting) and AC (electrical motors, pumps, fans, etc.).
As known, the PV array produce DC power and therefore DC/AC conversion is required. An inverter is a converter where the power flow is from the DC to the AC side, namely having a DC voltage, as input, it produces a desired AC voltage as output.

## 3.2 Mathematical and simulation models of the single components

### 3.2.1 PV module

*PV cell mathematical model*

The one-diode model shown on the Fig. 33 can be used as an equivalent circuit for PV cell. The parameters of interest in the model are the photon current *(Iph)*, the series resistance *(Rs)*, shunt resistance *(Rsh)*, the diode reverse saturation current *(Is)* and ideality factor *(m)*. The data sheets describe only the electrical characteristics of the PV module under STC (Standard Test Conditions, 1000 W/m², 25°C, AM 1.5) which is serial connections of 36 cells.
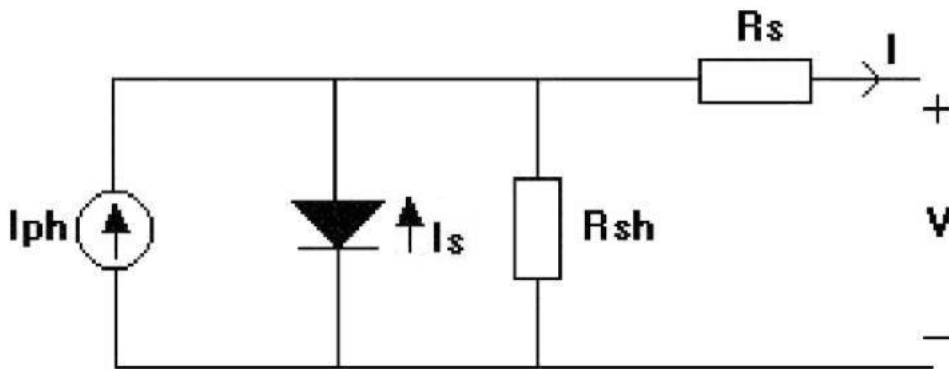
**Figure 33. PV cell equivalent circuit**

The model of a solar module (consisting of one string of 36 cells in series) is represented by the relation between current (I) and voltage (U) in below equation.

$$I = I_{ph} - I_r \times (\exp((U + I \times R_s)/(m \times U_T)) - 1) \qquad (3.5)$$

$$f(I) = I_{ph} - I_r \times (\exp((U + I \times R_s)/(m \times U_T)) - 1) - I = 0 \qquad (3.6)$$

Where:

$$I_{ph} = I_{phc} \times n_p$$
$$I_r = I_{sc} \times n_p$$
$$R_s = R_{sc} \times n_s / n_p$$
$$U_T = n_s \times k \times T_c / e$$
$$I_{phc} = I_{phc_{1000}} \times (E(t)/E_{1000})$$

$$I_{sc} = I_{sc0} \times T_c^3 \times \exp(-E_g /(k \times T_c))$$

$$m = 1$$

$$R_{sc} = 0.013558 \, \Omega$$

$$n_s = 36$$

$$n_p = 1$$

$$I_{phc_{1000}} = 3.27 \, A$$

$$E_{1000} = 1000 \, W/m^2$$

$$k = 1.3806 \times 10^{-23} \, J/K$$

$$e = 1.60219 \times 10^{-19} \, C$$

$$T_c = 342 \, K$$

$$I_{sc0} = 3.727873 \, A/K^3$$

$$E_g = 1.794 \times 10^{-19} \, J$$

*Model in Simulink for one PV module (Appendix ) (Fig. 34)*

By simulation of eq. 3.6, it is possible to obtain U-I characteristics (working characteristics) of the PV module under given constant PV cell temperature and given constant solar irradiation.

In order to find the needed I–U relationship, a systematic way for obtaining the best possible curve fit was developed according to the PV module characteristic given in Appendix .

The PV module is represented with one block in Simulink scheme. Input and output signals as used in Simulink are presented on Fig. 34.
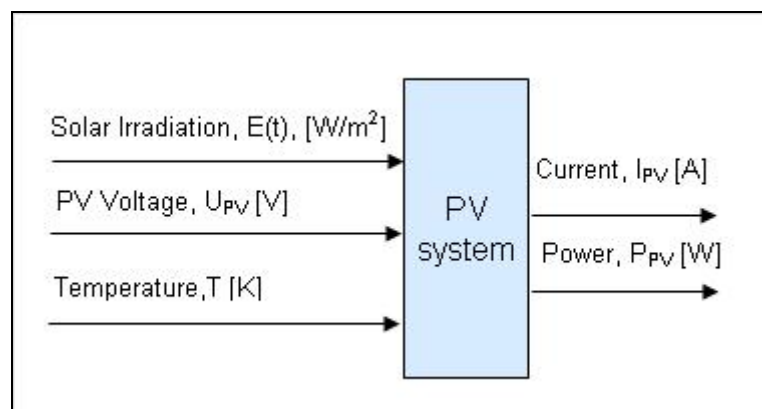


**Figure 34. PV module model input-output signals**

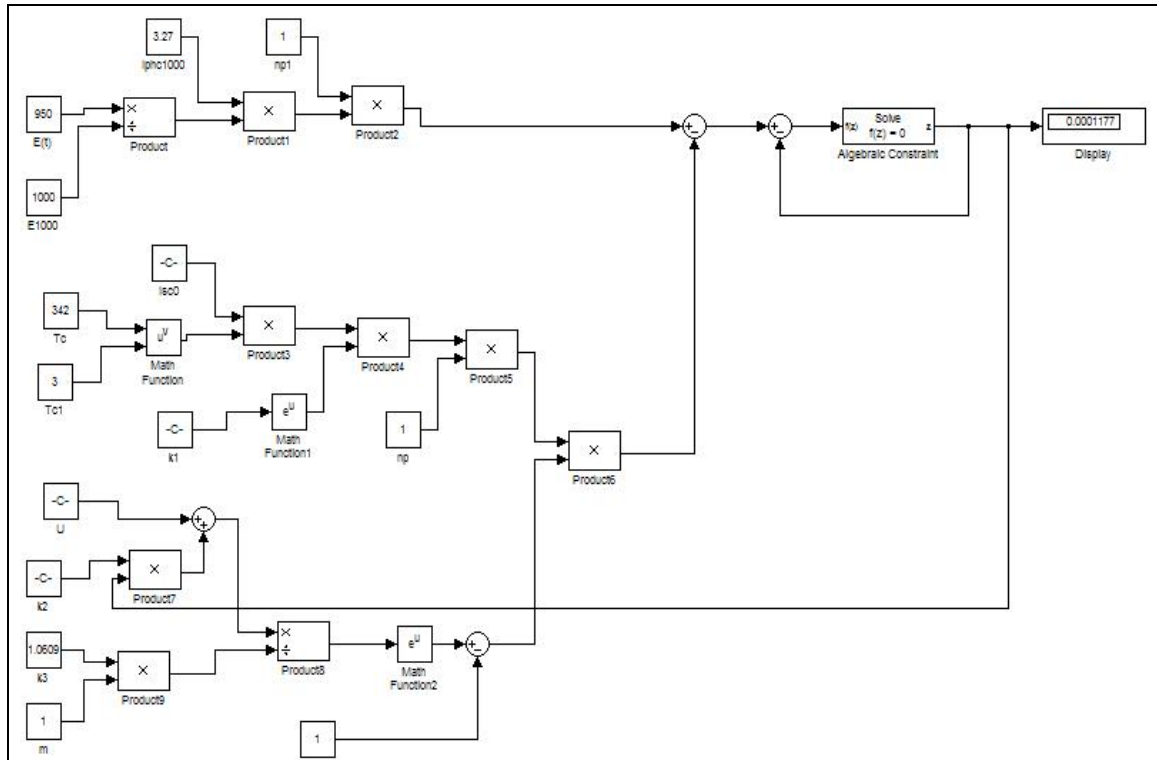PV module Simulink block in detail is shown in Fig. 35

**Figure 35. Simulink PV cell model**

Following data and graph shows the proof that the model shown in Fig. 35 works properly.

```
U=[0 1 2 3 4 5 6 7 8 9 10 11 12 13 14 15 16 17 18 19 20 21 21.5 21.54
21.5449];

I=[3.106 3.106 3.106 3.106 3.106 3.106 3.106 3.106 3.106 3.106 3.106
3.106 3.105 3.102 3.096 3.08 3.039 2.941 2.722 2.295 1.597 0.628
0.05404 0.006 0.0001];
plot(U,I)
hold on
grid on
```
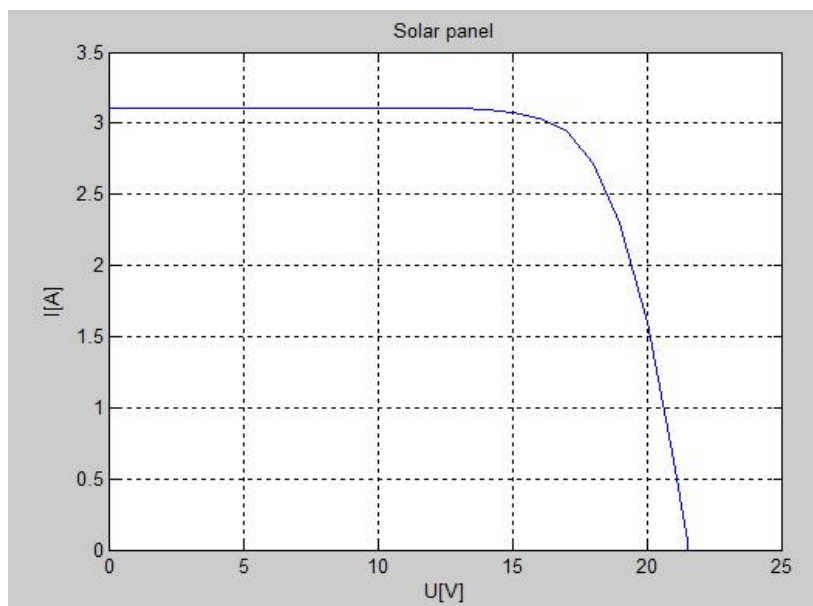


**Figure 36.  I-V characteristic of PV module**

In the Fig. 37 hourly solar radiation of island Hvar is given which is used as input data in the simulation.
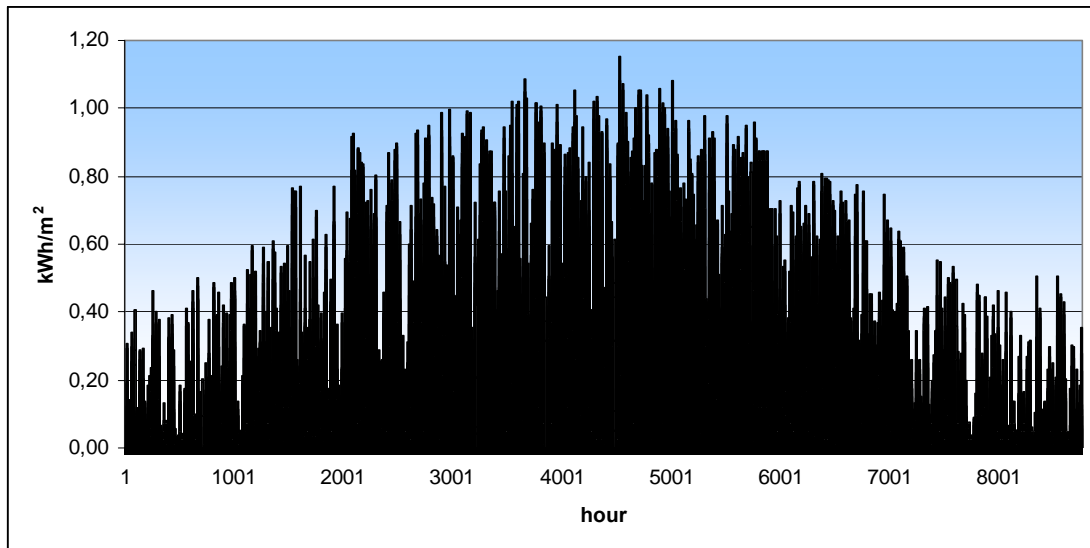


**Figure 37. Hourly solar radiation in island Hvar**

Fig. 38 shows a profile of the PV module-generated currents, which is simulated by the above model during a one year (8760 hours).
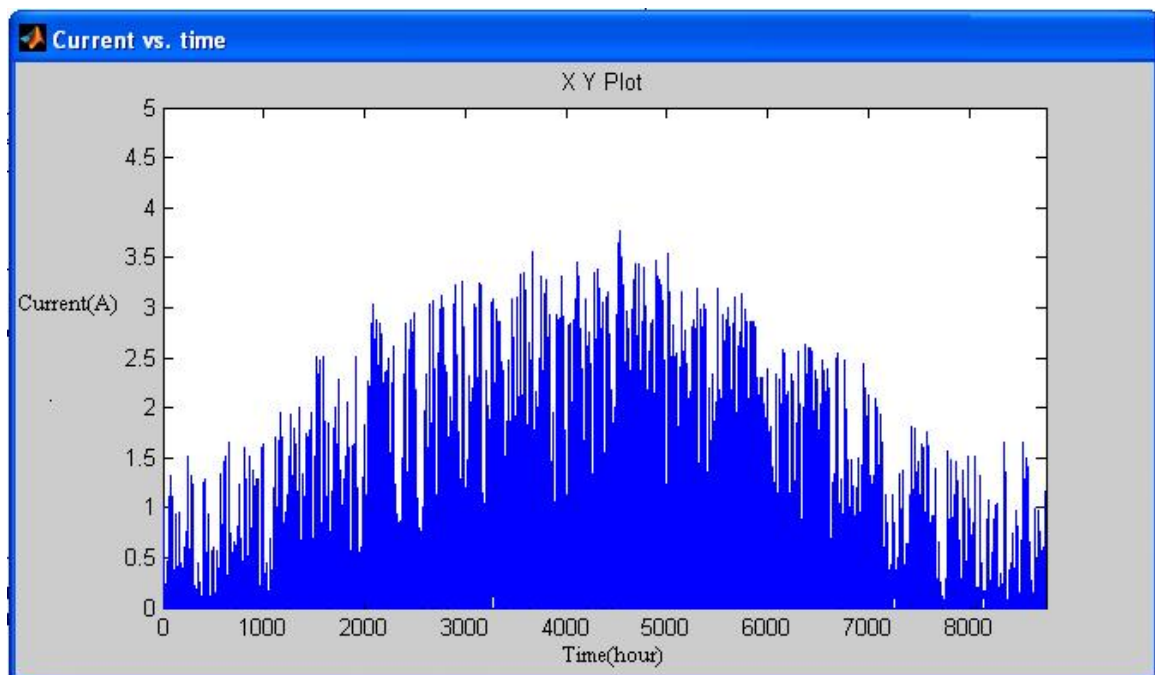


**Figure 38. Characteristic of current (A) vs. time (hourly) during one year for one PV module**

Under a constant temperature, values of Isc and Voc are simulated for different irradiance levels. Results are presented in Fig. 39.
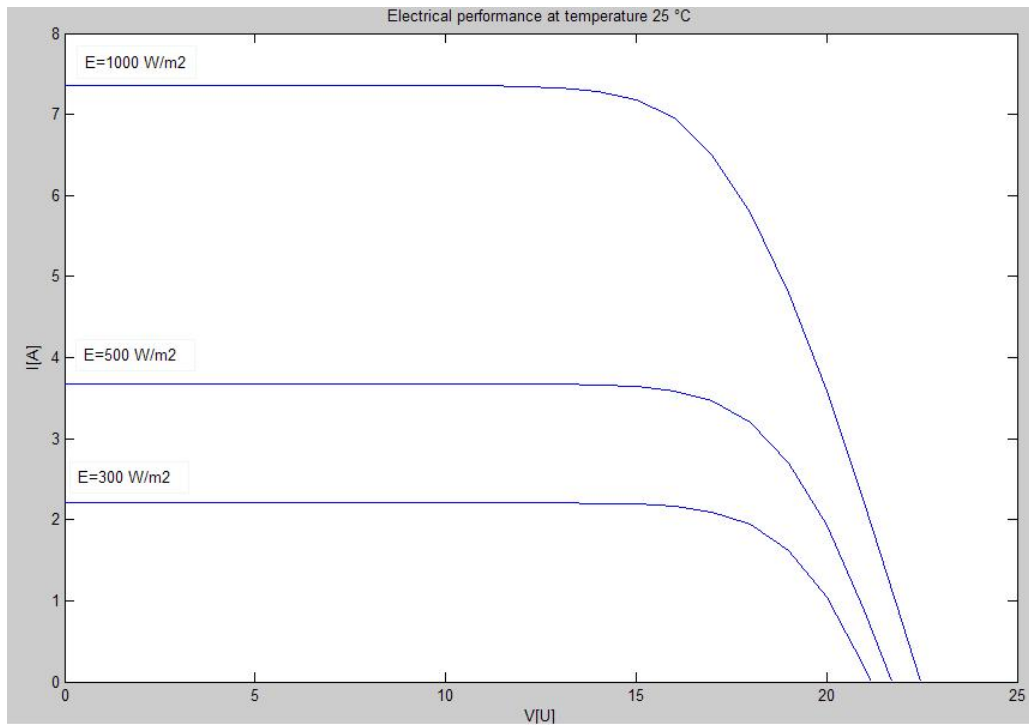
**Figure 39.  I-U characteristic of PV module (36cells)**

The modeling can be also adapted to the systems with different size of each PV. It is assumed that Ns is the number of the PV modules in series and the Np is the number of parallel strings of PV modules in series. A larger PV system can be modeled by Simulink as given in the following picture.



**Figure 40.  PV array system Simulink model (17in parallel and 3 in series)**

The operating characteristics of the PV system made of 3 modules in series and 17 modules in parallel under different irradiance levels are given in the Fig.41. (Again at PV cell temperature of 25 °C)
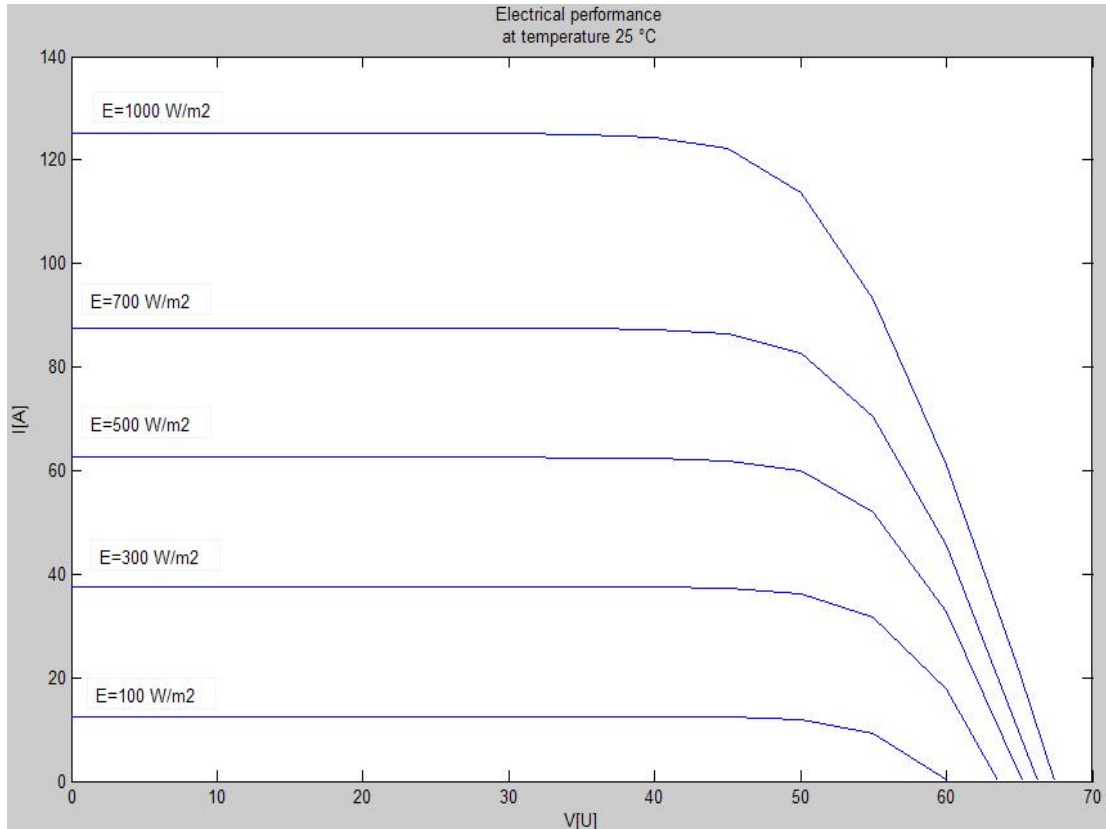
**Figure 41.  I-U characteristic of array in different solar irradiations**

Except for the solar panel characteristics, the amount of solar energy delivered by the solar cell panel depends on local 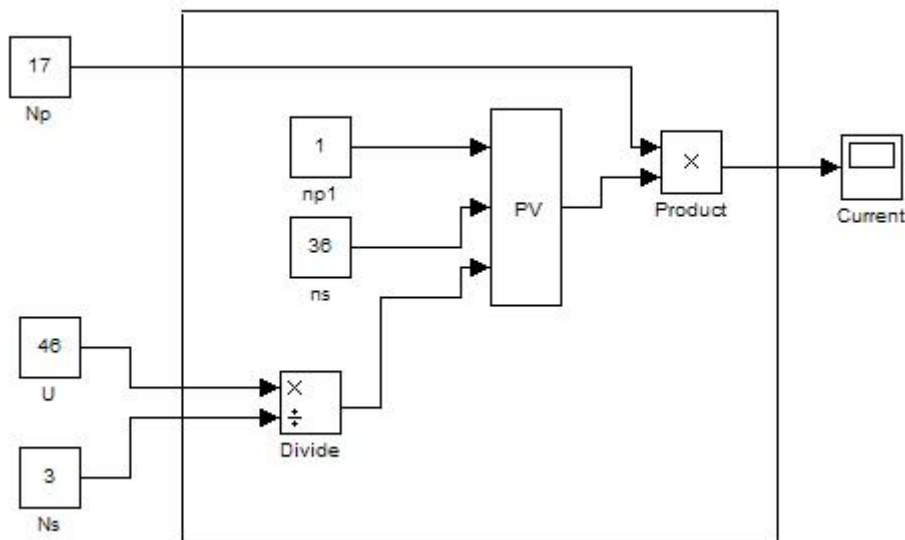weather conditions, such as the solar radiation, wind velocity and ambient temperature. According to [13] the experiments were performed to measure the average temperature of PV module during the measurement of each characteristic. It can be seen on Fig. 42 that at certain constant wind velocity (about 2 m/s), cell temperature (and module as a whole) increases with solar irradiation.



**Figure 42.  Solar irradiation vs. Temperature [13] at certain constant wind velocity**

The effect of the cell temperature on the PV system is not modeled (and simulated) by using thermal energy accumulation in PV modules than by using data given in Fig 42.

So based on these measurements the I-U characteristic of PV modules in different temperature and particular solar radiation are simulated and shown in Fig.43.



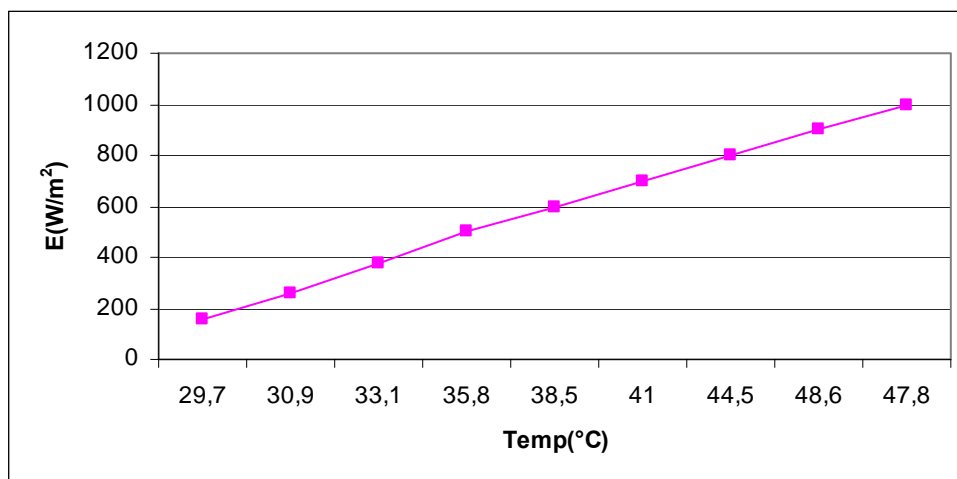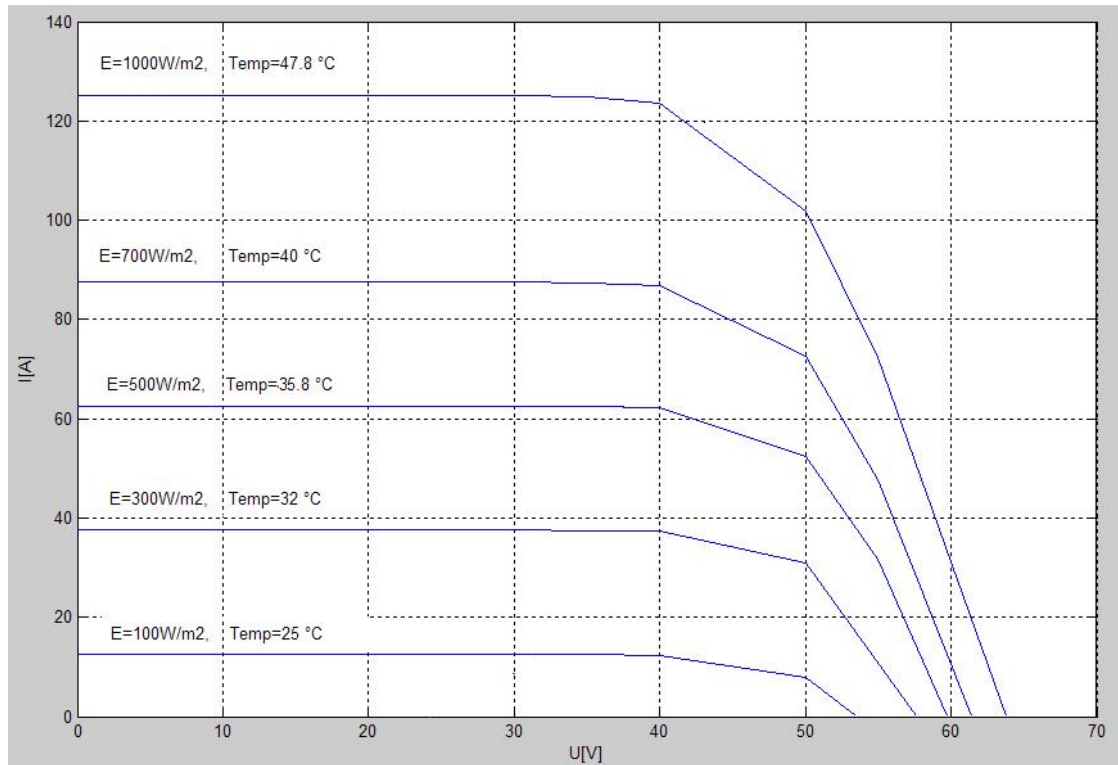**Figure 43. U-I characteristic of the array at different solar radiation when appropriate temperatures of modules are applied**

### 3.2.2 Electrolyser

*Electrolyser mathematical model*

In simulation of electrolyser, an empirical model which was suggested by Ulleberg [12] for a commercial electrolyser which for a known operation temperature is used:

$$U = n_c U_{rev} + a(\frac{I}{A}) + bLog[c(\frac{I}{A})+1] \qquad (3.7)$$

Where

$U$ - operation cell voltage, V
$U_{rev}$ - reversible cell voltage, V
$a$ - ohmic resistance of electrolyte, $\Omega m^2$
$b, c$ - coefficients for overvoltage on electrodes
$A$ - area of electrode, $m^2$
$I$ - current through cell, A
$n_c$ - number of cells in a stack

Coefficients $a, b, c$ are functions of temperature.

*Electrolyser specification*

In this work semi-commercial electrolyser have been selected: HySTAT  from Hydrogenics, Canada, Alkaline electrolyser (Appendix ). Technical data are as follows [14]:

Max H2 production          = 1 Nm$^3$/hr
Operating temperature      = 20-70 C
Operating pressure         = 25 bar
Stack voltage (at 25 bar)  = 40 V
Stack current (at 25 bar)  = 120 A
Number of cells            = 22
Surface area               = 300 cm$^2$


 A series of experimental U–I curves were obtained in the temperature range from 20 to 70 °C and pressure of 5 bar  as it can be seen in Fig. 48.
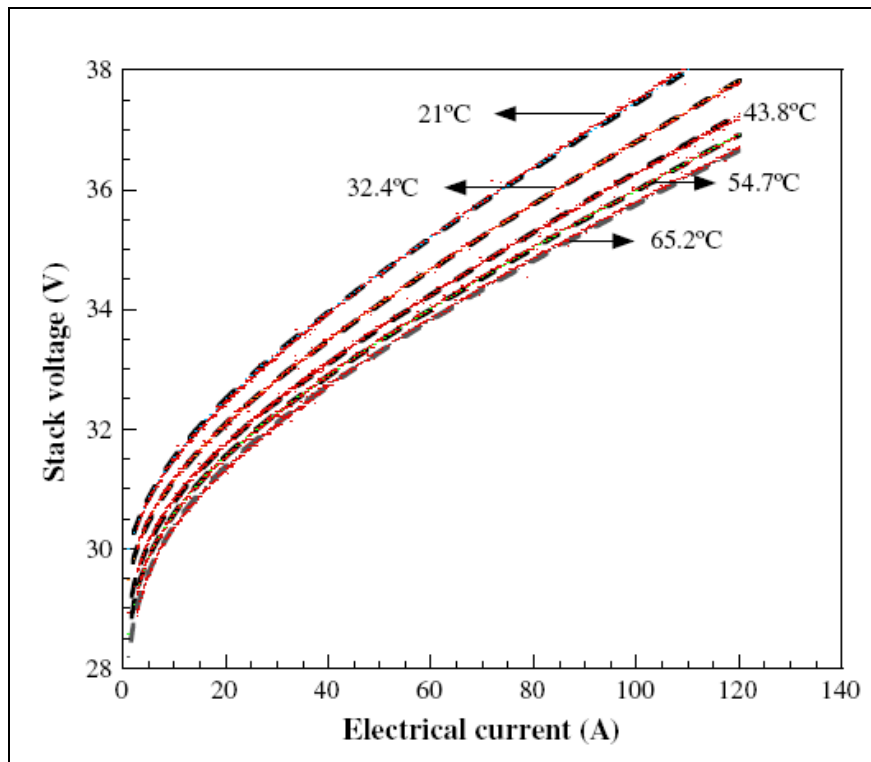


**Figure 44.  The effect of temperature on operation point of Electrolyser [14]**

Because there is no still published data for temperature dependence at higher pressure level that's why it has been chosen to approximate experimental characteristic U-I at 5 bars. Also, temperature dependence shown in Fig. 44 has not been taken into account in our model, i.e. curve for 25 °C was chosen.

In order to find a, b, c parameters in eq. 3.7, we need to have experimental data of electrolyser current and voltage, i.e. several points of its working characteristics. These data were taken from [14] as follows (and graphically shown on Fig.45, 5 green dots).
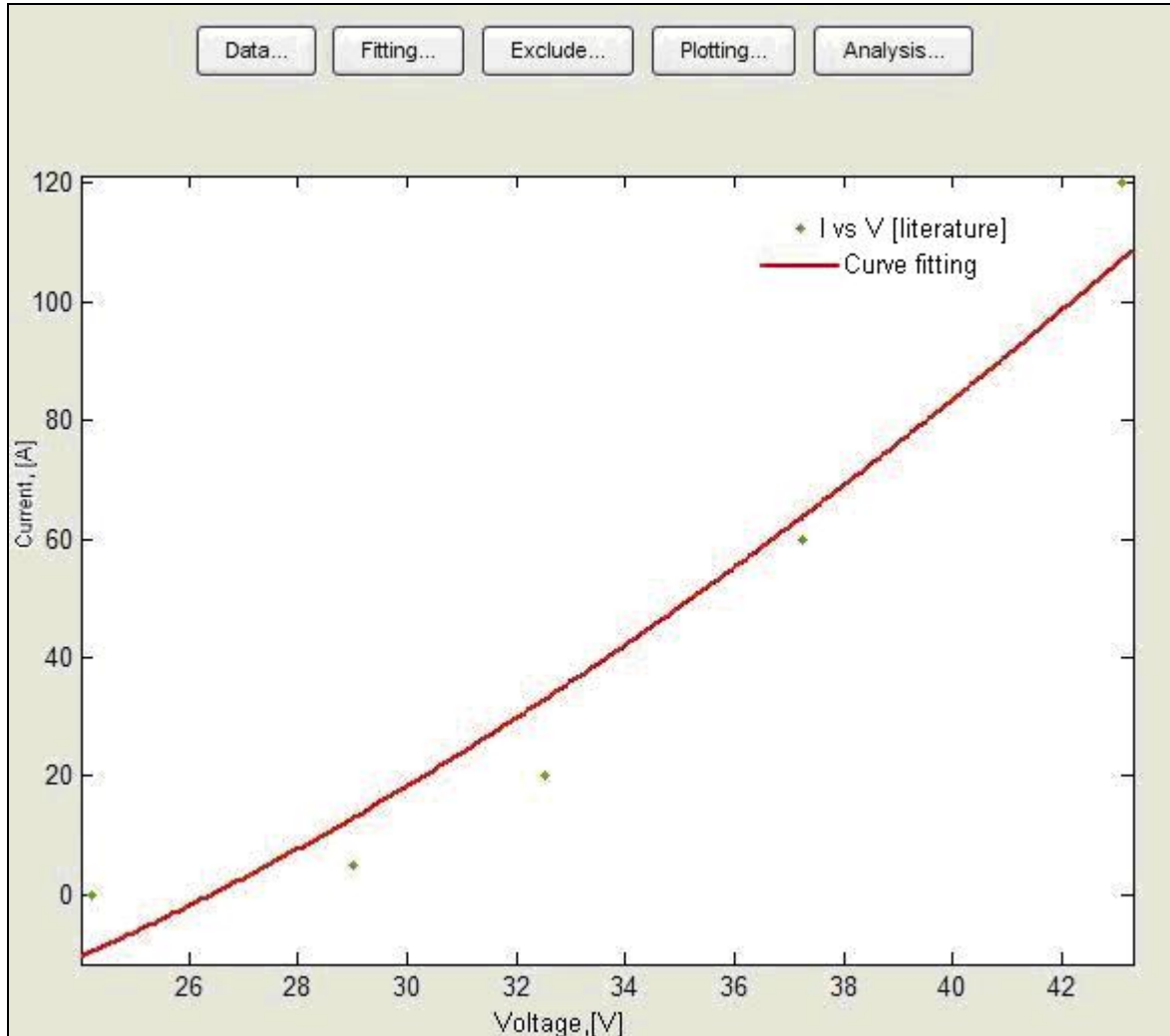
**Figure 45. Curve fitting to find a,b,c parameters**

The corresponding values of the chosen data points P(I,V) of electrolyser characteristics [14]:

P1 (0,  24.20)
P2 (5,  29.00)
P3 (20, 32.50)
P4 (60, 37.24)
P5 (120, 43.00)

Curve fitting procedure (Matlab function Curve fitting) was selected to calculate mentioned *a, b, c* parameters by using points P1, P2 and P3. Then after curve fitting:

a = 0.0025
b = 2.8946
c = 0.299

$$U = n_c U_{rev} + 0.0025(\frac{I}{A}) + 2.8946 Log[0.299(\frac{I}{A}) + 1] \qquad (3.8)$$

The resulting curve according to eq. 3.8 is shown on Fig 45. (red colored curve). It can be seen that the difference between experimentally obtained (green) points, and simulation results (red curve) are acceptable. The eq. 3.8 was adopted as electrolyser model in further text.

*Electrolyser model in Simulink*

Simulink block with input output signals are shown on Fig. 46.
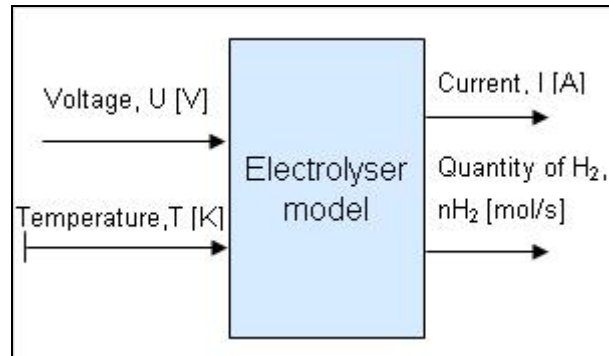


**Figure 46. Electrolyser model input-output signals**

Simulink model in detail (based on eq. 3.8) is shown in the Fig. 47.
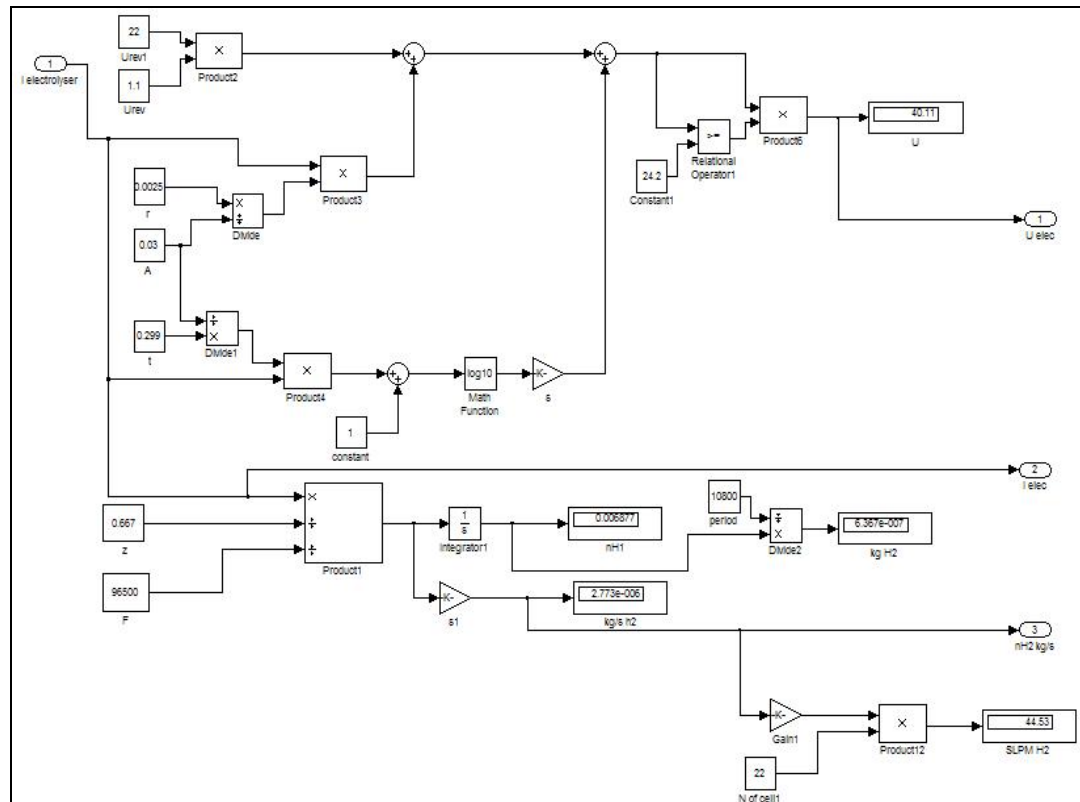


**Figure 47. Simulink Electrolyser model**

Following data and graph shows the proof that the model works appropriately

```
U=[24.2 30.83 32.53 33.87  35.06 37.24 39.27 41.21 43.11
44.04];
I=[0 10 20 30 40 60 80 100 120 130];
plot(U,I,'b')
hold on
grid on
```
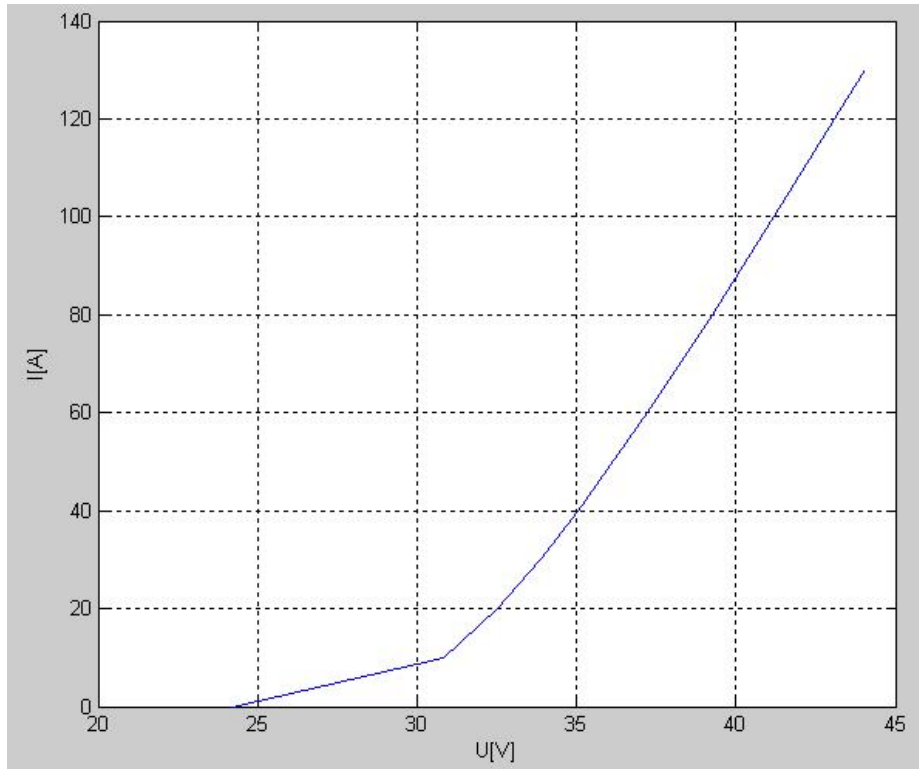


**Figure 48.  I-V characteristic of electrolyser at temp. 25°C**

### 3.2.3    Hydrogen storage tank

*Hydrogen storage mathematical model*

The hydrogen storage models are based on either the ideal gas law, or Van der Waals equation of state for real gases.
According to the ideal gas law, the pressure p of a gas storage tank can be calculated as

$$P_{H2} = n_{st.}RT/V_{st} \qquad\qquad (3.9)$$

Where:

$$n_{st} = \frac{1}{2F}\int\left(I_{el} - I_{FC}\right)dt \qquad\qquad (3.10)$$

Following table shows the compressibility factor depends on temperature, pressure and the substance represents the deviation of a real gas from the ideal gas model.

**Table 16. Hydrogen compressibility factors (Z) at 20°C[15]**

| Pressure (MPa) | 0.1013 | 5 | 10 | 20 | 30 | 35 | 40 | 50 | 70 | 100 |
|---|---|---|---|---|---|---|---|---|---|---|
| Z | 1 | 1.032 | 1.065 | 1.132 | 1.201 | 1.236 | 1.272 | 1.344 | 1.489 | 1.702 |

The use of the different equations of state leads to diverse predictions of the behaviour of hydrogen at high pressure. Figure 49 shows the density of hydrogen with pressure as calculated by considering the ideal gas model, the van der Waals model and the compressibility factor of hydrogen. For pressures up to 150 bar, the predictions of the 3 models are practically identical. However, at higher pressures the ideal gas model overestimates the density of hydrogen, compared to the real gas models; the deviation increases with pressure [15].
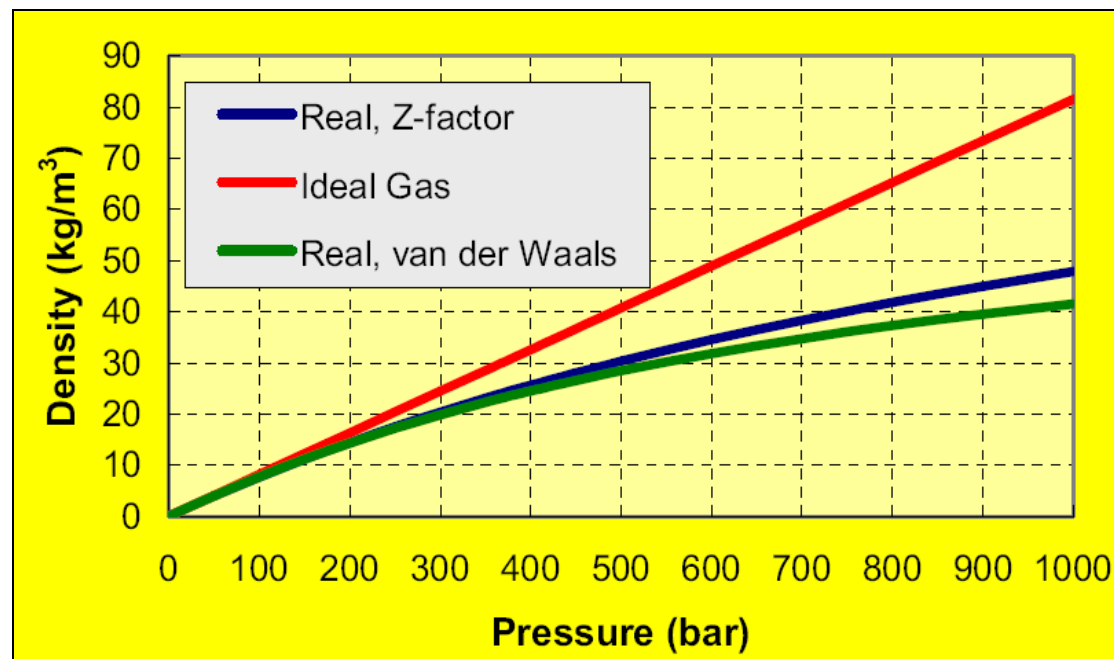


**Figure 49. Hydrogen density as a function of pressure [15]**

With applying the conservation of mass relation for storage tank which states the hydrogen mass in the tank.

$$\frac{dM}{dt} = m^\circ{}_{in} - m^\circ{}_{out} \tag{3.11}$$

Where, $m_{in}$ and $m_{out}$ are the total rates of mass flow into and out of the storage tank, respectively. And dM/dt is the rate of change of mass within the tank.

$$\frac{d(V\rho)}{dt} = V\frac{d\rho}{dt} \tag{3.12}$$

$$\rho = \rho(PT) \quad / \frac{\partial}{\partial t} \tag{3.13}$$

$$\frac{d\rho}{dt} = \frac{\partial\rho}{\partial P}\cdot\frac{dP}{dt} + \frac{\partial\rho}{\partial T}\cdot\frac{dT}{dt} \tag{3.14}$$

$$T = \text{constant, then } \frac{dT}{dt} = 0 \tag{3.15}$$

$$V\frac{d\rho}{\partial P}\cdot\frac{dP}{dt} = m°_{in} - m°_{out} \tag{3.16}$$

$$\rho = P/R_gT \quad \text{then} \quad \frac{\partial\rho}{\partial P} = \frac{1}{R_gT} \tag{3.17}$$

When we introduce compressibility factor Z for hydrogen in eq. 3.17, we get:

$$\frac{\partial\rho}{\partial P} = \frac{1}{ZR_gT} \tag{3.18}$$

Compressibility factor for hydrogen according to table 16 is:

$$Z = 0.99704 + 6.4149\times10^{-9}\,P \tag{3.19}$$

Then mathematical model: $\quad \dfrac{dP}{dt} = \dfrac{Z(P)\,R_g\,T}{V}\,(m°_{in} - m°_{out})$ (3.20)

Where:

P [N/m$^2$]
$\rho$ [kg/m$^3$]
T  [K]
M [kg]
V [m$^3$]
$R_g$ = 4124.18 Nm/(kg K)
Z= Compressibility factor for H$_2$

*Storage tank specification*

For the purpose of the simulation there is no need for selection of commercial available storage tank. It is only supposed maximum tank pressure of 25 bar because it is compatible with chosen electrolyser.

*Hydrogen  storage tank model in Simulink*

Hydrogen storage tank was modeled and simulated in Simulink by using of eq. 3.20., and input/output signals are given in Fig. 50 and expanded view is given in Fig. 51.
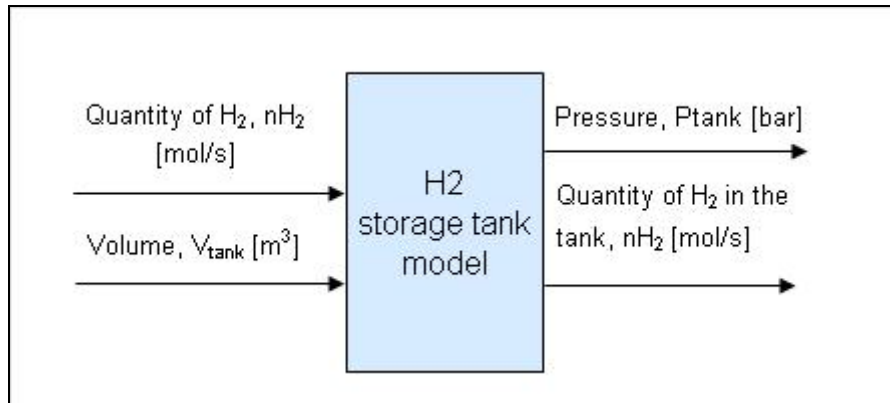


**Figure 50. Input-output signals for hydrogen storage tank model**
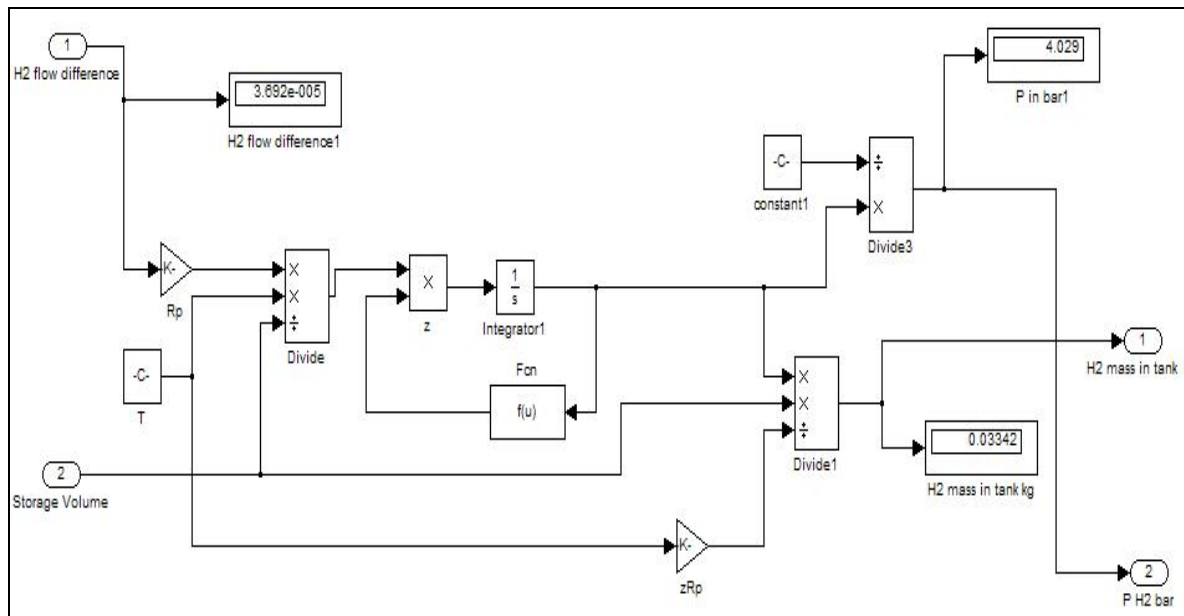


**Figure 51.  Gas storage tank model in Simulink**

In order to see the result of storage tank Simulation the flow rate of hydrogen is much more than the real just to show whether simulation model works properly. As it can be seen from the Fig. 52 it works as it was expected.
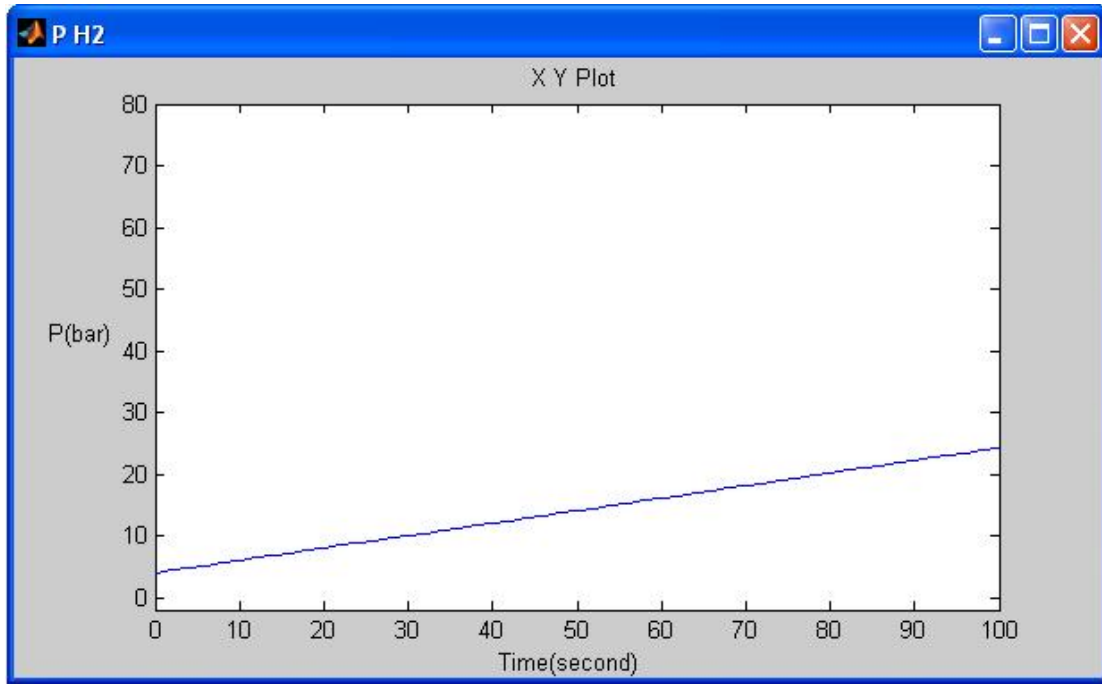
**Figure 52. Simulation result of storage tank**

Input data in storage tank model are assumed higher value in order to show that the simulation model works properly. That's why the pressure of the tank is increased very fast to the maximum level.

### 3.2.4   Compressor

*Compressor work model*

The compressor model is mainly based on a two stage polytropic compression process with inter-cooling. The total compressor work $W_{comp}$ required for this process is

$$W_{comp} = n_{gas} (W_l + W_{ll})/\eta_{comp} \tag{3.21}$$

And

$$Wl = \frac{\alpha R T_1}{\alpha - 1} \left[1 - \left[\frac{P_x}{P_1}\right]^{\left(\frac{\alpha-1}{\alpha}\right)}\right] \quad \text{and} \quad Wll = \frac{\alpha R T_1}{\alpha - 1} \left[1 - \left[\frac{P_2}{P_x}\right]^{\left(\frac{\alpha-1}{\alpha}\right)}\right] \tag{3.22}$$

Being W the total compressor work [W], $n_{gas}$ is the gas flow [mol/ s], Wl, Wll the polytropic work [J/ mol], ηcomp the compressor efficiency, α the polytropic coefficient, R the universal gas constant (8.314 J/K/mol), T the inlet gas temperature [K], and pi the pressure values [atm]

*Compressor work model in Simulink*

Simulink block o with input output signals is shown in Fig. 53.

60

**Figure 53. Compressor Simulink block input/output signals**

Two stage compressor works is given in the following Simulink model.



**Figure 54.  Compressor model in Simulink**

In this work model of compressor has been done but in the whole model simulation was not considered. It needs high pressure storage tank which is in fact hydrogen reservoir of the car. Because the process of filling hydrogen tank on the car is

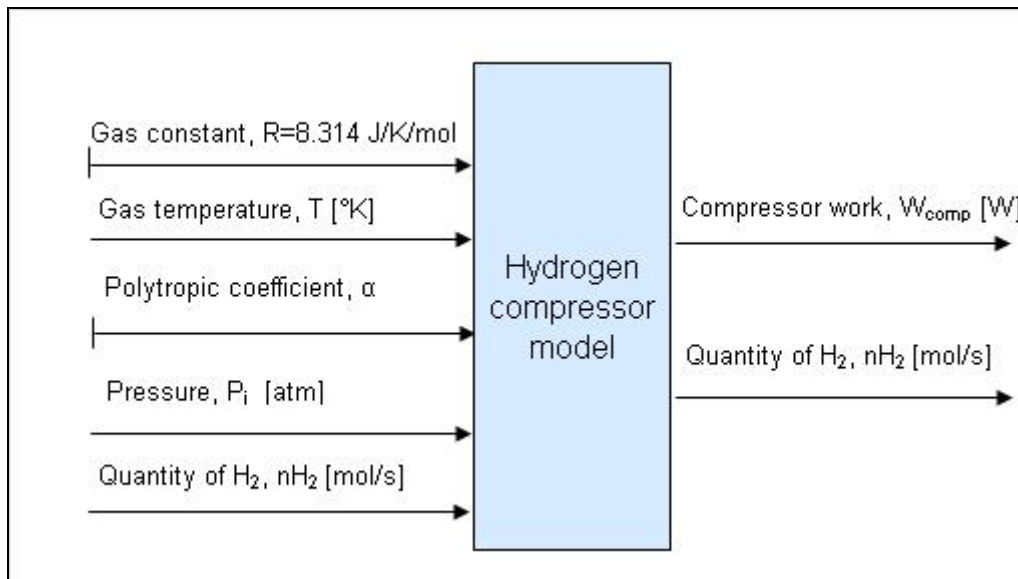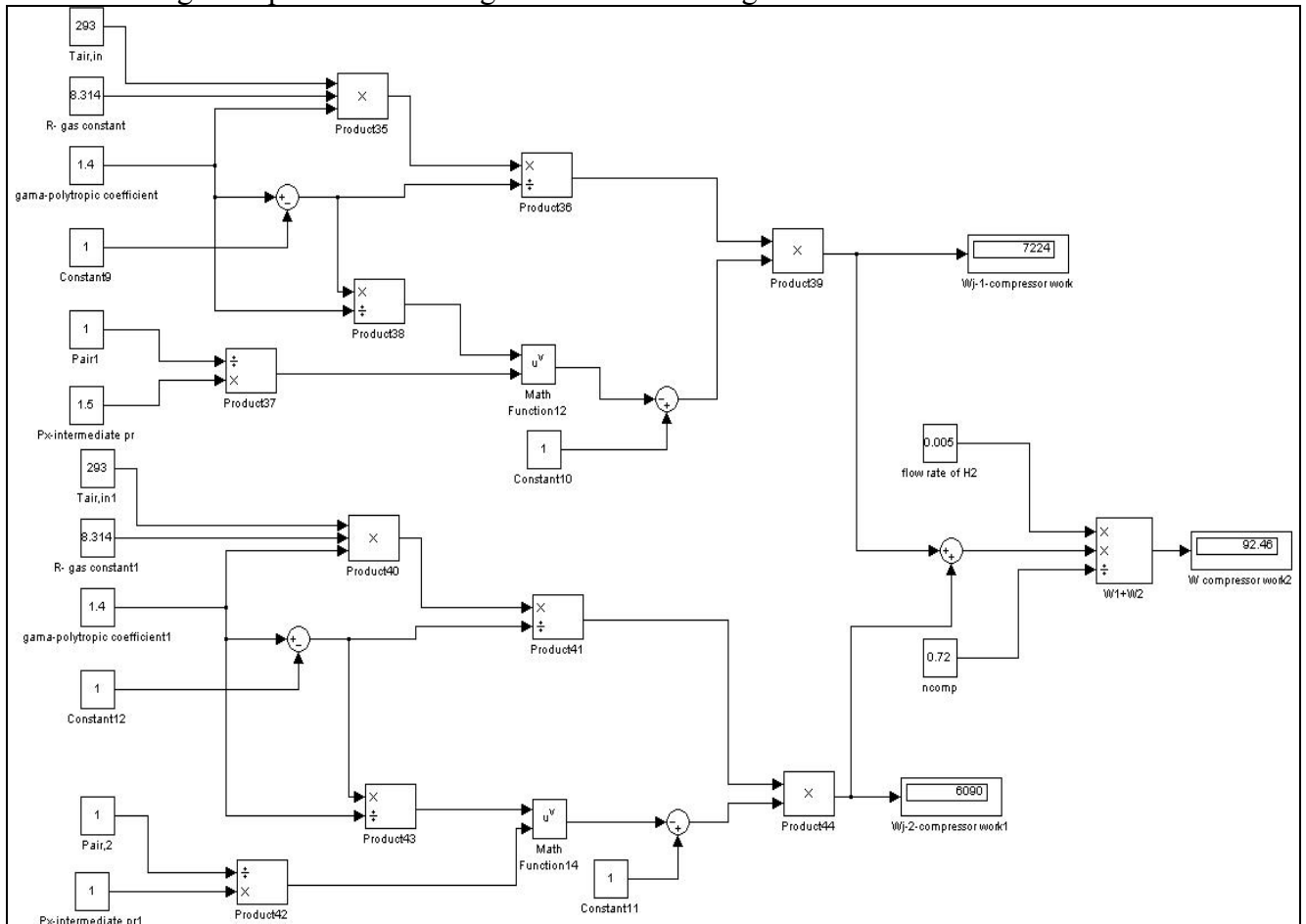manually controlled (this is not considered by controller simulated in Simulink), compressor model in Fig. 54 is not included in power system simulation.

### 3.2.5 Fuel cell

*Fuel cell mathematical model*

In order to model the fuel cell we have to calculate different voltage losses and consequently polarization curve. The first step in creating the polarization curve is to calculate the Nernst voltage.

The Nernst voltage can be calculated using the following equation [17]:

$$E_{Nernst} = \frac{G_{f,liq}}{2F} - \frac{RT_k}{2F} Ln(\frac{P_{H2O}}{P_{H2} P_{O2}^{1/2}})$$  (3.23)

Where:

$G_{f,liq}$- Gibbs free energy of hydrogen in liquid state, J/mol [228170 J/mol]
$T_k$- temperature in degrees K
i - current density, A/cm$^2$

For the purpose of the model simplicity at this level, theoretical value $E_{Nernst}$ =1.23 V was assumed.

Then, the cell voltage is calculated by following equation:

$$V_{cell} = E_{Nernst} - (V_{act} + V_{ohmic} + V_{conc})$$  (3.24)

Where the losses are composed of activation loss, concentration loss and ohmic losses and the cell potential is equal the difference between the $E_{Nernst}$ and voltage losses.

**-Equation of activation loss:**

$$\Delta V = a + b \log(i)$$  (3.25)

Where:

$$a = -2.3 \frac{RT}{\alpha F} \log(i_o), \text{ and } b = \frac{RT}{\alpha F}$$  (3.26)

$i_o$- exchange current density, [$i_o$= 3×10$^{-6}$ A/cm$^2$]
α- transfer coefficient,[ α=1]
n- number of electrons, [n=2]

**-Equation of ohmic losses:**

$$\Delta V_{ohm} = i R_i$$  (3.27)

Where:
i - current density, A/cm$^2$
$R_i$- total cell internal resistance (which include ionic, electronic and contact resistance, Ω cm$^2$)

Typical value for Ri are between 0.1 and 0.2 $\Omega$ cm$^2$ (In our model Ri = 0.15)

**-Equation of concentration polarization:**

$$\Delta V_{conc} = \frac{RT}{nF} Ln\left(\frac{i_L}{i_L - i}\right) \tag{3.28}$$

Where:
i - current density, A/cm$^2$
$i_L$ - limiting current density, A/cm$^2$ ,[$i_L$=1.6 A/cm$^2$]
F - Faraday's constant (F = 96500 Coulombs)

And power output:

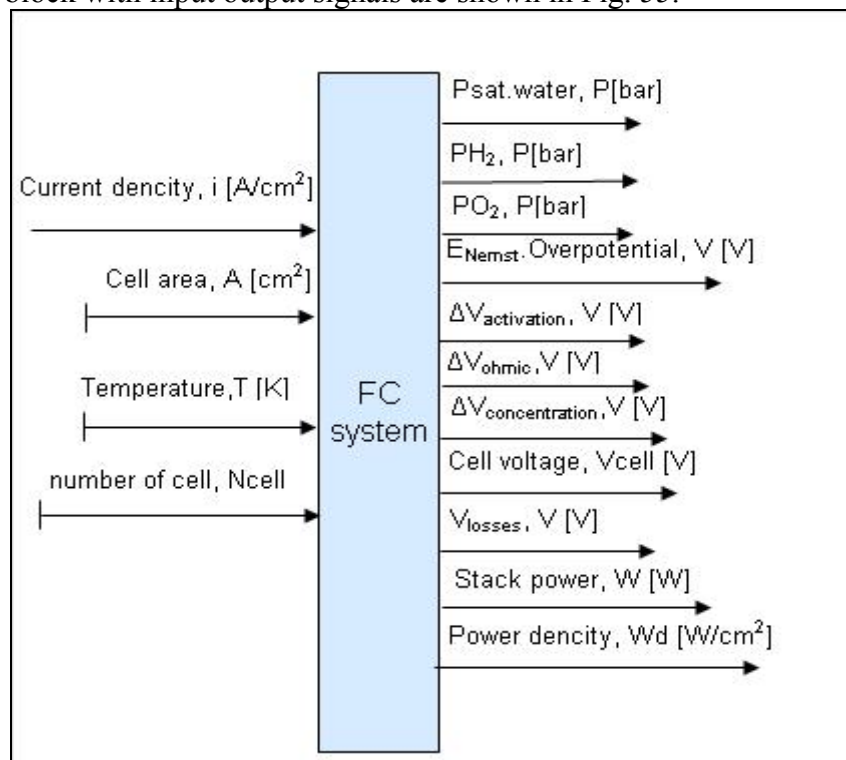$$W_{cell} = V_{cell} \; I_{FC} \; A_{FC} \tag{3.29}$$

where:

$I_{FC}$            fuel cell current, A ;   (i = $I_{FC}/A_{FC}$)

$A_{FC}$           the active area of the fuel cell electrode, cm$^2$

*Fuel cell model in Simulink*

Simulink block with input output signals are shown in Fig. 55.



**Figure 55. Fuel cell model input-output signals**

Using Simulink to solve it as it can be seen from the Fig. 56.
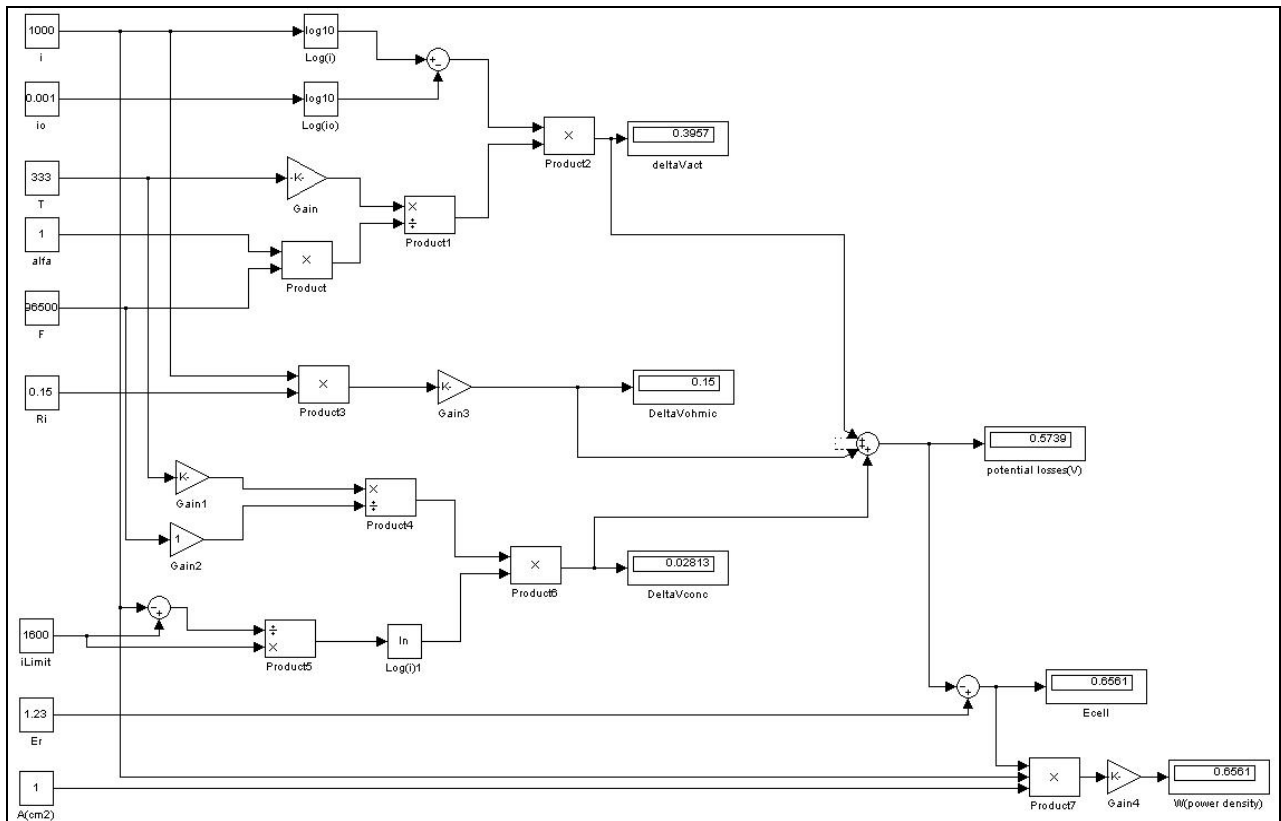


**Figure 56. Simulink fuel cell model**

**Table 17. Fuel cell voltage and losses(results from simulation)**

| | Current density [mA/cm²] | Potential losses (V) | | | | Ecell [V] | Power density [W/cm²] | Efficiency |
|---|---|---|---|---|---|---|---|---|
| | | Activation loss [V] | Ohmic loss [V] | Concentration loss [V] | Total potential losses [V] | | | |
| 1 | 0,005 | 0,0461 | 7,50E-07 | 8,96E-08 | 4,61E-02 | 0,954 | 4,76E-06 | 0,644 |
| 2 | 0,01 | 0,06595 | 1,50E-06 | 1,79E-07 | 0,06595 | 0,934 | 9,34E-06 | 0,630 |
| 3 | 1 | 0,1979 | 0,00015 | 1,79E-05 | 0,198 | 0,802 | 0,008 | 0,541 |
| 4 | 50 | 0,3099 | 0,0075 | 9,10E-04 | 0,3183 | 0,681 | 0,034 | 0,460 |
| 5 | 100 | 0,3298 | 0,015 | 1,85E-03 | 0,347 | 0,653 | 0,065 | 0,441 |
| 6 | 250 | 0,356 | 0,0375 | 4,80E-03 | 0,398 | 0,601 | 0,15 | 0,406 |
| 7 | 400 | 0,3695 | 0,06 | 8,20E-03 | 0,438 | 0,562 | 0,225 | 0,379 |
| 8 | 500 | 0,3759 | 0,075 | 1,07E-02 | 0,462 | 0,538 | 0,269 | 0,363 |
| 9 | 600 | 0,3811 | 0,09 | 1,35E-02 | 0,485 | 0,515 | 0,309 | 0,348 |
| 10 | 800 | 0,3893 | 0,12 | 1,98E-02 | 0,529 | 0,471 | 0,376 | 0,318 |
| 11 | 1000 | 0,3957 | 0,15 | 2,81E-02 | 0,574 | 0,426 | 0,426 | 0,287 |
| 12 | 1100 | 0,3985 | 0,165 | 3,33E-02 | 0,597 | 0,403 | 0,443 | 0,272 |
| 13 | 1200 | 0,401 | 0,18 | 3,97E-02 | 0,621 | 0,379 | 0,455 | 0,256 |
| 14 | 1300 | 0,4032 | 0,195 | 4,80E-02 | 0,646 | 0,353 | 0,460 | 0,238 |
| 15 | 1400 | 0,4054 | 0,21 | 5,96E-02 | 0,675 | 0,325 | 0,455 | 0,219 |
| 16 | 1500 | 0,4073 | 0,225 | 7,95E-02 | 0,712 | 0,288 | 0,432 | 0,194 |
| 17 | 1550 | 0,4083 | 0,2325 | 9,90E-02 | 0,740 | 0,260 | 0,402 | 0,175 |
| 18 | 1599 | 0,4092 | 0,2399 | 2,12E-01 | 0,861 | 0,139 | 0,228 | 0,094 |

Main types of losses in the fuel cell which are caused by different factors, cell potential and power density are given in table 17 and graphically in the following Figures.
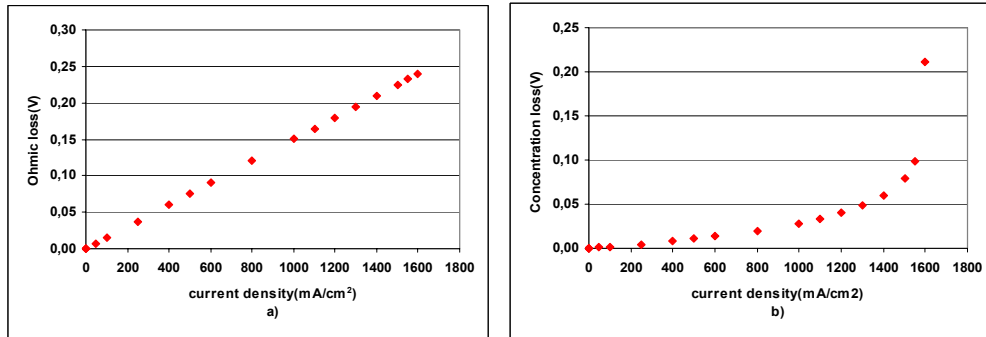


**Figure 57. Current density vs. losses   a) ohmic losses        b) concentration loss**
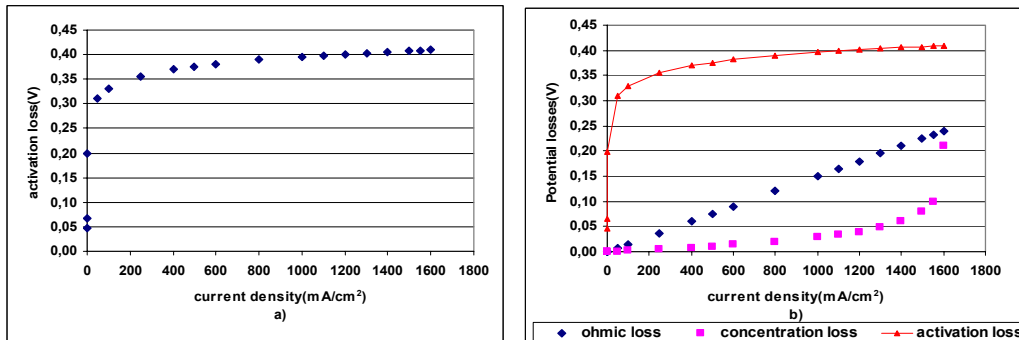


**Figure 58. Current density vs. losses in fuel cell  a)activation loss b)all  losses**

Polarization curve is the most important characteristic of a fuel cell [18]. This could help to identify particular problems.
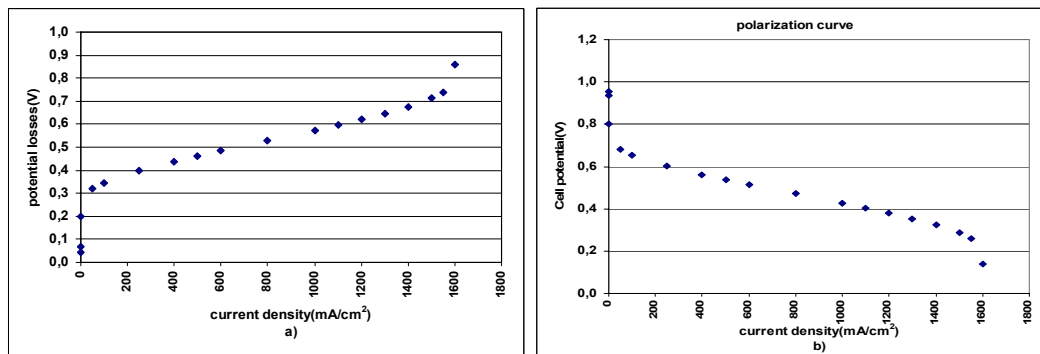


**Figure 59. Current density vs.  a) Potential losses   b) polarization curve**

Polarization curve and efficiency is given for a single cell. There are additional power losses and resulting efficiency loss due to auxiliary components in the fuel cell system (fans, pumps, relays and controllers).
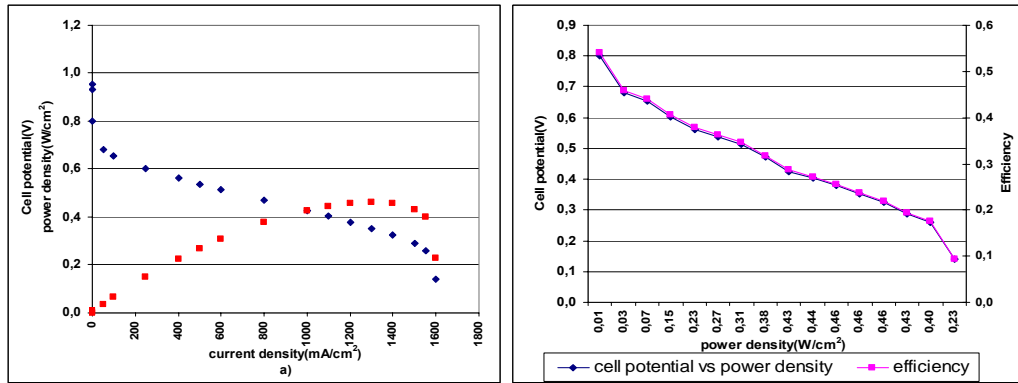
**Figure 60. Cell potential vs. a) current density b) power density**

### 3.2.6    Battery

*Mathematical model of the battery*

Battery state of charge (SOC):

$$SOC = \frac{\int I_B.dt}{C} \leq 1 \tag{3.30}$$

Battery clamps voltage (battery open circuit voltage which depends on SOC) (Appendix):

$$U_{oc} = 1.36\ SOC + 11.399 \tag{3.31}$$

Battery voltage:

$$U_B = U_{oc} + I_B.R_B \tag{3.32}$$
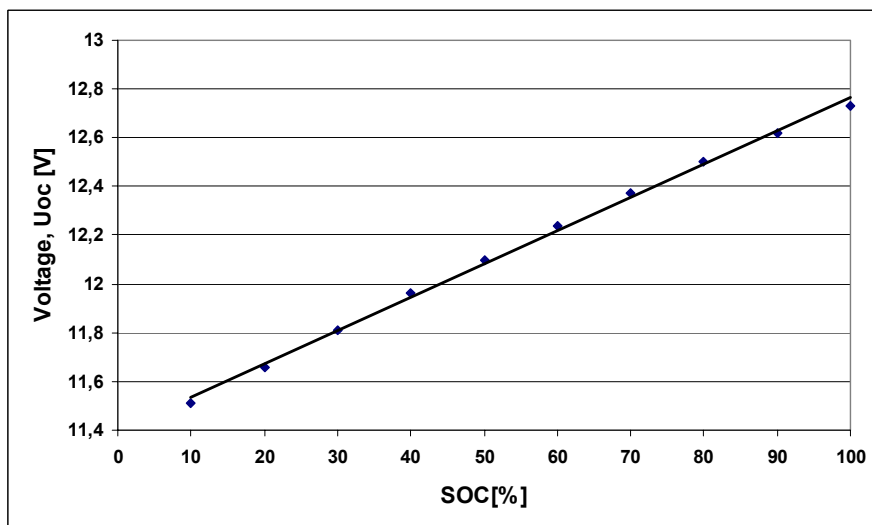


**Figure 61. Voltage vs. SOC given by producer [16]**

*Battery model in Simulink*

Simulink block with input output signals is shown in Fig. 62
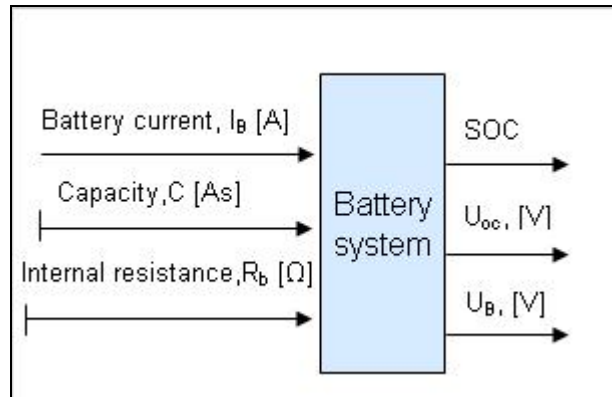


**Figure 62. Battery model input-output signals**
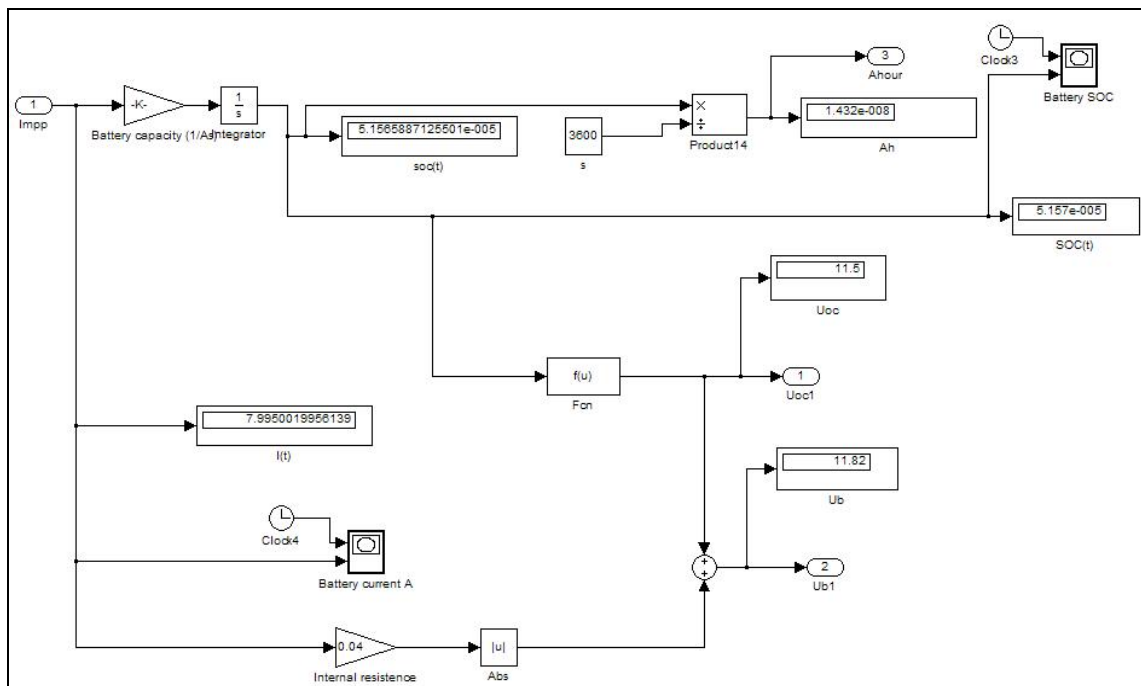


**Figure 63.  Battery model in Simulink**

In order to prove the model in Simulink, the result of simulation as battery SOC and voltage are plotted in Figure 64.

As it can be seen from Figure 64 when the battery voltage increases the SOC of the battery increases as well.
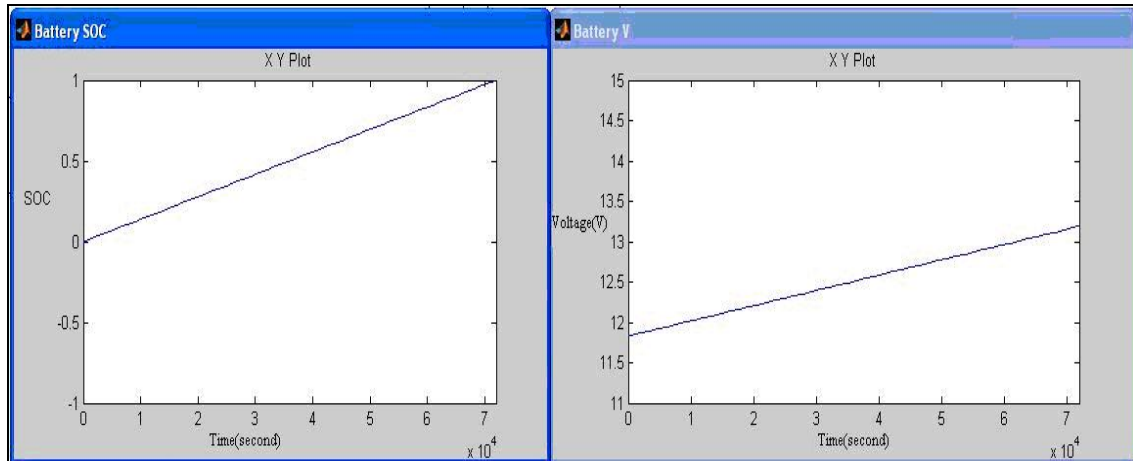
**Figure 64. Battery model result in Simulink**

### 3.2.7 DC/DC converter

The MPP trajectory of the PV array can be aligned with the U-I characteristic of the electrolyzer using appropriate designs of the PV array and electrolyzer (for example by varying the number of serial connected modules and the number of parallel module strings of the PV array [13]), or by using MPP tracker (part 3.1.7). That means that MPP tracker ensures that electrolyser use all available power delivered by PV array, even when solar irradiation is varying.

On the Fig. 65 it is shown what would be happen if PV system (consider in this work) would be connected with the electrolyser (from Appendix), without MPP tracker in between. The data for this Figure regards PV system are given in the Table 18. The electrolyser working characteristics are produced by data from Fig. 44.

**Table 18. Electrical performance of PV array [13]**

| $E$ [W/m$^2$] | $U$m [V] | $I$m [A] | $U$oc [V] | $I$sc [A] | $t$ [°C] | $FF$ |
|---|---|---|---|---|---|---|
| 1000 | 46 | 116 | 63.81 | 125.1 | 47.8 | 0,67 |
| 700 | 47 | 80.76 | 61,4 | 87.58 | 40 | 0,71 |
| 500 | 47 | 58.32 | 59.76 | 62.56 | 35.8 | 0,73 |
| 300 | 47 | 34.99 | 57.64 | 37.54 | 32 | 0,76 |
| 100 | 45 | 11.66 | 53.5 | 12.51 | 25 | 0,78 |
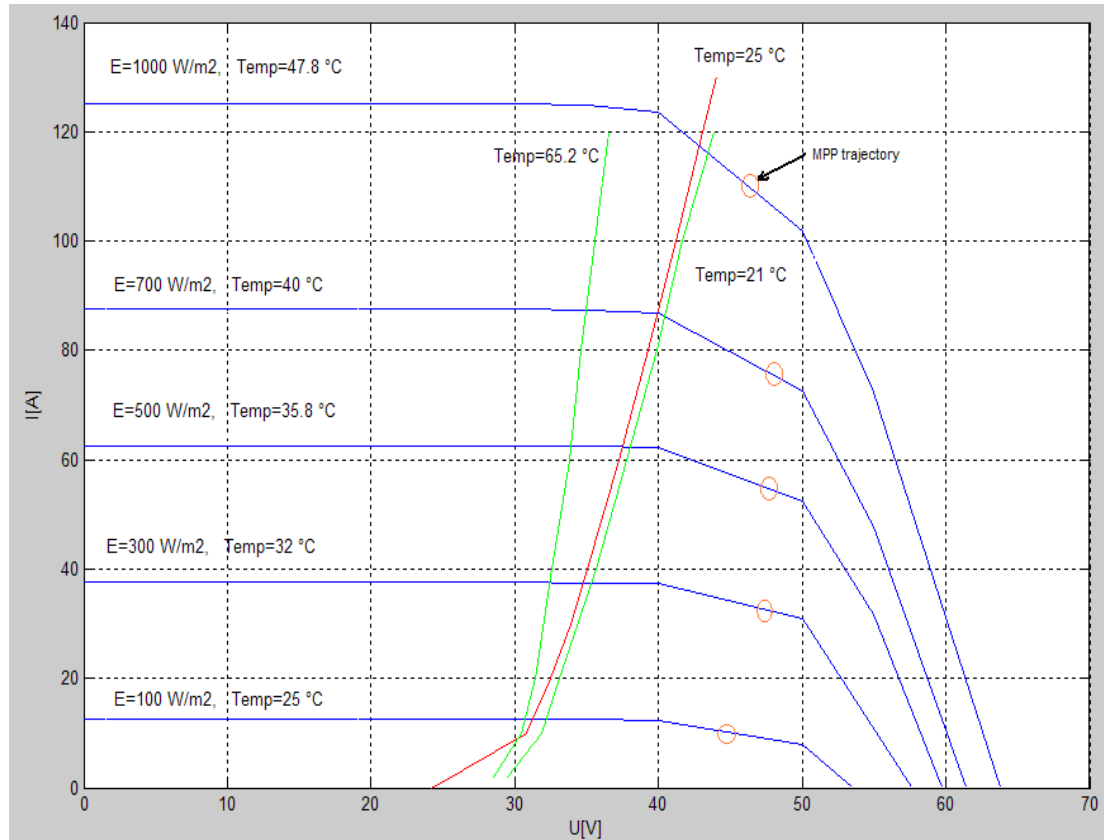
**Figure 65. Working points of the system PV array and electrolyser at different electrolyser and PV array temperatures**

PV array MPP trajectory depends on PV cell temperature and solar irradiation intensity, and electrolyser U-I characteristics (Fig.49) turns to the left with the rising of electrolyser temperature, which means even with the best arrangement of the standard modules in array (with the aim of the closest possible electrolyser working characteristics to the MPP trajectory), under real working conditions the MPP tracker will be needed.

In the simulations of the three scenarios (part 3.4) electrolyser characteristics at electrolyser temperature of 25 °C was used. Model of the electrolyser (eq. 3.8) was derived just for this temperature. In future work eq. 3.8 can be adapted with the influence of the temperature.

In this work only DC/DC conversion is used, both for electrolyser and battery. The same principle is applied to household appliances (chapter 3.1.9 and 3.2.9).

*Mathematical model of the DC/DC converter for electrolyser*

$$P_{in(electrolyser)} = P_{out(electrolyser)} \qquad\qquad (3.33)$$

$$U_{PV} I_{PV} = \eta_{DCDCE} U_E I_E \qquad\qquad (3.34)$$

$$I_E = P_{in(electrolyser)} / (\eta_{DCDCE} U_E) \qquad\qquad (3.35)$$

$$\eta = 0.95$$

*DC/DC model in Simulink for electrolyser*

Simulink block with input output signals for DC/DC convertor for electrolyser are shown on Fig. 66.
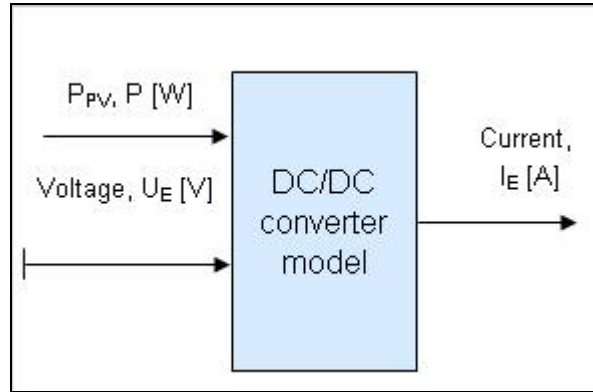

**Figure 66. DC/DC model input-output signals**

*DC/DC converter model in Simulink for electrolyser*

Simulink model in detail (based on eq. 3.35) is shown in the Fig. 67.
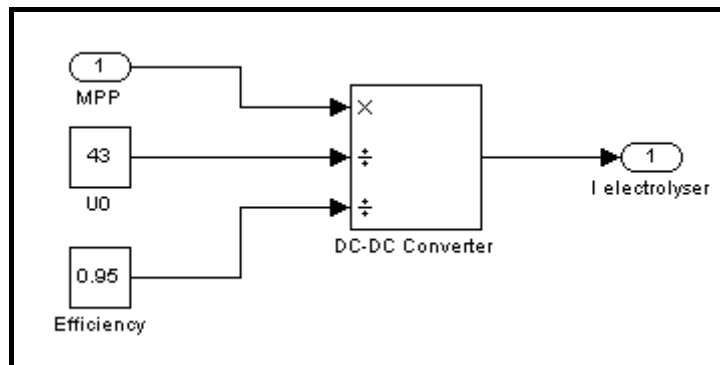

**Figure 67: Converter model in Simulink for electrolyser**

*Mathematical model of the DC/DC converter for battery*

$$P_{in(battery)} = P_{out(battery)} \qquad\qquad (3.36)$$

$$U_{PV}\, I_{PV} = \eta_{DCDCB}\, U_B\, I_B \qquad\qquad (3.37)$$

$$I_B = P_{in(battery)} / (\eta_{DCDCB}\, U_B) \qquad\qquad (3.38)$$

$$\eta_{DCDCB} = 0.95$$

*DC/DC model in Simulink for battery*

Simulink block with input output signals for DC/DC convertor for battery are shown on Fig. 68.
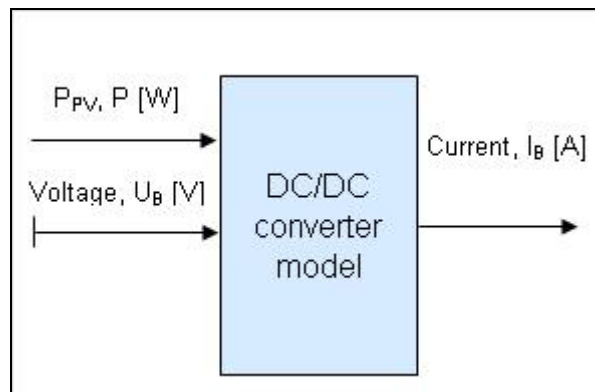


**Figure 68. DC/DC model input-output signals**

*DC/DC converter model in Simulink for battery*

Simulink model in detail (based on eq. 3.38) is shown in the Fig. 69.
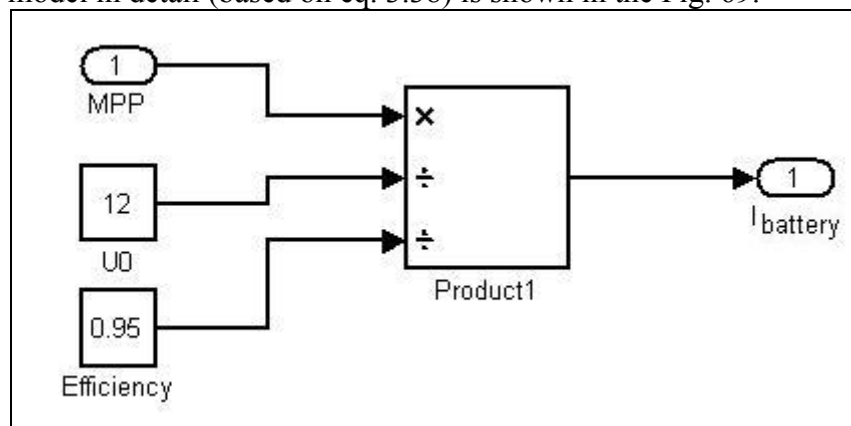


**Figure 69.  Converter model in Simulink for battery**

**3.2.8    Control system**

The task of the control system is that by default rules and working conditions switch on and off system components individually for the production and consumption of electricity. One of the main problems is the management strategy which ends up two options. Control system can manage the system very fast in the best mode or "planned" in a long-term.
Short-term goals usually include a period on a one day. Long-term objectives can be taken into account and predict future conditions, which are not discussed in this work. It is also possible to connect the control system with a weather station for short and/or long term system guidance.

*The concept of control system*

The control system must be able to identify conditions and on this basis switch on and off the components. The basic division of power flows can be divided in "Hydrogen" and "battery" sections. Each part has two states: charging and discharging. In "Hydrogen" charging is a part of the electrolyser work and discharge is to work of fuel cell. The battery can be charged and discharged, but not at the same time. In "hydrogen" section, the situation is different, because at the same time can work electrolyser to fill the storage tank and fuel cell to empty the tank.

From these explanations it is concluded that if the battery is in charging mode; all need to electricity is supplied from the fuel cell. If the battery is empty, then all the energy from the PV is used to run electrolyser and hydrogen production. The priority is to use battery as much as possible because of better efficiency compared to the hydrogen cycle. Actually the point is to use the battery for short periods on a daily basis or weekly and hydrogen for long-term needs.

The control system should have the information (signals) of the individual components such as SOC, $P_{H2}$ and the need for electricity consumption (load).

*Control system logic*

Since the models of components which controller should be managed, using Simulink, and then the controller is running in the same program. The control system is designed in Simulink and all analysis and descriptions is based on the Simulink model.

The controller is implemented using Simulink blocks "Embedded MATLAB function", and operating under the influence of input signals. It may be noted that there are output signals returning to the controller, and feedback. They are essentially known to the controller where state of the output variables, and then formed basis on that in the next steps.

To be able to run the simulation at all, it is necessary to adjust the feedback so not to cause numerical errors. Blocks of "Memory" which is located on the signal feedback connections are necessary in order not to generate algebraic loops that cause errors (stop simulation) during the simulation. "Memory" blocks retain the value of the last integration steps, thus effectively causing the delay of signals from one time step (step size). Therefore, the signal is no longer "closed" in itself directly, but with some delay. Of course, these adjustments cause errors, but at this level it is neglected.

Output variables of the controller are:

 BATTERY_CONSUMPTION_SWITCH_OUT
 SYS_VOLTAGE_SWITCH_OUT
 ELECTROLYSER_SWITCH_OUT
 FUEL_CELL_SWITCH_OUT

these variables are defined so that they can take the values 0 or 1. Their task is to manage the switches that have two positions as it turns on or off certain elements. Used block "Switch" is shown in Fig. 70.
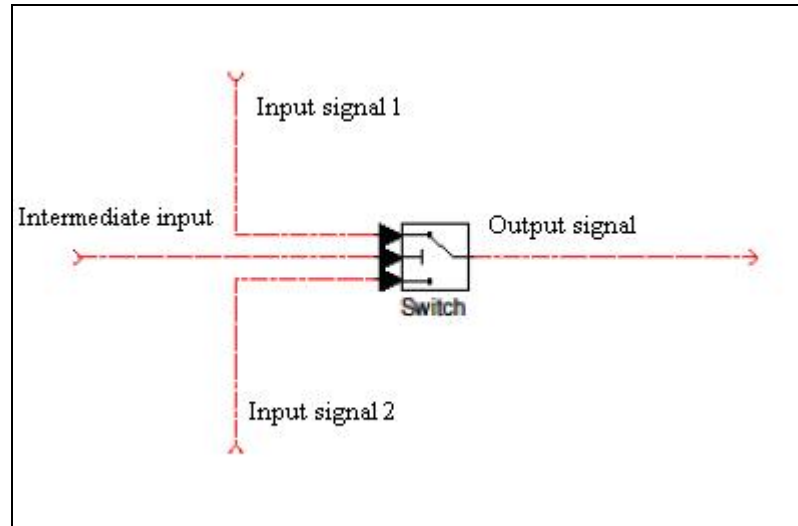
**Figure 70. Switch with input and output signals**

Intermediate input (Fig. 70) switch is in one of the above variables and in fact it determines the position of the switch. The remaining two signals are the real power flows from individual components. The output signal is actually one of the two input signals is based on control signal transmitted through a switch.

Input variables in the controller are:

LOAD
SOC
H2

These three variables represent the current electricity consumption (load), battery state of charge (SOC) and state of storage tank of hydrogen (H2).

The structure of the controller is defined by logical conditions. Based on the input variables, controller performs comparisons and other functions on the basis of which determines the state of output of variables. Here is applied approach as in [19]. The structure of the controller is as follows:

```
function
[BATTERY_CONSUMPTION_SWITCH_OUT,SYS_VOLTAGE_SWITCH_OUT,ELECTRO
LYSER_
SWITCH_OUT, FUEL_CELL_SWITCH_OUT]= fcn(LOAD, SOC,H2,
BATTERY_CONSUMPTION_SWITCH, SYS_VOLTAGE_SWITCH,
ELECTROLYSER_SWITCH,
FUEL_CELL_SWITCH)
BATTERY_CONSUMPTION_SWITCH_OUT=BATTERY_CONSUMPTION_SWITCH;
SYS_VOLTAGE_SWITCH_OUT=SYS_VOLTAGE_SWITCH;
ELECTROLYSER_SWITCH_OUT=ELECTROLYSER_SWITCH;
FUEL_CELL_SWITCH_OUT=FUEL_CELL_SWITCH;
if SOC >=0.4
BATTERY_CONSUMPTION_SWITCH_OUT=1;
SYS_VOLTAGE_SWITCH_OUT=1;
```

```
ELECTROLYSER_SWITCH_OUT=1;
FUEL_CELL_SWITCH_OUT=0;
end;
if SOC <=0.3
BATTERY_CONSUMPTION_SWITCH_OUT=0;
SYS_VOLTAGE_SWITCH_OUT=0;
ELECTROLYSER_SWITCH_OUT=0;
end;

if H2 < 30
    if BATTERY_CONSUMPTION_SWITCH_OUT==0
        ELECTROLYSER_SWITCH_OUT=1;
    end;
else
    ELECTROLYSER_SWITCH_OUT=0;
end;
```

The basic principle is to use the batteries whenever possible. Because there minimum level of battery charge is 30% which was selected based on recommendations. It is not allowed to go below that level. When the battery is on discharging phase and when it comes to the level charge drops 30%, consumption is shifted to fuel cell and battery switches the charging regime. Review of the system leads to the conclusion that the battery is able to switch to the regime of the discharge as soon as charging in a value that is only slightly greater than a given critical value of 30%. Such work would not be good because the battery and fuel cell constantly (or alternatively) turning on and off between themselves. Therefore, a certain upper limit to that the battery must be charged in order to reset the discharge regime. This value is selected 40%. Designed controller will actually keep the battery minimum voltage in the range of 30% to 40%.

The variables that determine the conditions previously mentioned variable ending "_OUT". One determines the position of switches.

Change switch positions during the simulation increases the likelihood of certain errors that prevent successful completion of the simulation. Here is an explanation of the problem and its solution. By changing the switch position the output variable changes momentarily (dt = 0) to new value. This means that at the same time there are two output values, which makes fatal error and simulation stops. In order to prevent these phenomena, the transfer function (Fig. 62) was put just after the switch.



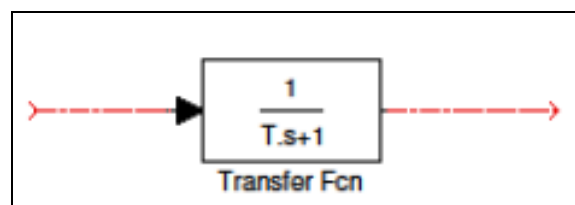**Figure 71. Transfer function that allows the simulation works**

The transfer function changes the shape of the signal in time. The time constant "T" in the transfer function can be assumed as "amount of the deformation of the signal." If the specified time constant was equal to zero, then in fact there would be no changes of the output signal but "fatal error" would arise. It is enough that the

constant has a certain small value, to simulation proceed. In the model the value of time constant is T = 0.001.

There is also a drawback to use these transfer functions. Due to very small values of the time constant, the simulation time can be significantly higher. The reason is that the maximum time integration steps (step size) should not be greater than half of the minimum time constant in the simulation model (this in according to Nyquist-Shanon theorem).

### 3.2.9 Appliances load model

In this study, the loads are battery, electrolyser and appliances. Electrolyser and battery are treated separately in parts 3.2.2 and 3.2.6. Here will be only appliances load discussed.

There are ten compact fluorescent lamps ($10 \times 18$ W), a TV (80 W), a computer (90 W), one refrigerator, one freezer, one washing machine, one dryer and one electric stove. They can be divided into two groups based on the type of power consumption: these are, continuous, and intermittent power consumption loads. Also they can be AC or DC type.

The loads, consuming constant electrical power and running continuously from the time they are turned on until they are turned off, are defined as the continuous power consumption loads. The power consumption of the refrigerator comes from two main components: the compressor and the accessories which include a thermostat, a control unit and an internal circulating fan.

The power demand of the appliances loads ($P_{Load}$) can then be expressed as:

$$P_{Load} = C1 P_{light} + C2 P_{computer} + C3 P_{TV} + C4 P_{refrigerator} + C5 P_{freezer} + C6 P_{washingmachine} + C7 P_{dryer} + C8 P_{electric\,stove} \quad (3.42)$$

$P_{light}$, $P_{computer}$, $P_{TV}$, $P_{refrigerator}$, $P_{feezer}$, $P_{washingmachine}$, $P_{dryer}$ and $P_{electricstove}$ are the power demands of the compact fluorescent lamps, TV, refrigerator, freezer, washing machine, dryer and electric stove, respectively.

C1, C2, C3, C4, C5, C6, C7 and C8 can be controlled functions corresponding to the appliances which they are associated with. They are equal to "1" when their corresponding loads are turned on; otherwise they are equal to "0". But they also can be distributed across the time (here for the purpose of simulation, one day).

For example, in this study for the purpose of simulation during one day period, the lamps and TV and computer are turned on from 18:00 hr until 22:00 hr every day while the refrigerator and freezer are always plugged in to the electrical receptacle. Washing machine and dryer work one hour per week (8,4 minutes per day) and electric stove for cooking one hour per day. The compressors in refrigerator and freezer are working like on and off during a day i.e. periodically.

As we can see, mathematical model of the appliances load ($P_{Load}$) can be very complicated function of time including AC or DC current needs. For the purpose of this work it is supposed that all appliances need DC current. Further, this current should be supplied by power system according to particular function in time during one day. This function was calculated separately, taking into account particular

appliance power, voltage, internal ohmic resistance and on/off working period. The result is the appliances load equivalent resistance given on Fig. 72. This (in fact input function to the whole "complete power system simulation block") in connection with Ohm's low (basic equation for Simulink block given on Fig. 74, and Fig. 75) presents how appliances load were modeled and simulated.

Thus, current, $I_L$, as output signal from the load block on Fig. 74, sometimes can represent current supplied by the battery and sometimes, by the fuel cell, depending upon the controller decision.

*Mathematical model of the electric loads (household appliances)*

$$I_L = U / R_L \qquad (3.39)$$

where

$U = U_{FC}$ when fuel cell works (hydrogen is consumed from the storage tank)
$U = U_B$ when battery is discharging

Because of simplifications of simulation, instead of $U_B$ which should be working voltage, $U_{OC}$ of the battery was used. It is assumed that introduced resulting error would be acceptable. $U_{OC}$ is at the same time corresponding of the SOC according to battery manufacturer (Appendix).
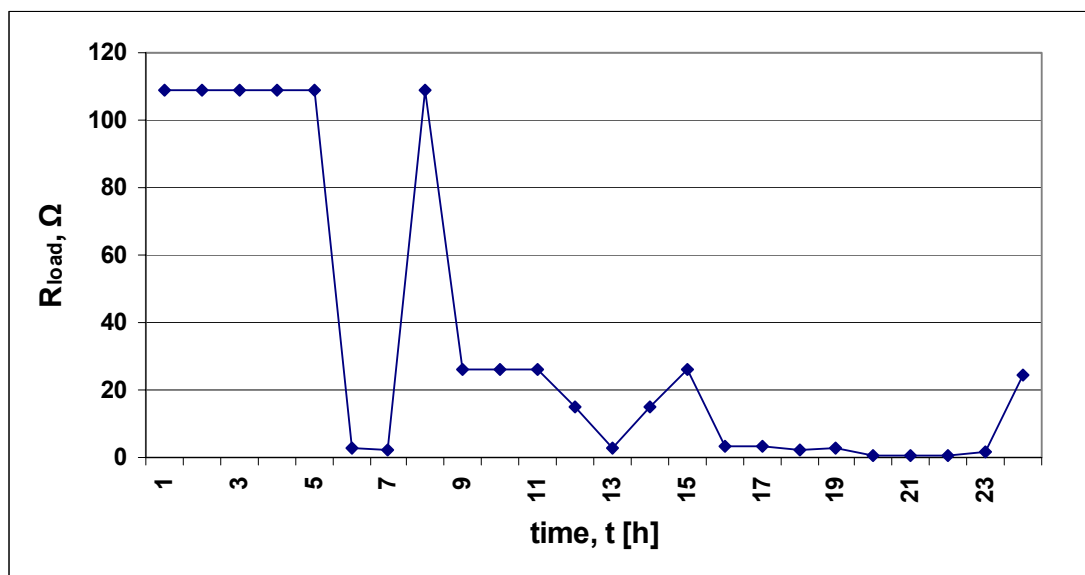


**Figure 72.  Equivalent DC electric load ohmic resistance profile for specified day (input signal to the "Complete power system simulation block" shown on Fig. 75 and Fig. 76.)**

Fig. 73 represents real equivalent power of the load.
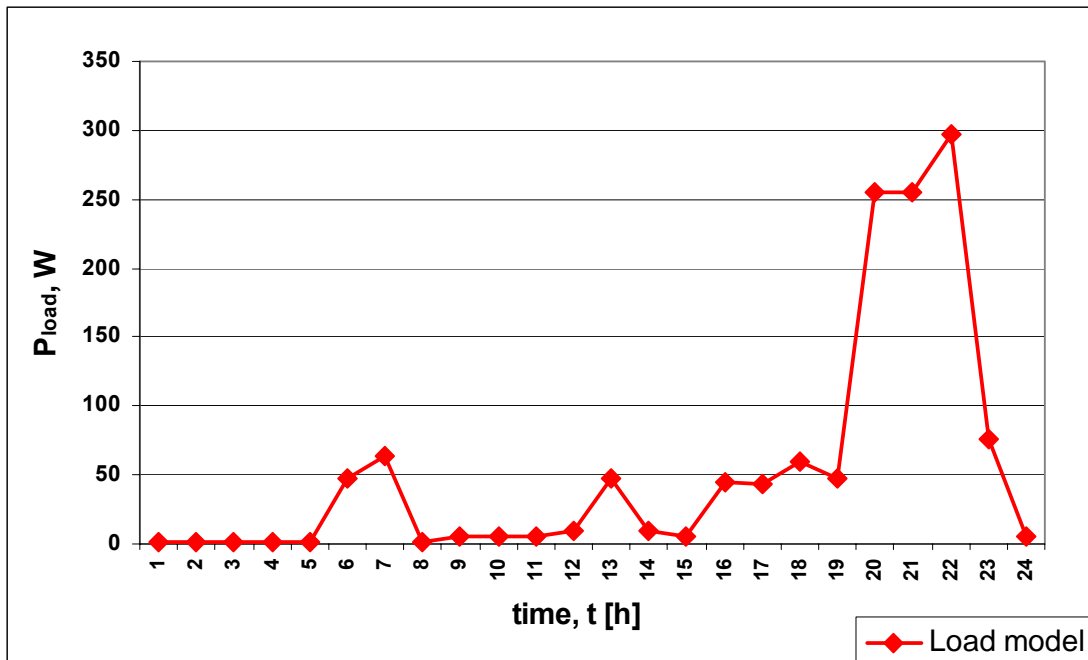
**Figure 73. Equivalent DC electric load power profile for specified day**

If equivalent resistance curve given on the Fig. 72 would be used as input for simulation, it would be very difficult interpret the simulations results. Because simulation should only to confirm that controller and system "Complete power system simulation block" performs as expected, more simply equivalent resistance curve will be supposed. Shape of this resistance curve in reciprocate form during one day is given as input signal on Fig. 81.

*Simulink model of the electric loads (household appliances)*
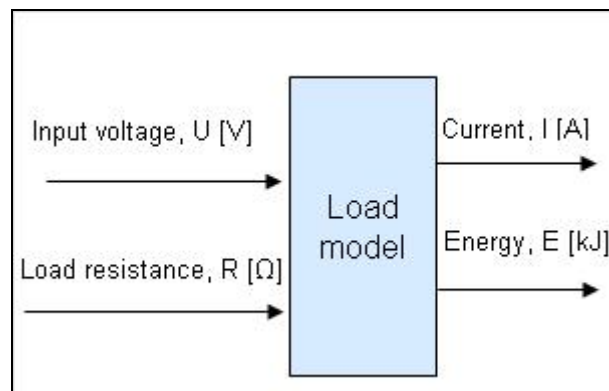


**Figure 74. Load model block input-output signals**
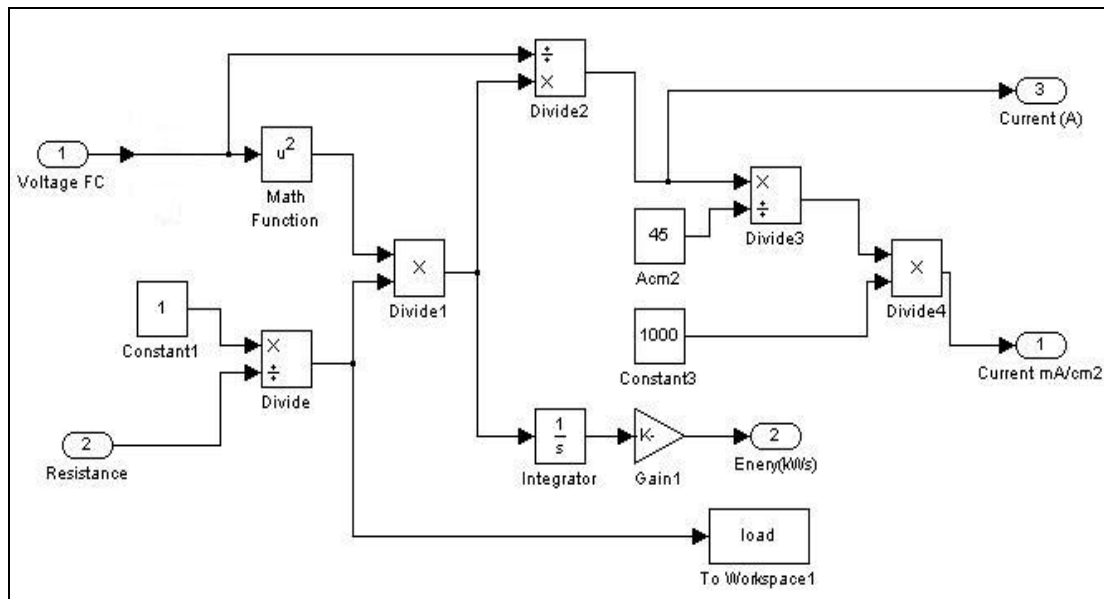
**Figure 75.  Appliances load model in Simulink**

In fact, equivalent appliances load resistance from Fig. 81 is the input signal to block "Load model" on Fig. 74, Fig. 75, Fig. 76 and Fig. 77.

## 3.3    Complete power system simulation model

The most important values of the power system are: PV surface, battery and hydrogen tank size. Solar energy is collected by the PV-modules MF120EC4, 120Wp, Mitsubishi. These modules have the originally 36 cells in series.

Simulations were performed with the following sizes:

   - Number of PV panels: Np = 17, Ns = 3 ; i.e. 51 modules
   - Battery capacity.  7751.9 As
   - The volume of hydrogen tank: 0.1 m$^3$

The initial conditions influence the results of the simulation. The initial conditions are equal and as follow:

   - Battery charge (SOC):                      1.00 (100%)
   - The pressure in the tank of hydrogen:    4 bar

The shape of solar radiation during the one day is also made simpler than it usually is. The shape is the curve "Solar irradiation" given on Fig. 81. As it can be seen, it has form of a triangle.

*Simulink model of the complete power system simulation block*
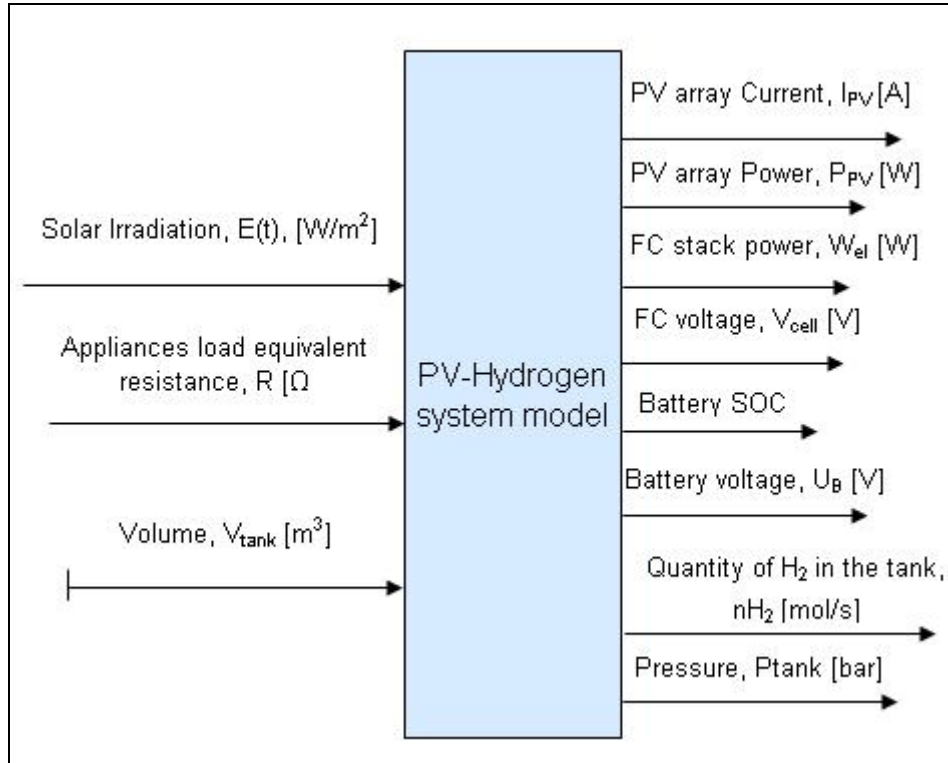


**Figure 76.  Input/output signals in "Complete power system simulation block"**
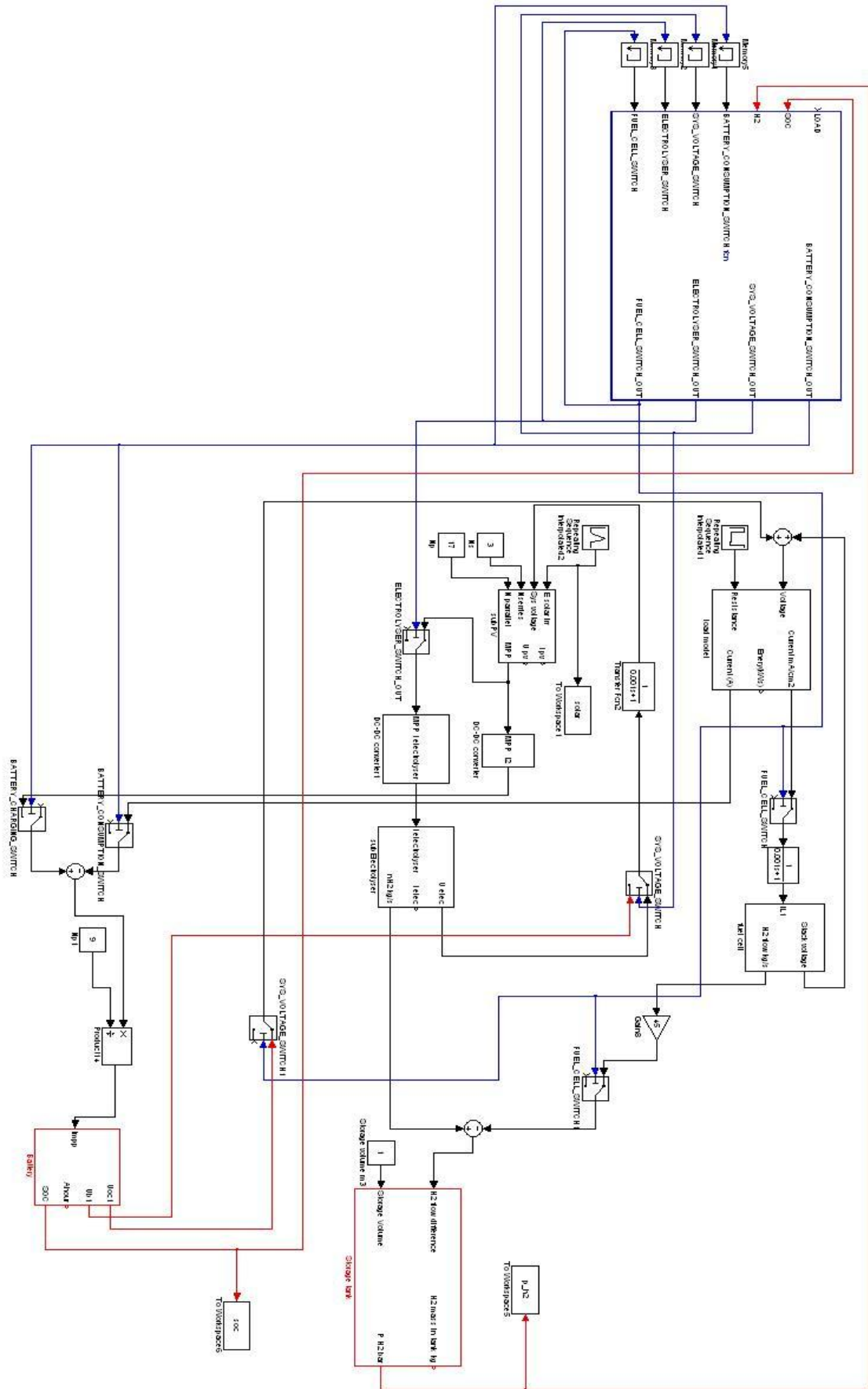
**Figure 77. Whole system simulation Simulink block scheme**

### 3.3.1 First scenario

In order to prove the controller system function, different scenarios are performed. The task of controller is based on some external conditions carry all three scenarios without manual intervention during the simulation. Therefore, the requirements of the scenario should be consistent with the strategy and the internal logic controllers. The scenarios are defined based on work status of individual system elements, and external conditions (solar radiation and energy consumption).

The conditions which are taken into account for first scenarios are as follow:

- Solar PV system works
- Battery is fully charged
- Load does not need electricity
- Fuel cell doesn't work
- Storage tank is partially full
- Electrolyser works

Components which are in function are highlighted with red color.
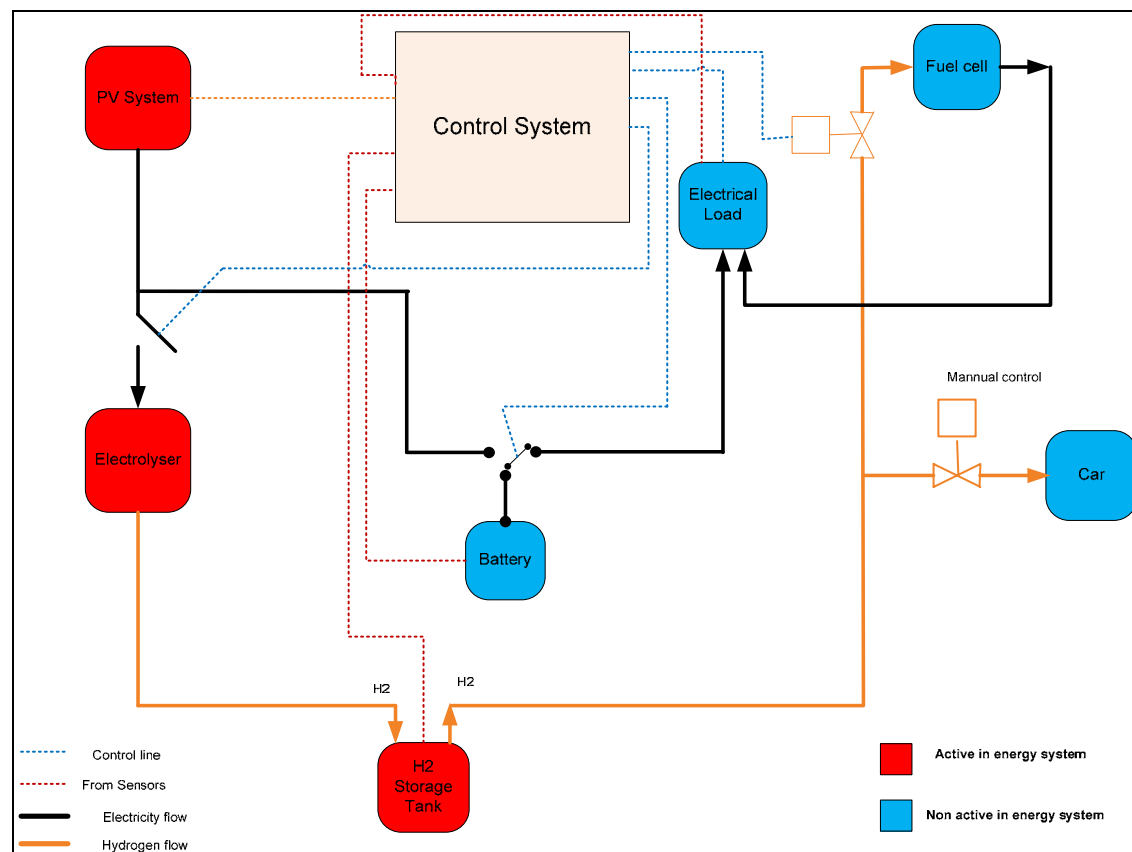


**Figure 78. Schematic of the model for first scenario (PV and electrolyser work)**

### 3.3.2    Second scenario

In the second scenario different conditions are considered which are given in below:

- Solar PV system does not work
- Battery SOC is 30%
- Minimum load request should be fulfilled
- Fuel cell works
- Storage tank should have enough hydrogen to supply and cover the need for minimum one day
- Electrolyser does not work
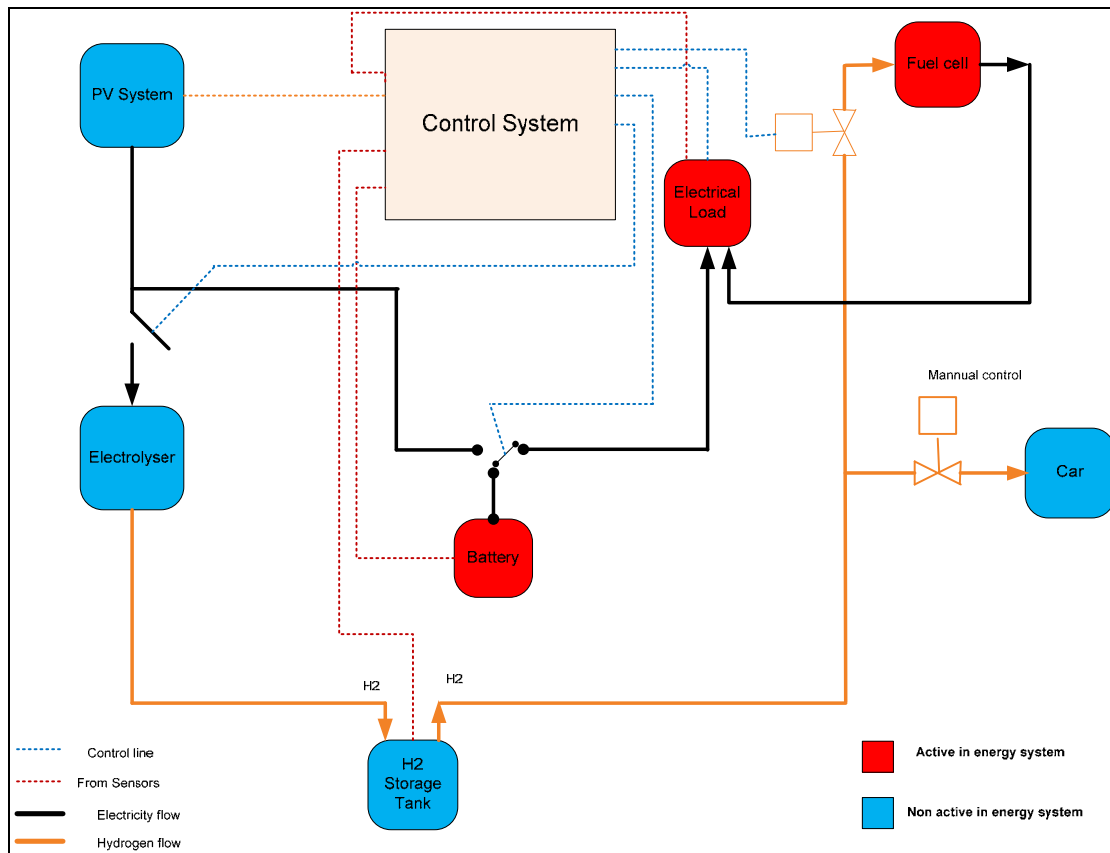


**Figure 79.  Schematic of second scenario (Just Fuel cell works)**

### 3.3.3    Third Scenario

In this scenario just battery is running and working to meet the load, other parts of the system are not in function.
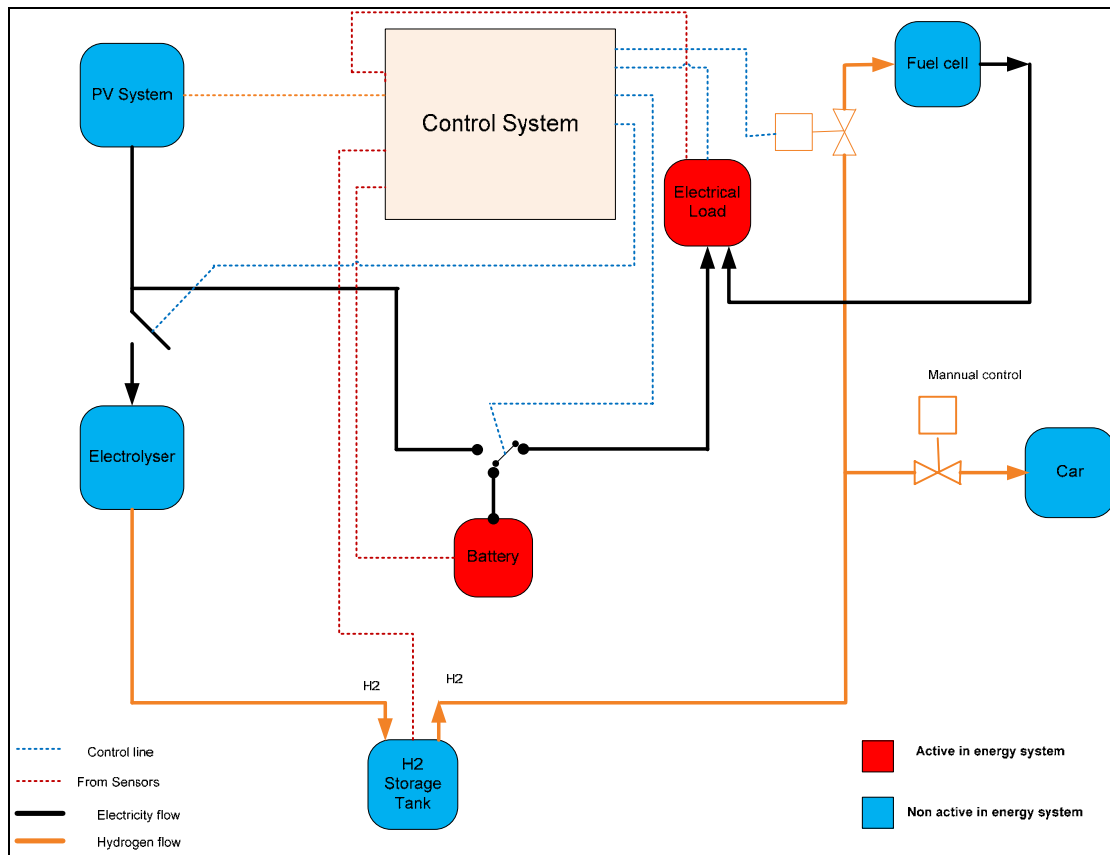
**Figure 80.  Schematic of third scenario (Just batteries work)**

## 3.4    Simulation results of the "whole system simulation block scheme"

The whole system simulation block scheme is given on the Fig. 77.
External conditions which affect on the operation of system are solar radiation (curve "Solar irradiation" on Fig. 81) and energy consumption (curve "Electricity consumption" on the same Fig. 81). Initial conditions are given in 3.3.

### 3.4.1    Simulation results covering all three considered scenarios(for the purpose of  the proving "whole system simulation block scheme")

Result of scenarios can be seen in the diagram shown in Fig. 81.
*Period 0 h - 6 h* Only very small electricity consumption exists (0.001). This is quite visible on the curve "Electricity consumption". Solar radiation does not exist. This is visible on curve "Solar irradiation". Pressure in the hydrogen tank is equal 4 bar. This is visible on the curve "Hydrogen storage tank pressure", and shows that fuel cell stack does not produce electricity. Battery covers small electricity consumption because it has higher priority than fuel cell stack. SOC of the battery slightly drops. This is visible in the curve "SOC battery".
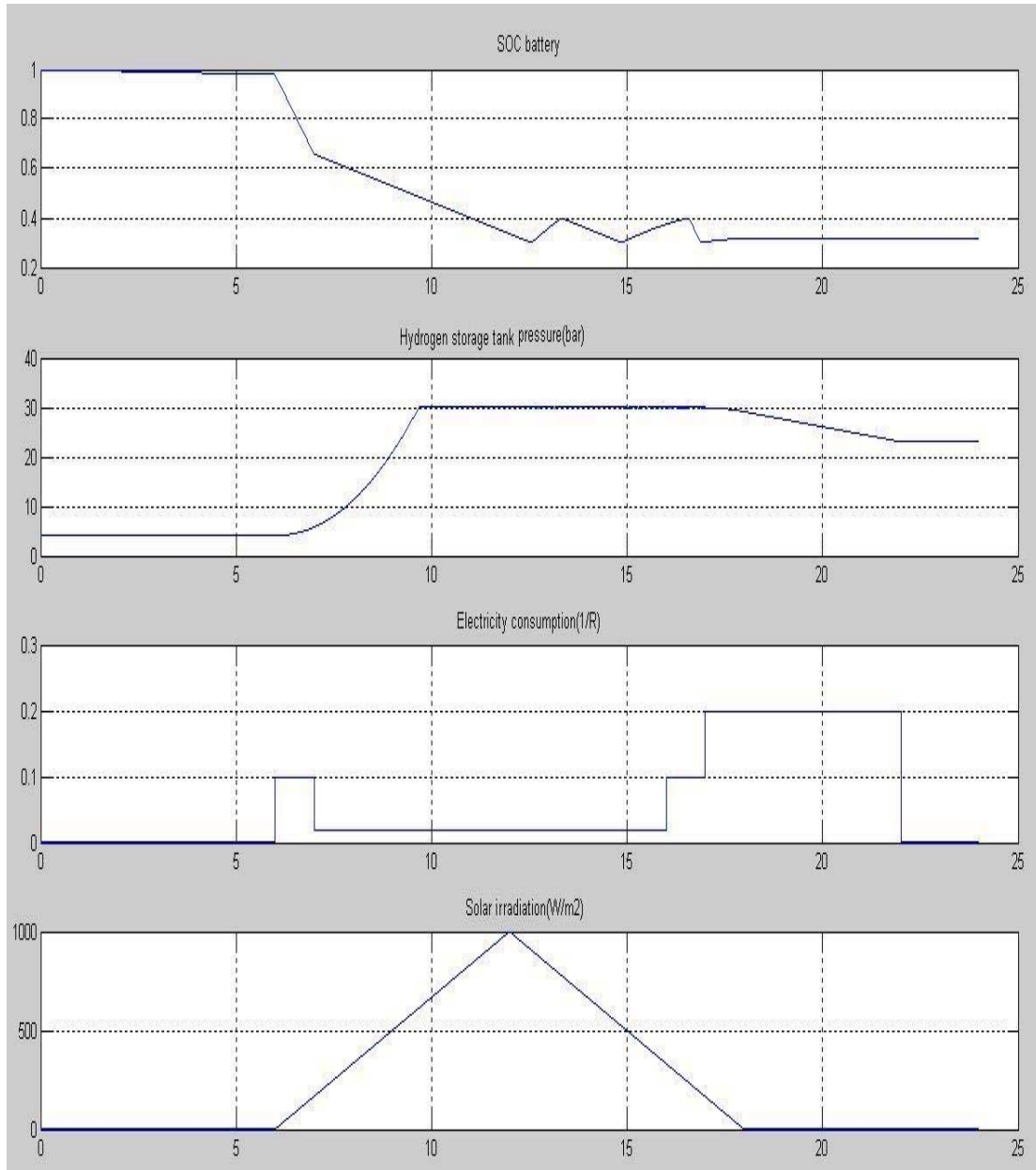
**Figure 81. Simulation results according to scenarios**

*Period 6 - 7 h* Electricity consumption sharply jumps and during period of 1 h has the constant value (0.1). At the same time solar irradiation starts to rise. Because of higher priority battery supply the requested bigger amount of energy and because of that curve "SOC battery" sharply drops in this period. At the same time electrolyser starts produce hydrogen which is stored in the tank. Hydrogen pressure start to rise as it can be seen from the curve "Hydrogen storage tank pressure".

*Period 7 - 16 h* Electricity consumption sharply drops at 7h and take the constant value 0.02. During this period solar irradiation continue to rise up to 1000 W/m2 at 12h and then gradually decrease (to 0 W/m$^2$ at 18h). Hydrogen pressure continues to rise and when it comes to the tank limit (30 bar) it stay constant. Battery SOC continues to gradually decrease up to the value of 30 % what is allowable minimum.

Within this period we have interesting situation between 12.5 and 16 h. This is charging, and discharging the battery, work of electrolyser at the same time as the fuel cell stack (filing and emptying of the hydrogen storage tank).

84

*Period 16 - 22 h* Electricity consumption rises step by step to 0.2. This is quite high consumption, battery is between 30 and 40% SOC and fuel cell stack uses hydrogen, so pressure in the tank drops gradually, especially because there is not more hydrogen production, i. e. there is not solar irradiation.

*Period 22 - 24 h* Again electricity consumption is very small (0.001), battery is empty, electrolyser does not work, but fuel cell stack works and draw only very small hydrogen quantity so hydrogen pressure drops extremely slow.

# 4   Discussion

## 4.1   Passive house in terms of energy consumption

The reason that in this work was selected passive house concept is to minimize the energy demand in accordance with the global principle of sustainability, while at the same time improving the comfort experienced by building occupants. It thus creates the basis on which it is possible to meet the remaining energy demand of new buildings completely from renewable sources.

Through the Passive House concept a considerable energy saving compared to the Existing one can be obtained. This energy saving potential for a single residence goes together with $CO_2$ emission reductions of about 50% to 65%. So if we wanted to design autonomous solar-hydrogen system, for the conventional system it would be at least two times bigger for PV system, fuel cell stack, electrolyser and all other relevant components.

The small heating load is roughly equivalent with an annual space heat requirement of 15 kWh/(m$^2$a). Passive houses thus need about 85% less space heat than new buildings designed to the various national building in Europe and specially in Croatia.
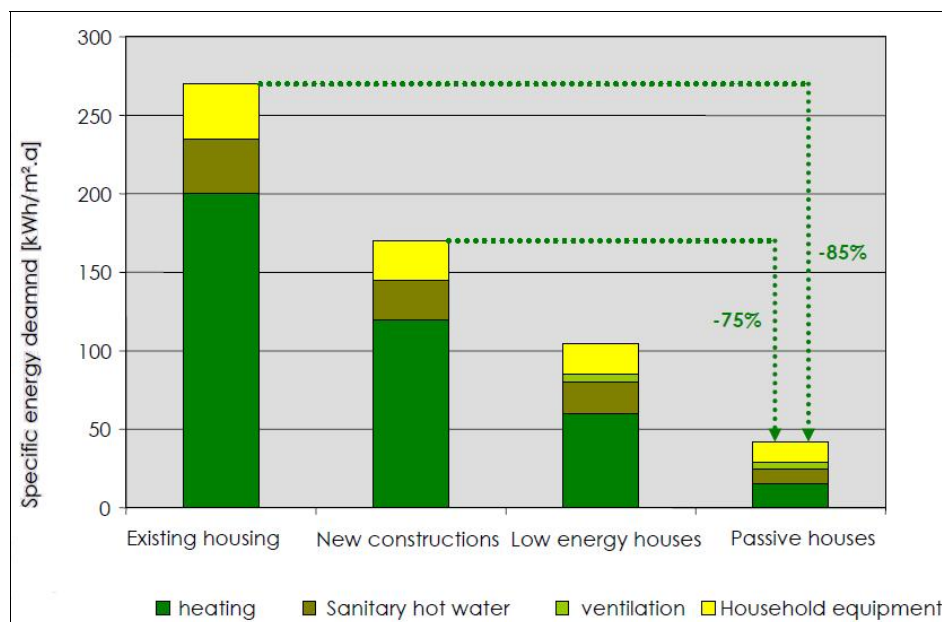


**Figure 82. Comparison of energy consumption of passive house and other buildings**

## 4.2 Summary of household energy system

In the Table 20 the summary of energy system used in the passive house are given.

**Table 19. Summary of energy system in the passive house**

| Components and quantities | Dimension | Value |
|---|---|---|
| Space heating system | | |
| Total heating load | kWh/year | 4395.7 |
| Solar collectors area | $m^2$ | 7 |
| Solar thermal collectors area | $m^2$ | 3 |
| Water tank volume | $m^3$ | 0,750 |
| Space cooling system | | |
| Type of system: solar desiccant cooling | | |
| Total cooling load | kWh/year | 5204.1 |
| Cooling power capacity | kW | 10 |
| Power of motor for desiccant wheel | kW | 0,12 |
| Power of cooling power pump | kW | 0,3 |
| Ventilation rate of conditioned space | $m^3/h$ | 500 |
| Power system | | |
| Photovoltaic array total area | $m^2$ | 46,94 |
| Number of modules | pcs | 51 |
| Nominal power of module | kW | 0,12 |
| Total power of PV array | kW | 6,12 |
| Fuel cell | | |
| Installed power of fuel cell stacks | kW | 2,4 |
| Maximum hydrogen consumption | SLPM* | 36 |
| Maximum water production | l/h | 1,6 |
| Maximum heat production | kW | 4,8 |
| Maximum FC system efficiency | % | 50 |
| Electrolyser | | |
| Power of electrolyser | kW | 5 |
| Number of electrolysis cells | pcs | 22 |
| Rate of hydrogen production | $Nm^3/h$ | 1 |
| Overall energy consumption | $kWh/Nm^3 H_2$ | 4,9 |
| Surface area | $cm^2$ | 300 |

*SLPM   - standard litter per minute

# 5    Conclusion

In this work was performed stationary state calculation of heat flows of passive house and modeling and simulation of dynamics of the off grid passive house power system. The house is located on island Hvar, Croatia. The passive house consists of heating system, cooling system and power system. Heating system provides heat from solar collectors for space heating. Cooling system uses solar thermal energy for space cooling.(desiccant system). Power system consists of photovoltaic array and hydrogen technology based energy storage system. Energy storage system consists basically of electrolyser, hydrogen storage and fuel cell stack. Excess solar energy can be used by electrolyser for hydrogen production. Produced hydrogen is stored in the tank for subsequent use in fuel cell stuck for power production. Also alternatively it can be compressed on the higher level pressure to use as fuel in hydrogen based truck. The household has electrical appliances, lights and DC motors. All of that are supposed to be as DC loads.
Power system is controlled by automatic control provided by controller.

Above mentioned power system was mathematically modeled and simulated using Matlab Simulink software. The power system consists of commercially available components except electrolyser. The electrolyser was produced only once for research purpose from Hystat company. This allows a real input data to be used in simulation. Such one model with real input data can produce real outputs according to chosen scenario.

Model of the system components were checked by simulation in Simulink individually and in groups of two subsystems (PV array and electrolyser or fuel cell and load). Also controller has been checked using two scenarios.

In the first scenario it was considered the daily PV system works to supply electricity to the electrolyser to produce hydrogen while other components were not working.

In the second scenario night period when PV system and electrolyser are not in function and storage tank has enough hydrogen to supply fuel cell also battery SOC is in 30% level for critical situation.

It should be mentioned that there are lots of scenarios which can be considered but in this work in order to prove that simulation works properly, two most interesting situation are given.

The results of this work are mathematical model of the off-grid power system consisting of photovoltaic and hydrogen technology based components. This model can be used as a tool to test different scenarios corresponding to different purposes as follows:

a) for given solar radiation time sequences different hardware parameters can be tested.(for studying the influence PV surface area, number of cells in electrolyser, volume of hydrogen storage tank, etc…) to study energy availability  profile during the same time sequences

b) For given fixed hardware parameters to study energy availability of the household under influences of changing solar radiation during the time sequences.

There are some differences between supposed thesis proposal requests and achieved results. This mainly concerns the insufficient computing power needed for detailed one year simulation of the stand-alone power system.

# References

[1] Dr. Wolfgang Luther, Application of nanotechnologies in energy sector, Volume 9 of series Aktionslinie Hessen Nanotech of the Hessian Ministry of Economy, August 2008, pp.18

[2] Fuel Cells-Green power, Sharon Thomas and Marcia Zalbowitz, New Mexico

[3] http://passiv.de/en/index.html

[4] http://www.cepheus.de/eng/index.html

[5 ] http://www.mca.si/fsi/mca/2007_mca/marles/catalog-hise_2007.html

[6] http://heatweb.com/literature/Solar and Heat Pumps/Viessmann Heat Pumps and Solar/HeatingGuide.pdf

[7] http://ec.europa.eu/energy/efficiency/labelling/labelling_en.htm

[8] Applied solar Technology, FSB Zagreb, Edition 2004, Damir Duvić

[9] Hans-Martin Henning, Solar – assisted air- conditioning in buildings, Handbook for planners, Springer, Wien, 2004, pp. 25

[10] http://www.etecevs.com/pdf/h2_ice.pdf

[11] Studying and Improving the Efficiency of Water Electrolysis Using a Proton Exchange Membrane Electrolyser, by IOANNIS PAPAGIANNAKIS, 2005

[12] Øystein Ulberg, stand-alone power systems for the future: optimal design, operation & control of solar-hydrogen energy systems, December 1998, pp.184

[13] Firak, M., et al.: An investigation into the effect of photovoltaic module electric properties on maximum power point trajectory with the aim of its alignment with electrolyser U-I characteristic, Thermal science: Year 2010, Vol. 14, No. 3, pp. 729-738

[14] Thermal performance of a commercial alkaline water electrolyser: Experimental study and mathematical modelling, P.M. Dieguez, A. Ursua, P. Sanchis, C. Sopena, E. Guelbenzu, L.M. Gandıa, International journal of hydrogen energy 33 ( 2 0 0 8 ), pp 7338 – 7354

[15] E. Tzimas, C.Filiou, S.D. Peteves and J.-B. Veyret Petten, The Netherlands, "Hydrogen storage:state of the art and future perspective", pp:15

[16] http://www.wholesalesolar.com/batteries.html ,Trojan battery user guide, pp 15

[17] Colleen Spiegel, "PEM fuel cell modeling and simulation using Matlab", 2008, pp.69

[18] Barbir, F., PEM Fuel Cells: Theory and Practice, 2005, pp. 39-65

[19] Kovačić, T.: Projektiranje kontrole energetskog sustava pasivne kuće, seminarski rad (voditelj prof. dr. sc. M. Firak), Fakultet strojarstva u brodogradnje Sveučilišta u Zagrebu, siječanj 2012.

[20] METEONORM, http://meteonorm.com/

[21] Fuel cell handbook, US, Department of energy, 2004,  www.ott.doe.gov

[22] Ballard Power Systems Inc.,NexaTM Power Module User's Manual, pp. 12

[23] Quaschning, Understanding renewable energy systems, chapter 4, pp. 150

# Appendix

Data sheets of the commercially available power system components used in this work

| PV module | |
|---|---|
| Model name | PV-MF120EC4-MITSUBISHI PV MODULE |
| Cell type | Polycrystalline silicon 150mm square |
| No. of cells | 36 in series |
| Maximum power rating [Pmax] | 120W |
| Open circuit voltage [Voc] | 22.0V |
| Short circuit current [Isc] | 7.36A |
| Maximum power voltage [Vmp] | 17.6V |
| Maximum power current [Imp] | 6.84A |
| Dimensions | 1425x646x56mm |
| Weight | 11.5kg (25.4lb) |
| Module efficiency | 13.0% |
| **Fuel cell** | |
| Electrical rated power | 2.4kW (2 × 1.2kW)- Ballard PEM FC |
| Maximum electric power | 3kW (2 × 1.5kW) |
| Open circuit voltage | 2 × ca. 48V |
| Rated electric current | 45A |
| Rated electric voltage | 26V |
| Maximum electric current per stack | 50A |
| Hydrogen consumption at rated electric power | <18.5 SLPM |
| Operating pressure of hydrogen | 70 – 1720kPa |
| Maximum operating pressure of hydrogen | 50kPa |
| Connection pressure of hydrogen | 500kPa |
| Water production | 870ml/hr(max.) |
| L x W x H | 56cm x 25cm x 33cm |
| Permissible ambient temperature | 3 to 40°C |
| Permissible relative humidity | 5 to 95% |
| **Electrolyser** | |
| Supplier | Hydrogen systems(now Hystat) |
| Model | 22 Cells of 300 $cm^2$ surface area connected in series |
| Operation Pressure | 25bar |
| Nominal Voltage and Current | 43V- 120A |
| Ambient Temperature | 2 to 40°C |
| Electrolyte Temperature | 85°C (max) |
| Maximum Power | 5.16kW |
| Module Conversion Efficiency | 4.9kWh/Nm³ |
| Current Density | 1A/cm² (max) |
| Hydrogen Production | 0.8Nm³/h at 30bar |

| Battery | |
|---|---|
| Model name | Trojan J185H- deep cycle 12 Volt |
| Capacity (minutes) at 25 Amps | 415 minutes |
| Ampere Hour Capacity:C20 | 215 AH |
| Voltage: | 12V |
| Dimentions(L×W×H) | 381mm×178mm×371mm |
| Weight | 55kg |
| Compressor | |
| Model name | TKH 36/18-100-50- Hofer |
| Suction Pressure (min. allowable) | 15bar |
| Capacity | 2Nm3/h |
| Suction Pressure (max.) | 50bar |
| Capacity | 8Nm3/h |
| Discharge Pressure (max.) | 500bar |
| Installed Motor Power: | 2kW |

# Životopis

Motalleb Miri rođen je 3. svibnja 1973. u Neki (Iran). Završio je srednju, matematičko-fizičku, školu u Neki 1991. Potom je 1997. diplomirao procesno inženjerstvo na Inženjersko tehničkom fakultetu sveučilišta Tehran. Magistrirao je (stekao MSc. diplomu) na Strojarskom fakultetu Abbaspur Sveučilišta u Tehranu 2000. godine. Nakon toga bio je zaposlen u Iranskoj organizaciji za energetsku učinkovitost (Iran Energy Efficiency Organization – IEEO) u odjelu za energetsku učinkovitost u industriji i energetskim postrojenjima. U IEEO-u je radio kao ekspert i ujedno vodio nekoliko projekata iz analize energetskih sustava u industriji. U 2003. pohađao je 3,5 mjesečni kurs iz održivog energetskog planiranaja u zgradarstvu na Sveučilištu Oslo, Norveška. Od 2006 do sada zaposlen je u Elma Kurtalj d.o.o. u Zagrebu kao projektni menadžer u odjelu za upravljanje energetskom učinkovitošću s radnim iskustvom na EU projektima i programima energetskog audita u zgradama. Sudjelovao je na više od 15 kurseva u Iranu, Njemačkoj, Finskoj, Turskoj i Hrvatskoj. Govori Engleski, Hrvatski, Arapski i Perzijski. Oženjen je i ima jedno dijete.

# Biography

Motalleb Miri was born on 03 May 1973 in Neka (Iran), accomplished high school in mathematics and physics in Neka in 1991. He was graduated from technical engineering faculty in process engineering from Tehran University in 1997. He earned his master degree in energy systems in 2000 from mechanical engineering faculty in Abbaspour University in Tehran. After that he was employed in Iran energy Efficiency Organization (IEEO) in the department of energy efficiency in industries and power plants. He has worked in IEEO as expert and also conducted several projects in energy system analysis in industries. In 2003 attended in the course of sustainable energy planning in buildings in university of Oslo, Norway. From 2006 he was employed in Elma Kurtalj Ltd. as project manager in the department of energy efficiency management with work experiences in EU projects and energy auditing programs in buildings. He has participated in more than 15 professional training courses in energy field in Iran, Germany, Finland, Turkey and Croatia.
He speaks English, Croatian, Arabic and Persian. He got married and has one son.